

WALL TEICHOIC ACID ASSEMBLY

**USING AUTHENTIC SUBSTRATES TO PROBE WALL TEICHOIC ACID
ASSEMBLY**

By Robert Tait Gale, B.Sc.

A thesis submitted to the School of Graduate Studies in partial fulfillment of the
requirements for the degree of Doctor of Philosophy

McMaster University © Robert Tait Gale, March 2018

DOCTOR OF PHILOSOPHY (2018) McMaster University

(Biochemistry and Biomedical Sciences) Hamilton, Ontario, Canada

TITLE: Using authentic substrates to probe wall teichoic acid assembly

AUTHOR: Robert Tait Gale, B.Sc.

SUPERVISOR: Eric D. Brown, Ph.D.

NUMBER OF PAGES: xii, 147

Abstract

Some of the most successful antibiotics in the clinic inhibit bacterial cell wall assembly. However, the continued emergence of multidrug-resistant bacteria is rapidly eroding the efficacy of these drugs - like all other antibiotics - and is a significant threat to human health. New treatment options are urgently needed that hinder bacterial viability, growth, and/or pathogenesis. Wall teichoic acids (WTAs) are integral components of Gram-positive bacterial cell walls and are critical to physiology and pathogenesis. WTA assembly is a *bona fide* drug target in several pathogens like *Staphylococcus aureus*. Many whole-cell screens have been performed to find small molecule inhibitors of this process. These efforts require a deep understanding of WTA assembly to help identify, characterize, and exploit high potential targets and therapeutic strategies. Challenges involved in the isolation of authentic substrates have hampered detailed biochemical study of WTA biosynthesis. Many features of the process remain uncharacterized. In this thesis, I detail a novel chemoenzymatic method to prepare authentic WTA substrates. I show that these materials can be used to study WTA biosynthetic enzymes *in vitro* and to probe enigmatic features of WTA assembly. With authentic WTA substrates, I reconstituted the final step of *B. subtilis* WTA synthesis *in vitro*, which involves ligation of WTAs to peptidoglycan. This process eluded biochemical characterization for decades. I investigated the catalytic requirements and substrate preferences for the LytR-CpsA-Psr family of enzymes that mediate this glycopolymer transfer reaction. Further, I discuss the attractiveness of these enzymes as antibiotic drug targets. Authentic WTA substrates will likely continue to be useful tools in understanding molecular features of WTA assembly and serve to assist drug discovery and development efforts targeting this process.

Acknowledgements

Dr. Eric Brown – thank you for the opportunity to pursue graduate research in your lab. The independent, creative, and engaging environment pushed me. It was a transformative experience. I am grateful for your support and guidance during pivotal periods along the way.

Drs. Gerry Wright and Russell Bishop – thank you for your wise counsel, constructive criticism, and thought-provoking questions.

Kalinka – I'm indebted to you for teaching me the crafts of analytical chemistry and chemical synthesis.

Cullen – I thoroughly enjoyed our brainstorming sessions. Your insight was crucial to this research. You kept morale high through it all. It was an honour, my friend.

Nigel – your unwavering belief in me allowed me to express myself. I could not have done this without your support.

Mom and Casey – thank you for the support and for lending a sympathetic ear in times of need.

Dawn – you introduced me to research, setting me on my path. I'm forever grateful. You have nurtured me and encouraged me to grow. Thank you for refusing to believe I wasn't going to make it. And for the wholesomeness. I love you deeply.

Table of contents

Preface

| | |
|-----------------------------|------|
| Abstract..... | iii |
| Acknowledgements..... | iv |
| Table of contents | v |
| List of figures..... | viii |
| List of tables..... | x |
| List of abbreviations | xi |

Chapter I - Introduction

| | |
|---|----|
| Preface..... | 2 |
| The Gram-positive bacterial cell wall: a formidable structure and prized antibiotic target..... | 3 |
| The rising threat of antimicrobial resistance and a lean drug pipeline..... | 4 |
| A clarion call to find new drug targets within cell wall assembly..... | 6 |
| Peptidoglycan assembly and organization..... | 8 |
| New tools to probe peptidoglycan assembly and aid drug discovery | 9 |
| Wall teichoic acids: the other major component of the Gram-positive cell wall | 11 |
| WTA biosynthesis machinery as antibacterial drug targets..... | 13 |
| Understanding WTA assembly and the need for authentic substrates..... | 15 |
| The LytR-CpsA-Psr (LCP) family - putative glycopolymer transferases..... | 17 |
| Genetic and phenotypic work underpin LCP functional characterization | 19 |
| LCP biochemical characterization..... | 20 |
| Contents herein..... | 22 |
| References..... | 22 |
| Figures..... | 38 |

Chapter II – Reconstituting poly(glycerol phosphate) wall teichoic acid biosynthesis *in vitro* using authentic substrates

| | |
|--------------------|----|
| Preface..... | 44 |
| Summary..... | 45 |
| Introduction | 45 |

| | |
|--|-----|
| Results and discussion | 47 |
| Conclusions | 52 |
| Experimental | 54 |
| Acknowledgements | 58 |
| References..... | 58 |
| Figures..... | 63 |
| Scheme..... | 66 |
| Table..... | 67 |
| Supplementary methods | 68 |
| Supplementary figures | 75 |
| Chapter III – <i>B. subtilis</i> LytR-CspA-Psr enzymes transfer wall teichoic acids from authentic lipid-linked substrates to mature peptidoglycan <i>in vitro</i> | |
| Preface..... | 89 |
| Summary..... | 90 |
| Introduction | 90 |
| Results | 93 |
| Discussion..... | 100 |
| Significance..... | 105 |
| Author contributions | 106 |
| Acknowledgements | 106 |
| References..... | 106 |
| Star methods..... | 113 |
| Figures..... | 122 |
| Table..... | 125 |
| Supplemental figures | 126 |
| Supplemental table | 129 |
| Chapter IV - Conclusion | |
| Summary..... | 131 |
| Practical applications for authentic WTA substrates | 131 |
| Probing the glycopolymer transfer reaction..... | 134 |
| Are LCP proteins druggable antibiotic targets?..... | 137 |
| Screening for small molecule inhibitors of LCP enzymes | 139 |

| | |
|--------------------------|-----|
| Concluding remarks | 141 |
| References..... | 142 |
| Figure..... | 147 |

List of figures

Chapter I

| | |
|---|----|
| Figure 1: <i>B. subtilis</i> peptidoglycan biosynthesis..... | 38 |
| Figure 2: <i>B. subtilis</i> peptidoglycan structure and chemical diversity | 39 |
| Figure 3: <i>B. subtilis</i> 168 wall teichoic acid structure..... | 40 |
| Figure 4: <i>B. subtilis</i> 168 wall teichoic acid biosynthesis | 41 |
| Figure 5: Structure of the wall teichoic acid biosynthetic intermediate Lipid α and analogs thereof | 42 |

Chapter II

| | |
|--|----|
| Figure 1: Poly(glycerol phosphate) WTA biosynthesis in <i>B. subtilis</i> 168..... | 63 |
| Figure 2: Semisynthetic Lipid α can be used to reconstitute the activities of pure, recombinant WTA biosynthetic enzymes TagA and TagB <i>in vitro</i> . | 64 |
| Figure 3: Authentic late-stage WTA intermediates are substrates for polymerization and glucosylation | 65 |
| Scheme 1: Semisynthetic preparation of lipid α | 66 |
| Figure S1: HRMS of WTA intermediates produced <i>in vitro</i> | 75 |
| Figure S2: Negative-ion collision-induced dissociation mass spectra (MS/MS) of WTA intermediates produced <i>in vitro</i> | 76 |
| Figure S3: TagF and TagE reaction products are polyanionic..... | 78 |
| Figure S4: The TagF reaction product shows typical WTA lability patterns..... | 79 |
| Figure S5: Radioactive standards for anion exchange HPLC analysis | 80 |
| Figure S6: HRMS of synthesized materials | 82 |
| Figure S7: NMR analysis of synthesized materials..... | 87 |

Chapter III

| | |
|--|-----|
| Figure 1: <i>B. subtilis</i> LCP enzymes transfer WTA intermediates to peptidoglycan <i>in vitro</i> | 122 |
| Figure 2: TagU-mediated activity varies with alternative acceptor/donor substrates and is linear with time and enzyme concentration | 123 |
| Figure 3: Hydrolysis and HPLC analysis confirm the transfer of WTAs to peptidoglycan by <i>B. subtilis</i> TagU..... | 124 |
| Figure S1: Purification of truncated <i>B. subtilis</i> LCP enzymes | 126 |
| Figure S2: Synthesis of WTA intermediates for LCP transferase assays . | 127 |

| | |
|---|-----|
| Figure S3: HPLC analysis of radiolabeled standards..... | 128 |
| Chapter IV | |
| Figure 1:..... | 147 |

List of tables

Chapter II

| | |
|---|----|
| Table 1: Nomenclature for undecaprenyl-linked WTA intermediates | 67 |
|---|----|

Chapter III

| | |
|---|-----|
| Table 1: WTA intermediates and analogs | 125 |
| Table S1: Polyisoprenoid-linked WTA and peptidoglycan intermediates | 129 |

List of abbreviations

| | |
|------------|--|
| WHO | World Health Organization |
| VRSA | vancomycin-resistant <i>Staphylococcus aureus</i> |
| MRSA | methicillin-resistant <i>Staphylococcus aureus</i> |
| R&D | Research and Development |
| WTA | wall teichoic acid |
| UDP | uridine diphosphate |
| GlcNAc | <i>N</i> -acetylglucosamine |
| MurNAc | <i>N</i> -acetylmuramic acid |
| FDA | Food and Drug Administration (USA) |
| GlcNAc-1-P | <i>N</i> -acetylglucosamine-1-phosphate |
| ManNAc | <i>N</i> -acetylmannosamine |
| mDAP | <i>meso</i> -diaminopimelic acid |
| GroP | <i>sn</i> -glycerol-3-phosphate |
| Und | undecaprenol |
| Glu | glucose |
| CDP | cytidine diphosphate |
| ESI-MS | electrospray ionization mass spectrometry |
| HRMS | high resolution mass spectrometry |
| LC/MS | liquid chromatography/mass spectrometry |
| MS/MS | tandem mass spectrometry |
| NMR | nuclear magnetic resonance |
| HPLC | high-performance liquid chromatography |
| UPLC | ultra-performance liquid chromatography |
| Q-TOF | quadrupole time-of-flight |
| MOA | mechanism of action |
| ABC | ATP-binding cassette |
| LCP | LytR-CpsA-Psr |
| IPTG | isopropyl β -D-1-thiogalactopyranoside |
| TLC | thin layer chromatography |

SEDS shape, elongation, division, and sporulation
PBP penicillin-binding protein
CPS..... capsular polysaccharides
TB tuberculosis
SDS..... sodium dodecyl sulphate
EDTA..... ethylenediaminetetraacetic acid
TCA..... trichloroacetic acid

CHAPTER I – Introduction

Preface

Some parts of this chapter were adapted from a previously published review:

Gale, R.T., and Brown, E.D. (2015). New chemical tools to probe cell wall biosynthesis in bacteria. *Curr. Opin. Microbiol.* 27, 69–77.

Permission has been granted by the publisher to reproduce the material herein.

I wrote and edited the manuscript with input from Dr. Eric Brown.

The Gram-positive bacterial cell wall: a formidable structure and prized antibiotic target

Almost all eubacteria synthesize a cell wall. This structure protects the cell from environmental challenges, imparts shape, resists turgor pressure, modulates surface adhesion, and assists in pathogenesis and antibiotic resistance (Brown et al., 2013; Höltje, 1998; Navarre and Schneewind, 1999). Several large macromolecules make-up the bulk of the cell wall in Gram-positive bacteria. These include peptidoglycan, proteins, and glycopolymers like wall teichoic acids (WTAs).

The cell wall is a crucial structure for those bacteria that have it. Disruption of its synthesis or specific degradation of this barrier means certain lysis. Chemotherapeutic agents that interdict cell wall synthesis are among the most successful and effective of all antibiotics. The use of these agents, notably the β -lactam and glycopeptide classes of antibiotics that target peptidoglycan synthesis, have provided the mainstay of treatment regimes for bacterial infections in the clinic (Singh et al., 2017; Van Boeckel et al., 2014). Indeed, cell wall biosynthesis inhibitors have totaled as much as 50% of the antibiotics prescribed globally in recent decades (Singh et al., 2017; Van Boeckel et al., 2014).

Some consider the cell wall biosynthetic machinery to be a privileged antibiotic target (Silver, 2017). The spectacular success of cell wall inhibitors is attributed to their targets being essential, conserved across bacteria, absent in mammals, and mostly located on the cell surface. These features mitigate target-based cytotoxicity and drug permeability/efflux issues that plague antibiotic drug discovery efforts. Yet, success is further explained by some inhibitors having many targets, and others targeting non-protein molecules. Both of these features make resistance development more challenging. For instance, β -lactams inhibit

the actions of many penicillin-binding proteins (PBPs) that build the peptidoglycan layer (Curtis et al., 1979; Silver, 2007). Moreover, glycopeptides, lantibiotics, depsipeptides, and defensins all bind and sequester cell wall precursors (Müller et al., 2017; Ulm and Schneider, 2016).

The rising threat of antimicrobial resistance and a lean drug pipeline

The rapid emergence and spread of antibacterial resistance have tempered the clinical efficacy of all antibiotics - not least the cell wall-targeting agents. A well-publicized report from the World Health Organization (WHO) in 2017 underscores this problem by naming pathogens resistant to one or more cell wall-targeting antibiotics as priority pathogens to guide research and development of new antibiotics (World Health Organization, 2017a). Several Gram-positive pathogens are listed. These include vancomycin- and methicillin-resistant *Staphylococcus aureus* (VRSA and MRSA), vancomycin-resistant *Enterococcus faecium*, and penicillin-non-susceptible *Streptococcus pneumoniae*.

There are increasing reports of multidrug-resistant bacteria in which there are few available treatment options (Almeida Da Silva and Palomino, 2011; Higgins et al., 2010). Many experts agree that we are on the periphery of a post-antibiotic age (Brown and Wright, 2016; Luepke et al., 2017; Unemo and Nicholas, 2012). This threat has spurred government and public health agencies to commit to combating antimicrobial resistance. The Public Health Agency of Canada, for instance, recently released reports highlighting their federal action plans on antimicrobial resistance and use. These reports focus on increased surveillance, stewardship, and innovation (Public Health Agency of Canada, 2014, 2015).

A waning antibiotic drug pipeline over the past decades (Spellberg, 2014) has failed to subvert the looming resistance problem. Experts blame the precipitous decline of antibiotics on scientific barriers, regulatory challenges, difficulties in clinical development, and little return on financial investments (Luepke et al., 2017; Silver, 2017). These issues played a role in the exodus of major pharmaceutical companies from antibiotic discovery and development. This has left mainly universities and small R&D companies to fill the void. However, recently forged private-public partnerships like the Combating Antibiotic-Resistant Bacteria initiative: Xccelerating global antibacterial innovation (CARB-X; <http://www.carb-x.org>) and the Innovative Medicines Initiative: New Drugs for Bad Bugs (ND4BB; <http://www.nd4bb.eu>) offer some recourse. These initiatives promise to bring novel research and innovations to the fight in the coming years.

We saw thirty new antibiotics enter the market between 2008-2015 (Butler et al., 2016). Only five of these drugs are first-in-class antibiotics. Most are chemical modifications of old chemical lead classes (Singh et al., 2017). Thirty percent of these new antibiotics are cell wall assembly inhibitors and belong to the well-known antibiotic classes of carbapenems (Biapenem, Ertapenem, Doripenem, and Tebipenem pivoxil), cephalosporins (Ceftobiprole medocaril and Ceftaroline fosamil), and glycopeptides (Telavancin, Dalbavancin, and Oritavancin) (Butler et al., 2016). There is a clear paucity of approved first-in-class antibiotics that inhibit cell wall assembly.

The current antibiotic pipeline (as of early 2017) echoes a similar tale. The WHO and the Pew Charitable Trusts report ~ 40 antibiotics in various phases of clinical development (World Health Organization, 2017b; Pew Charitable Trusts, 2017). Only a handful of these drugs are cell wall synthesis inhibitors, and again, belong to known antibiotic classes. These include three cephalosporins (Cefiderocol, S-649266, and GSK-3342830), a penem (Sulopenem), and a monobactam (LYS-

228). While progress has been made, experts agree that these chemical entities – both recently approved or still in the pipeline – are insufficient to tackle the current threat of antimicrobial resistance (Butler et al., 2016; Singh et al., 2017). Overcoming existing resistance requires first-in-class antibiotics with new cellular targets.

A clarion call to find new drug targets within cell wall assembly

Empirical screening of actinomycetes extracts was a fruitful path to discover new antibiotics until the early 1980s (Silver, 2016). But, the dearth of new chemical matter from overmining this platform, along with the advent of genomics, bioinformatics, and other technologies like high-throughput robotic screening platforms shifted the discovery paradigm to a target-centralized one. In this approach, potential antibacterial targets are first identified, then screened via whole-cell, *in vitro*, and/or *in silico* methods to find novel small molecule inhibitors from chemical libraries. Unfortunately, target-based drug discovery has been unsuccessful (Brown and Wright, 2016). The shortcomings are well documented (Payne et al., 2007; Tommasi et al., 2015). They are the inability of many small molecule inhibitors to traverse the cellular envelope to interact with targets (particularly problematic in Gram-negative bacteria); rapid resistance development to single-enzyme target inhibitors; and a lack of chemical diversity in large chemical libraries. Moreover, it is challenging to rank and leverage the real druggable targets from other candidates without a deep understanding of each targets complex biology (Sutterlin et al., 2017).

Discovering new antibiotics is difficult. Some have suggested that the way forward is to resolve the challenges and bottlenecks identified from the unsuccessful target-centralized approach (Lewis, 2017). Focusing discovery efforts on targets within cell wall biosynthesis pathways - which are druggable

and mostly located outside the cytoplasmic membrane - promises to ease some of the hardships in modern drug discovery. Indeed, many experts believe that we should screen the established cell wall targets with more diverse chemical matter (Lange et al., 2007; Projan, 2002; Silver, 2016). But, these proven targets represent only a small subset of gene products and/or intermediates in cell wall assembly. Thus, it is reasonable to assume that there are still many unexploited targets to use for drug discovery. Small molecule inhibitors of these new targets could be leads and developed/optimized for the generation of first-in-class antibiotics.

To identify and leverage unexploited targets, we need a more fundamental understanding of cell wall biology. Accordingly, there is a renewed emphasis on studying cell wall enzyme-mediated reactions at the molecular level. Moreover, many in the field have pushed to develop new chemical tools and substrates to probe enigmatic features of cell wall assembly (reviewed in Gale and Brown, 2015). These efforts motivated the research presented in this thesis (Chapters 2 & 3), where I endeavored to prepare authentic substrates - and use them - to characterize enigmatic features of Gram-positive bacterial cell wall assembly. These features surround the assembly of wall teichoic acids (WTAs). Many proteins involved in WTA assembly have been the target of screening campaigns searching for new antimicrobial matter (Farha et al., 2013; Lee et al., 2010; 2016; Matano et al., 2017; Swoboda et al., 2009; Wang et al., 2013).

Peptidoglycan and WTAs make up the bulk of the Gram-positive bacterial cell wall. These large macromolecules join in the final stages of cell wall assembly. I provide a brief background of the biosynthesis of these structures, along with recent discoveries and attractive druggable targets in their pathways, for context and to further explain motivations behind the research presented herein.

Peptidoglycan assembly and organization

The construction of the peptidoglycan meshwork may have underpinned the explosive bacterial radiation that took place 3-4 billion years ago (Errington, 2013). Gram-positive bacteria, in particular, make a very thick, multilayered peptidoglycan meshwork using extracytoplasmic proteins to concatenate peptidoglycan precursors (Silhavy et al., 2010).

The assembly of the peptidoglycan sacculus occurs in distinct stages. Figure 1 details the process in *Bacillus subtilis*. The pathway begins with the cytoplasmic generation of UDP-*N*-acetylmuramic acid pentapeptide (Barreteau et al., 2008). This precursor is coupled to a membrane-embedded undecaprenyl phosphate (C₅₅-P) lipid carrier on the cytoplasmic face of the bacterial membrane and glycosylated to form Lipid II (Bouhss et al., 2008). Lipid II is translocated across the bacterial membrane and polymerized to form long glycan chains (Meeske et al., 2015; Sham et al., 2014). These nascent glycan strands are cross-linked to the existing meshwork through flexible peptides to form part of the multi-gigadalton peptidoglycan sacculus that surrounds the cytoplasmic membrane (Vollmer et al., 2008).

To accommodate bacterial growth and division, peptidoglycan synthesis, modification, and degradation are in constant flux (Egan and Vollmer, 2012). Peptidoglycan biosynthetic enzymes incorporate nascent peptidoglycan chains into the inner layers of the mature meshwork, whereas autolysins degrade the outer-most glycans inwards (Koch and Doyle, 1985). Newly-formed glycan layers are likely in a relaxed conformation until they brace the turgor pressure once held by older layers that have degraded (Beeby et al., 2013).

Peptidoglycan seems to adhere to several distinct architectural arrangements/models. *Escherichia coli*, which have average glycan chain lengths

of ~21 disaccharides, arrange chains circumferentially across the long axis of the cell (Harz et al., 1990). Gram-positive *Staphylococcus aureus*, on the other hand, has short peptidoglycan strands (~6-8 disaccharide units) that likely orient perpendicular to the plasma membrane in a “scaffold” model (Boneca et al., 2000). The peptidoglycan architecture of rod-shaped *B. subtilis* has been the subject of much debate – its long glycan strands (~100 - 5000 disaccharide units) could form coiled-cable structures or arrange circumferentially like in *E. coli* (Beeby et al., 2013; Hayhurst et al., 2008).

Despite β -1,4-linked GlcNAc-MurNAc disaccharides being a ubiquitous feature of all peptidoglycan, there is chemical diversity in structures across bacterial species (Turner et al., 2014; Vollmer et al., 2008). Several enzyme-mediated reactions modify the peptidoglycan wall. In Gram-positive bacteria, these modifications include *N*-deacetylation at the C(2) position of GlcNAc and/or MurNAc residues, and *O*-acetylation at the C(6) hydroxyl group of MurNAc (Moynihan et al., 2014). Relevant to research/discussions presented in Chapter 3, this same C(6) hydroxyl group of MurNAc is also the site of attachment for glycopolymers like WTAs and capsular polysaccharides. Post-synthetic peptidoglycan modifications protect the cell from exogenous antimicrobial peptides. They also protect against host immunity-derived proteins like lysozyme, and from endogenous autolysins involved in peptidoglycan metabolism (Moynihan and Clarke, 2011). Figure 2 shows the structure of *B. subtilis* peptidoglycan and these sites of modification.

New tools to probe peptidoglycan assembly and aid drug discovery

The cytoplasmic stages of peptidoglycan assembly are viable antibacterial targets (Silver, 2012). Yet, most cell wall-targeting antibiotics inhibit the later lipid-

linked steps of the pathway. The emergence of resistance to cell wall inhibitors has sparked interest to better understand the molecular details of these steps and to develop new tools and assays that identify and progress novel biosynthetic inhibitors. Thorough biochemical studies of this nature need milligram quantities of peptidoglycan biosynthetic intermediates. Attempts to isolate intermediates Lipid I and Lipid II from natural bacterial sources are futile due to minute supply in cells (van Heijenoort et al., 1992). Thus, research groups have focused efforts on synthetic strategies to get them (Breukink et al., 2003; Lebar et al., 2013; Qiao et al., 2014; Schwartz et al., 2001; VanNieuwenhze et al., 2001; 2002; Ye et al., 2001).

There have been several important applications for authentic peptidoglycan substrates. For example, Braddick et al. used enzyme-prepared Lipid II to develop quantitative assays that track Lipid II polymerization by the *S. aureus* transglycosylase MGT (Braddick et al., 2014). Schneider and co-workers employed the same substrate to capture *S. aureus* pentaglycine interpeptide assembly *in vitro* (Schneider et al., 2004). Furthermore, Lipid I and Lipid II were used in biochemical assays to define the ligand preferences for the semisynthetic glycopeptide oritavancin and the highly-publicized novel depsipeptide teixobactin (Ling et al., 2015; Münch et al., 2015). Lastly, Huang *et al.* synthesized truncated Lipid II analogues containing Förster Resonance Energy Transfer donor/acceptor pairs. The authors used these molecules in high-throughput screens to search for *Clostridium difficile* PBP transglycosylase inhibitors (Huang et al., 2013).

These herculean efforts highlight the utility of authentic substrates. These tools help investigators: understand more fundamental aspects of peptidoglycan assembly; identify the cellular targets of antibiotics; and design novel screens for inhibitors. Peptidoglycan biosynthesis has experienced the lions-share of

biochemical focus directed at the cell wall. However, WTAs are another major component of this structure in Gram-positive bacteria. Furthermore, these glycopolymers influence antibiotic resistance and pathogenesis. Thus, part of the focus of our laboratory is to better understand fundamental aspects of WTA biology. Information from these studies might drive the discovery, validation, and development of novel cell wall inhibitors. It was clear that these efforts would benefit from advancements akin to those described above for the peptidoglycan pathway.

Wall teichoic acids: the other major component of the Gram-positive cell wall

The peptidoglycan meshwork in most Gram-positive bacteria is heavily modified with glycopolymers, the most abundant being anionic WTAs. WTAs can account for up to 60% of the total mass of the cell wall in some organisms (Neuhaus and Baddiley, 2003). These polymers anchor to the C(6) hydroxyl group of peptidoglycan *N*-acetylmuramic acid – tethered to about every ninth residue (Bera et al., 2007; Kojima et al., 1985) - and consist of repeating polyol phosphate residues tailored with D-alanyl and glycosyl groups. WTA polymers are 40-60 polyol phosphate units in length and protrude beyond the thick peptidoglycan sacculus (Kojima et al., 1985; 1983). Figure 3 shows the structure of *B. subtilis* 168 WTA anchored to peptidoglycan.

While the precise biological function of WTAs remains unclear, these polymers participate in bacterial growth, division, morphogenesis (D'Elia et al., 2006), autolysis (Schlag et al., 2010), and even the modulation of sensor kinase activity (Botella et al., 2014). Work in pathogenic *S. aureus* and *S. pneumoniae* reveals a critical role for WTAs in mechanisms of host infection and virulence (Hong et

al., 2017; Wanner et al., 2017; Weidenmaier et al., 2004; Winstel et al., 2015; Xu et al., 2015), along with β -lactam resistance (Farha et al., 2013; Wang et al., 2013). Furthermore, our group has recently investigated the role of WTA degradation in the phosphate starvation response (Myers et al., 2016). Studies also reveal that peptidoglycan and WTA biosynthesis are intimately linked (Atilano et al., 2010), particularly during cell wall stress, like upon challenge with glycopeptides (Chang et al., 2017; Singh et al., 2017).

Like peptidoglycan biosynthetic intermediates, WTAs are assembled on membrane-embedded undecaprenyl-linked precursors (C_{55}). One of the better-characterized biosynthetic pathways is *B. subtilis* 168 poly(glycerol phosphate) WTA assembly. This process is shown in Figure 4. The first step of this pathway involves the transfer of *N*-acetylglucosamine-1-phosphate to the undecaprenyl phosphate lipid carrier in a reaction catalyzed by the transmembrane protein TagO, producing intermediate Lipid α (Soldo et al., 2002). TagA catalyzes the first committed step of the pathway with the addition of *N*-acetylmannosamine to the C(4) hydroxyl group of the Lipid α GlcNAc moiety to yield Lipid β (D'Elia et al., 2009). TagB catalyzes the incorporation of a single *sn*-glycerol-3-phosphate residue to the lipid-linked disaccharide to form Lipid ϕ .1 (Bhavsar et al., 2005). TagF then polymerizes ~50 glycerol-3-phosphate units on Lipid ϕ .1 (Pereira et al., 2008; Schertzer and Brown, 2003). TagE modifies these polymers with α -linked glucose residues, generating Lipid γ . The ATP-binding cassette (ABC) transporter TagGH transports Lipid γ to the extracellular leaflet of the plasma membrane (Allison et al., 2011; Lazarevic and Karamata, 1995). Uncharacterized enzymes likely modify these lipid-linked glycopolymers with D-alanyl substituents (Kovács et al., 2006). The recently characterized TagTUV proteins (Gale et al., 2017) transfer WTAs from their lipid anchors to the C(6) hydroxyl group of peptidoglycan *N*-acetylmuramic acid (demonstrated in Chapter 3).

WTA biosynthetic machinery as antibacterial drug targets

Given the importance of WTAs to bacterial physiology and pathogenesis, the WTA biosynthetic machinery has emerged as an attractive target for novel antibacterial agents (Pasquina et al., 2013; Sewell and Brown, 2013). Proteins in this pathway may also be viable targets for antivirulence (Silver, 2012) and/or β -lactam potentiation therapeutic strategies (Brown et al., 2013). The WTA synthesis machinery is essential during infection and proven to be druggable. Inactivation of the early-step gene *tarO* results in WTA-deficient *S. aureus* mutants. These mutants have impaired pathogenesis during murine infection models and in other *in vitro* assays (Baur et al., 2014; Wanner et al., 2017; Weidenmaier et al., 2004). Furthermore, whole-cell target-based screens have identified several valid inhibitors of WTA assembly (discussed below).

Genes involved in *B. subtilis* and *S. aureus* WTA biosynthesis exhibit paradoxical gene dispensability patterns. Inactivation of early-step genes results in viable but non-infectious organisms. Late-step genes are indispensable and result in bacteriostatic phenotypes if inactivated (likely due to an accumulation of essential cell wall precursors) (D'Elia et al., 2009; 2006a; 2006b; Pereira et al., 2008). Interestingly, simultaneous inactivation of early-step genes alleviates the lethality of late-step gene inactivation. Several whole-cell based screens have leveraged this unique conditional essential phenotype to identify inhibitors of the WTA biosynthetic pathway. For example, the Walker group and Merck Research laboratories have identified inhibitors of TarG (the translocase component of the ABC complex) in screens looking for agents that phenocopy lesions in late-step genes (Matano et al., 2017; Swoboda et al., 2009; Wang et al., 2013). Researchers at Merck also found inhibitors of TarO through chemical suppression-based screens designed to phenocopy lesions in early-step

processes (Lee et al., 2016). Our laboratory first published on this screen design, which resulted in the discovery of several inhibitors of undecaprenyl pyrophosphate synthase (Czarny and Brown, 2016; Farha et al., 2015).

Antibiotic resistance is rife and new chemical classes of antibiotics are lacking. Because of this, considerable effort has gone into restoring the clinical efficacy of work-horse β -lactam antibiotics. One strategy to overcome β -lactam resistance is through combination therapy that pairs a β -lactam with a β -lactamase inhibitor. Indeed, we have seen two new β -lactam/ β -lactamase combinations enter the clinic since 2000, and the current pipeline contains many more (Butler et al., 2016; World Health Organization, 2017b). The inhibition or alteration of WTA biosynthesis has also emerged as a viable method to re-tool β -lactam therapies. This strategy is particularly effective against MRSA that exploits alternative routes to resistance other than β -lactamase production (Fuda et al., 2005). Genetic inactivation of early step genes or small-molecule inhibition of WTA assembly restores the sensitivity of MRSA to β -lactams *in vitro* and during murine infection (Campbell et al., 2011; Wang et al., 2013; Maki 1994). Thus, small molecule inhibitors of early WTA biosynthetic steps have great potential to act as β -lactam potentiators in combination therapies. With this in mind, Farha *et al.* executed a chemical combination screen that paired approved drugs with the β -lactam antibiotic cefuroxime. These efforts identified ticlopidine as an inhibitor of *S. aureus* TarO catalysis (Farha et al., 2013). TarA and TarS may also be attractive β -lactam potentiator targets (Brown et al., 2012). Although, it appears that targeting the WTA molecule itself with cationic polymers might also be a viable option for β -lactam potentiation against MRSA (Foxley et al., 2017).

Understanding WTA assembly and the need for authentic substrates

Armstrong et al. conducted early work on the biochemistry of WTAs from several Gram-positive bacteria (Armstrong et al., 1958). Various genetic experiments and sequence analyses later identified the genetic requirements for WTA assembly (Karamata et al., 1987; Lazarevic et al., 2002; Ward, 1981). While advancements in molecular biology granted access to recombinant WTA biosynthetic enzymes, inaccessibility of the (C₅₅) undecaprenyl-linked substrates hindered their detailed characterization. To overcome these issues, our lab and the Walker lab synthesized soluble WTA intermediate analogues for use in biochemical assays. These analogues contain truncated polyisoprenoid tails (Zhang et al., 2006) or short aliphatic tridecyl (C₁₃) chains (Ginsberg et al., 2006; Pereira et al., 2008) in place of the C₅₅ moiety found in authentic WTA biosynthetic substrates. Figure 5 shows the structure of the early WTA biosynthetic intermediate Lipid α and analogs thereof. These intermediate analogues are simpler to prepare and do not aggregate during biochemical assays. Investigators have characterized several WTA biosynthetic enzymes from *B. subtilis* and *S. aureus* using these substrates. These WTA glycosyltransferases mediate WTA linkage unit formation (Ginsberg et al., 2006; Zhang et al., 2006), priming (Brown et al., 2008; Ginsberg et al., 2006), polymerization (Pereira et al., 2008; Sewell et al., 2009) and modification (Allison et al., 2011; Brown et al., 2012).

But, many of the WTA glycosyltransferases are membrane-associated. These enzymes operate on undecaprenyl-linked substrates at the lipid-water interface. Thus, the soluble *in vitro* systems that use truncated substrates are unable to mimic true physiological features for catalysis. Many whole-cell screening platforms were being developed against WTA biosynthetic proteins. To learn more about these targets in a physiologically-relevant context, we felt it was

necessary to probe WTA glycosyltransferase-mediated catalysis using authentic substrates. We speculated that these materials, reconstituted into an interfacial system, would influence enzyme catalysis compared to what was observed using soluble analogues. Changes could occur in catalytic efficiency, processivity, and mode/mechanism. Indeed, early work from our lab showed that the WTA polymer-length regulatory function of TagF depends on authentic substrate/membrane-interaction alone (Schertzer and Brown, 2003; Sewell et al., 2009). Moreover, as described in Chapter 3, we were optimistic that authentic WTA substrates would illuminate enigmatic features surrounding the last step of WTA biosynthesis. These biochemical studies needed access to authentic WTA substrates.

Tanja Schneider's group published the first preparation of authentic WTA substrates. Her team solubilized *S. aureus* TagO - a protein bearing 13 transmembrane helices - and reconstituted its *N*-acetylhexosamine-1-phosphate transferase activity *in vitro*. They used commercial undecaprenyl-phosphate reconstituted in mixed-micelles as an acceptor substrate (Müller et al., 2012). Lipid α was produced by this enzyme-mediated reaction. Lipid α could be elaborated to Lipid β by the addition of UDP-GlcNAc and recombinant proteins TagA and MnaA to the system. The Schneider group used these WTA precursors to confirm the mechanism of action for several cell-wall antibiotics including nisin, the lantibiotic NAI-107, and teixobactin (Ling et al., 2015; Munch et al., 2014; Müller et al., 2012).

Undecaprenyl pyrophosphate-linked sugars are intermediates in peptidoglycan and WTA assembly pathways. These molecules are also used in *O*-polysaccharide biosynthesis, *N/O*-protein glycosylation, and capsule polysaccharide production (Larson and Yother, 2017; Li et al., 2016). Many

research groups have designed strategies to prepare these intermediates (Holkenbrink et al., 2011; Weerapana et al., 2005; Woodward et al., 2010). The use of these authentic intermediates in biochemical assays has elucidated many molecular features of these pathways (Li et al., 2010; Musumeci et al., 2013; Woodward et al., 2010).

Taken together, these works inspired our efforts to synthesize authentic undecaprenyl pyrophosphate-linked sugars of the WTA pathway (Gale et al., 2014). Chapter 2 details these efforts.

The LytR-CpsA-Psr (LCP) family – putative glycopolymer transferases

Gram-positive bacteria affix many glycopolymers to their developing peptidoglycan sacculus. Glycopolymers destined for the wall include WTAs, capsular polysaccharides, teichuronic acids, and other neutral or acidic polysaccharides (Schäffer and Messner, 2005). These glycopolymers have diverse compositions and equip the cell with a vast toolset to withstand environmental change. The importance of WTAs to physiology and pathogenesis was discussed at length above. We also speculate that these structures and other secondary cell wall polymers serve as nutrient sources in deplete environments (Myers et al., 2016). Furthermore, oligomeric capsule polysaccharides allow pathogens to evade host immunity and resist bacteriophage infection (Hyams et al., 2010; Rajagopal and Walker, 2015). Lastly, while we have restricted our discussion thus far to the cell walls of Firmicutes, Actinobacteria like *Mycobacterium tuberculosis* attach an intricate arabinogalactan layer to peptidoglycan. This unique structure provides protection from traditional cell wall-targeting antibiotics and host macrophages (Alderwick et al., 2007; Pieters, 2008).

Until 2016, no one had reconstituted glycopolymer transfer to peptidoglycan *in vitro*. Even the exact substrates and enzymes involved were unknown. Our lab and others were unsuccessful in characterizing this event for WTA biosynthesis. Decades-old analysis of cell wall preparations revealed that WTAs anchor to the C(6) hydroxyl group of peptidoglycan *N*-acetylmuramic acid. So, there must be machinery in place to transfer them from lipid anchors on the extrafacial leaflet of the cytoplasmic membrane to this peptidoglycan moiety. Substantial genetic and phenotypic evidence suggested that the *LytR*-*CpsA*-*Psr* (LCP) family of enzymes perform bacterial glycopolymer transfer functions.

The LCP proteins take their name after the first three representatives described - *LytR*, *CpsA*, and *Psr*. LCP enzymes are ubiquitous in Gram-positive bacteria. Most Gram-negative bacteria do not encode these proteins (Hübscher et al., 2008). Investigators used *lcp* gene-deficient mutants to probe protein function. From these experiments, LCP proteins were annotated as cell envelope-associated transcriptional attenuators. *B. subtilis* *LytR* was proposed to be a transcriptional regulator of the *lytRABC* divergon that encodes itself and several putative autolysins (Lazarevic et al., 1992). *CpsA* was believed to act as an activator for capsule polysaccharide gene transcription in *Streptococcus agalactiae* (Cieslewicz et al., 2000). *Psr* was thought to repress PBP5 expression in *Enterococcus hirae* (Ligozzi et al., 1993). However, the transcriptional attenuation observed during these studies were likely indirect consequences of defective cell wall synthesis in these mutants (Baumgart et al., 2016; Kawai et al., 2011). Still, interest in the LCP protein family piqued when they were shown to influence virulence (Bae et al., 2004; Hübscher et al., 2009; Maadani et al., 2007; Wen et al., 2006), antibiotic resistance (Rossi et al., 2003), and other cell wall-maintenance functions in Gram-positive bacteria.

Genetic and phenotypic work underpin LCP functional characterization

Jeff Errington's group first proposed that LCP proteins mediate glycopolymer transfer to peptidoglycan. These researchers used genetic and phenotype studies to prove that WTA-peptidoglycan ligation requires LCP enzymes in *B. subtilis* (Kawai et al., 2011). *B. subtilis* encodes three LCP enzymes – TagT (YwtF), TagU (LytR), and TagV (YvhJ). Kawai et al. found that single and double *lcp* gene deletion mutants (any combination) had no major cell defects. A mutant lacking all three genes ($\Delta tagTUV$), however, was not viable. Interestingly – and like the conditional essentiality of other late-stage WTA genes – a $\Delta tagTUV$ mutant was possible with simultaneous deletion of the *tagO* gene. Errington's group generated a triple *lcp* deletion-like mutant by placing *tagV* under the control of an IPTG-inducible promoter in a $\Delta tagTU$ background. This mutant had cell shape defects and reduced WTA content in low IPTG levels (Kawai et al., 2011).

Many research groups adopted this genetic and phenotypic approach to investigate LCP function. Studies of this nature were conducted in *Streptococcus mutans* (Bitoun et al., 2013; De et al., 2017), *S. pneumonia* (Eberhardt et al., 2012), *S. agalactiae* (Rowe et al., 2015), *E. hirae* (Maréchal et al., 2016), *Bacillus anthracis* (Liszewski Zilla et al., 2015; Zilla et al., 2015), and *S. aureus* (Chan et al., 2014; Dengler et al., 2012; Over et al., 2011). In the last few years, there has been a surge of interest in LCP members of Actinobacteria. Studies have been conducted in *Actinomyces oris* (Wu et al., 2014), *Streptomyces coelicolor* (Sigle et al., 2016), *Mycobacterium marinum* (Wang et al., 2015), *Corynebacterium glutamicum* (Baumgart et al., 2016), and *M. tuberculosis* (Grzegorzewicz et al., 2016; Harrison et al., 2016; Köster et al., 2017). Together, these studies suggest that LCP enzymes not only transfer glycopolymers like wall teichoic acids to peptidoglycan, but in some organisms, also capsular polysaccharides,

arabinogalactan components, and other secondary cell wall polymers. There is even data showing a role for LCP members in protein glycosylation.

Many *lcp* genes localize close to genetic regions responsible for cell wall synthesis (Baumgart et al., 2016; Eberhardt et al., 2012; Harrison et al., 2016; Kawai et al., 2011; Maréchal et al., 2016; Rowe et al., 2015; Sigle et al., 2016). Gram-positive bacteria can encode between 1-11 LCP homologues. Some have suggested that the presence of multiple LCP members in bacteria indicates functional variability and/or redundancy amongst the proteins (Over et al., 2011). LCP proteins display high sequence-divergence (i.e. low amino acid identity; 17-39%) but have conserved charged residues in LCP domains. Conserved residues include aspartic acid, arginine, and lysine (Hübscher et al., 2008). Secondary structure predictions and topology experiments suggest that most LCP members adhere to a common structural organization. This organization follows a short N-terminal cytoplasmic domain, a transmembrane-spanning region (with one or three helices), and a C-terminal extension that contains a mixed α -helical/ β -sheet LCP catalytic domain (approximately 150 amino acids in length) (Hübscher et al., 2008). Therefore, LCP proteins are considered extramembrane non-Leloir glycosyltransferases. That is, they utilize polyprenol pyrophosphate sugar donors instead of canonical sugar nucleotide donors for catalysis (Dufrisne et al., 2016; Larson and Yother, 2017).

LCP biochemical characterization

An enormous body of genetic and phenotypic work highlighted LCP members as glycopolymer transferases. Yet, their activity eluded *in vitro* biochemical characterization. Advancements in molecular biology provided access to recombinant LCP enzymes, but, generating functional assays to monitor activity proved difficult. Challenges stemmed from the complex chemical nature and

accessibility of peptidoglycan and glycopolymer substrates. Progress was further hampered by a lack of understanding of specific reaction requirements. For instance, the identity of the peptidoglycan substrate was unknown. As Figure 1 shows, many peptidoglycan biosynthetic intermediates contain the *N*-acetylmuramic acid C(6) hydroxyl moiety for glycopolymer attachment. Moreover, it was unclear if the reaction necessitated authentic glycopolymer substrates. We were not sure if soluble WTA substrate mimics would be acceptable donors in the transfer reaction.

There are only a handful of published biochemical studies of LCP members. Most of these report pyrophosphatase activity for LCP enzymes on polyisoprenyl pyrophosphate molecules (Baumgart et al., 2016; Grzegorzewicz et al., 2016; Kawai et al., 2011). The first successful reconstitution of LCP-mediated glycopolymer transfer came from a collaboration between Gurdyal Bersa and Luke Alderwick laboratories in 2016. These authors utilized a membrane-based radiolabeling assay to show that *M. tuberculosis* Lcp1 tethers arabinogalactan components to purified peptidoglycan preparations *in vitro* (Harrison et al., 2016). *Mycobacterium smegmatis* membranes were used as a source of polyisoprenoid-linked arabinogalactan donor molecules in these reactions. Unfortunately, these preparations also came charged with endogenous LCP enzymes that caused high background signal in assays. Furthermore, to monitor reaction progression, a laborious work-up involving many extraction and sedimentation techniques was used. In Chapter 3, we reconstituted WTA transfer to peptidoglycan *in vitro* using *B. subtilis* LCP enzymes and authentic substrates. We took inspiration from the above work in these efforts. But, we wanted to create a more defined and facile glycopolymer transfer assay. While our investigations were concluding, Suzanne Walker's laboratory reported WTA ligase activity of *S. aureus* LCP enzymes. We discuss this work in Chapter 3.

Contents herein

We hypothesized that with authentic WTA substrates we could probe enigmatic features of WTA assembly. We felt that information gained from these studies would be complementary to the screening/discovery efforts against the WTA pathway. To this end, Chapter 2 details our semisynthetic synthesis of authentic WTA substrates. In Chapter 3, we employed these molecules to provide the first detailed biochemical characterization of *B. subtilis* LCP enzymes. We show that these enzymes ligate WTAs to cross-linked peptidoglycan *in vitro*. Chapter 4 highlights areas of future research. We discuss studies to further probe LCP-mediated catalysis and provide suggestions on how to exploit this enzyme family for novel antibiotic drug discovery.

References

- Alderwick, L.J., Birch, H.L., Mishra, A.K., Eggeling, L., and Besra, G.S. (2007). Structure, function and biosynthesis of the *Mycobacterium tuberculosis* cell wall: arabinogalactan and lipoarabinomannan assembly with a view to discovering new drug targets. *Biochem. Soc. Trans.* *35*, 1325–1328.
- Allison, S.E., D’Elia, M.A., Arar, S., Monteiro, M.A., and Brown, E.D. (2011). Studies of the genetics, function, and kinetic mechanism of TagE, the wall teichoic acid glycosyltransferase in *Bacillus subtilis* 168. *J. Biol. Chem.* *286*, 23708–23716.
- Almeida Da Silva, P.E.A., and Palomino, J.C. (2011). Molecular basis and mechanisms of drug resistance in *Mycobacterium tuberculosis*: classical and new drugs. *J. Antimicrob. Chemother.* *66*, 1417–1430.
- Armstrong, J.J., Baddiley, J., Buchanan, J.G., Carss, B., and Greenberg, G.R. (1958). 882. Isolation and structure of ribitol phosphate derivatives (teichoic acids) from bacterial cell walls. *J. Chem. Soc.* *0*, 4344–4354.
- Atilano, M.L., Pereira, P.M., Yates, J., Reed, P., Veiga, H., Pinho, M.G., and Filipe, S.R. (2010). Teichoic acids are temporal and spatial regulators of peptidoglycan cross-linking in *Staphylococcus aureus*. *Proc. Natl. Acad. Sci. U.S.A.* *107*, 18991–18996.

- Bae, T., Banger, A.K., Wallace, A., Glass, E.M., Aslund, F., Schneewind, O., and Missiakas, D.M. (2004). *Staphylococcus aureus* virulence genes identified by bursa aurealis mutagenesis and nematode killing. *Proc. Natl. Acad. Sci. U.S.A.* **101**, 12312–12317.
- Barreteau, H., Kovač, A., Boniface, A., Sova, M., Gobec, S., and Blanot, D. (2008). Cytoplasmic steps of peptidoglycan biosynthesis. *FEMS Microbiol. Rev.* **32**, 168–207.
- Baumgart, M., Schubert, K., Bramkamp, M., and Frunzke, J. (2016). Impact of LytR-CpsA-Psr proteins on cell wall biosynthesis in *Corynebacterium glutamicum*. *J. of Bacteriol.* **198**, 3045–3059.
- Baur, S., Rautenberg, M., Faulstich, M., Faulstich, M., Grau, T., Severin, Y., Unger, C., Hoffmann, W.H., Rudel, T., Autenrieth, I.B., and Weidenmaier, C. (2014). A nasal epithelial receptor for *Staphylococcus aureus* WTA governs adhesion to epithelial cells and modulates nasal colonization. *PLoS Pathog.* **10**, e1004089.
- Beeby, M., Gumbart, J.C., Roux, B., and Jensen, G.J. (2013). Architecture and assembly of the Gram-positive cell wall. *Mol. Microbiol.* **88**, 664–672.
- Bera, A., Biswas, R., Herbert, S., Kulauzovic, E., Weidenmaier, C., Peschel, A., and Götz, F. (2007). Influence of wall teichoic acid on lysozyme resistance in *Staphylococcus aureus*. *J. Bacteriol.* **189**, 280–283.
- Bernard, R., Ghachi, El, M., Mengin-Lecreulx, D., Chippaux, M., and Denizot, F. (2005). BcrC from *Bacillus subtilis* acts as an undecaprenyl pyrophosphate phosphatase in bacitracin resistance. *J. Biol. Chem.* **280**, 28852–28857.
- Bhavsar, A.P., Truant, R., and Brown, E.D. (2005). The TagB protein in *Bacillus subtilis* 168 is an intracellular peripheral membrane protein that can incorporate glycerol phosphate onto a membrane-bound acceptor in vitro. *J. Biol. Chem.* **280**, 36691–36700.
- Bitoun, J.P., Liao, S., McKey, B.A., Yao, X., Fan, Y., Abranches, J., Beatty, W.L., and Wen, Z.T. (2013). Psr is involved in regulation of glucan production, and double deficiency of BrpA and Psr is lethal in *Streptococcus mutans*. *Microbiology* **159**, 493–506.
- Boneca, I.G., Huang, Z.H., Gage, D.A., and Tomasz, A. (2000). Characterization of *Staphylococcus aureus* cell wall glycan strands, evidence for a new beta-N-acetylglucosaminidase activity. *J. Biol. Chem.* **275**, 9910–9918.

- Botella, E., Devine, S.K., Hubner, S., Salzberg, L.I., Gale, R.T., Brown, E.D., Link, H., Sauer, U., Codée, J.D., Noone, D., and Devine, K.M. (2014). PhoR autokinase activity is controlled by an intermediate in wall teichoic acid metabolism that is sensed by the intracellular PAS domain during the PhoPR-mediated phosphate limitation response of *Bacillus subtilis*. *Mol. Microbiol.* *94*, 1242–1259.
- Bouhss, A., Trunkfield, A.E., Bugg, T.D.H., and Mengin-Lecreulx, D. (2008). The biosynthesis of peptidoglycan lipid-linked intermediates. *FEMS Microbiol. Rev.* *32*, 208–233.
- Braddick, D., Sandhu, S., Roper, D.I., Chappell, M.J., and Bugg, T.D.H. (2014). Observation of the time-course for peptidoglycan lipid intermediate II polymerization by *Staphylococcus aureus* monofunctional transglycosylase. *Microbiology* *160*, 1628–1636.
- Breukink, E., van Heusden, H.E., Vollmerhaus, P.J., Swiezewska, E., Brunner, L., Walker, S., Heck, A.J.R., and de Kruijff, B. (2003). Lipid II is an intrinsic component of the pore induced by nisin in bacterial membranes. *J. Biol. Chem.* *278*, 19898–19903.
- Brown, E.D., and Wright, G.D. (2016). Antibacterial drug discovery in the resistance era. *Nature* *529*, 336–343.
- Brown, S., Xia, G., Luhachack, L.G., Campbell, J., Meredith, T.C., Chen, C., Winstel, V., Gekeler, C., Irazoqui, J.E., Peschel, A., and Walker, S. (2012). Methicillin resistance in *Staphylococcus aureus* requires glycosylated wall teichoic acids. *Proc. Natl. Acad. Sci. U.S.A.* *109*, 18909–18914.
- Brown, S., Santa Maria, J.P., Jr., and Walker, S. (2013). Wall teichoic acids of Gram-positive bacteria. *Annu. Rev. Microbiol.* *67*, 313–336.
- Brown, S., Zhang, Y.-H., and Walker, S. (2008). A revised pathway proposed for *Staphylococcus aureus* wall teichoic acid biosynthesis based on *in vitro* reconstitution of the intracellular steps. *Chem. Biol.* *15*, 12–21.
- Butler, M.S., Blaskovich, M.A., and Cooper, M.A. (2016). Antibiotics in the clinical pipeline at the end of 2015. *J. Antibiot.* *70*, 3–24.
- Campbell, J., Singh, A.K., Santa Maria, J.P., Jr., Kim, Y., Brown, S., Swoboda, J.G., Mylonakis, E., Wilkinson, B.J., and Walker, S. (2011). Synthetic lethal compound combinations reveal a fundamental connection between wall teichoic acid and peptidoglycan biosyntheses in *Staphylococcus aureus*. *ACS Chem.*

Biol. 6, 106–116.

Chan, Y.G.-Y., Kim, H.K., Schneewind, O., and Missiakas, D. (2014). The capsular polysaccharide of *Staphylococcus aureus* is attached to peptidoglycan by the LytR-CpsA-Psr (LCP) family of enzymes. J. Biol. Chem. 289, 15680–15690.

Chang, J., Coffman, L., and Kim, S.J. (2017). Inhibition of d-Ala incorporation into wall teichoic acid in *Staphylococcus aureus* by desleucyl-oritavancin. Chem. Commun. (Camb.) 53, 1420.

Cieslewicz, M.J., Kasper, D.L., Wang, Y., and Wessels, M.R. (2000). Functional analysis in Type Ia Group B *Streptococcus* of a cluster of genes involved in extracellular polysaccharide production by diverse species of *Streptococci*. J. Biol. Chem. 276, 139–146.

Curtis, N.A., Orr, D., Ross, G.W., and Boulton, M.G. (1979). Affinities of penicillins and cephalosporins for the penicillin-binding proteins of *Escherichia coli* K-12 and their antibacterial activity. Antimicrob. Agents Chemother. 16, 533–539.

Czarny, T.L., and Brown, E.D. (2016). A small-molecule screening platform for the discovery of inhibitors of undecaprenyl diphosphate synthase. ACS Infect. Dis. 2, 489–499.

D'Elia, M.A., Henderson, J.A., Beveridge, T.J., Heinrichs, D.E., and Brown, E.D. (2009). The N-acetylmannosamine transferase catalyzes the first committed step of teichoic acid assembly in *Bacillus subtilis* and *Staphylococcus aureus*. J. Bacteriol. 191, 4030–4034.

D'Elia, M.A., Millar, K.E., Beveridge, T.J., and Brown, E.D. (2006a). Wall teichoic acid polymers are dispensable for cell viability in *Bacillus subtilis*. J. Bacteriol. 188, 8313–8316.

D'Elia, M.A., Pereira, M.P., Chung, Y.S., Zhao, W., Chau, A., Kenney, T.J., Sulavik, M.C., Black, T.A., and Brown, E.D. (2006b). Lesions in teichoic acid biosynthesis in *Staphylococcus aureus* lead to a lethal gain of function in the otherwise dispensable pathway. J. Bacteriol. 188, 4183–4189.

De, A., Liao, S., Bitoun, J.P., Roth, R., Beatty, W.L., Wu, H., and Wen, Z.T. (2017). Deficiency of RgpG causes major defects in cell division and biofilm formation, and deficiency of LCP proteins leads to accumulation of cell wall antigens in culture medium by *Streptococcus mutans*. Appl. Environ. Microbiol.

AEM.00928–17.

Dengler, V., Meier, P.S., Heusser, R., Kupferschmied, P., Fazekas, J., Friebe, S., Stauffer, S.B., Majcherczyk, P.A., Moreillon, P., Berger-Bächi, B., and McCallum, N. (2012). Deletion of hypothetical wall teichoic acid ligases in *Staphylococcus aureus* activates the cell wall stress response. *FEMS Microbiol. Lett.* **333**, 109–120.

Dufrisne, M.B., Petrou, V.I., Clarke, O.B., and Mancina, F. (2016). Structural basis for catalysis at the membrane-water interface. *Biochim. Biophys. Acta.* **1862**, 1368-1385.

Eberhardt, A., Hoyland, C.N., Vollmer, D., Bisle, S., Cleverley, R.M., Johnsborg, O., Håvarstein, L.S., Lewis, R.J., and Vollmer, W. (2012). Attachment of capsular polysaccharide to the cell wall in *Streptococcus pneumoniae*. *Microb. Drug Resist.* **18**, 240–255.

Egan, A.J.F., and Vollmer, W. (2012). The physiology of bacterial cell division. *Ann. N. Y. Acad. Sci.* **1277**, 8–28.

Errington, J. (2013). L-form bacteria, cell walls and the origins of life. *Open Biol.* **3**, 120143.

Farha, M.A., Czarny, T.L., Myers, C.L., Worrall, L.J., French, S., Conrady, D.G., Wang, Y., Oldfield, E., Strynadka, N.C.J., and Brown, E.D. (2015). Antagonism screen for inhibitors of bacterial cell wall biogenesis uncovers an inhibitor of undecaprenyl diphosphate synthase. *Proc. Natl. Acad. Sci.* **112**, 11048–11053.

Farha, M.A., Leung, A., Sewell, E.W., D’Elia, M.A., Allison, S.E., Ejim, L., Pereira, P.M., Pinho, M.G., Wright, G.D., and Brown, E.D. (2013). Inhibition of WTA synthesis blocks the cooperative action of PBPs and sensitizes MRSA to β -lactams. *ACS Chem. Biol.* **8**, 226–233.

Foxley, M.A., Wright, S.N., Lam, A.K., Friedline, A.W., Strange, S.J., Xiao, M.T., Moen, E.L., and Rice, C.V. (2017). Targeting wall teichoic acid *in situ* with branched polyethylenimine potentiates β -lactam efficacy against MRSA. *ACS Med. Chem. Lett.* **8**, 1083–1088.

Fuda, C.C.S., Fisher, J.F., and Mobashery, S. (2005). Beta-lactam resistance in *Staphylococcus aureus*: the adaptive resistance of a plastic genome. *Cell. Mol. Life Sci.* **62**, 2617–2633.

Gale, R.T., and Brown, E.D. (2015). New chemical tools to probe cell wall biosynthesis in bacteria. *Curr. Opin. Microbiol.* **27**, 69–77.

- Gale, R.T., Li, F.K.K., Sun, T., Strynadka, N.C.J., and Brown, E.D. (2017). *B. subtilis* LytR-CpsA-Psr enzymes transfer wall teichoic acids from authentic lipid-linked substrates to mature peptidoglycan *in vitro*. *Cell Chem. Biol.* **24**, 1537-1546.
- Gale, R.T., Sewell, E.W., Garrett, T.A., and Brown, E.D. (2014). Reconstituting poly(glycerol phosphate) wall teichoic acid biosynthesis *in vitro* using authentic substrates. *Chem. Sci.* **5**, 3823–3830.
- Ginsberg, C., Zhang, Y.-H., Yuan, Y., and Walker, S. (2006). *In vitro* reconstitution of two essential steps in wall teichoic acid biosynthesis. *ACS Chem. Biol.* **1**, 25–28.
- Grzegorzewicz, A.E., De Sousa-d'Auria, C., McNeil, M.R., Huc-Claustre, E., Jones, V., Petit, C., Angala, S.K., Zemanová, J., Wang, Q., Belardinelli, J.M., Gao, Q., Ishizaki, Y., Mikusova, K., Brennan, P.J., Ronning, D.R., Chami, M., Houssin, C., and Jackson, J.M. (2016). Assembling of the *Mycobacterium tuberculosis* cell wall core. *J. Biol. Chem.* **291**, 18867–18879.
- Harrison, J., Lloyd, G., Joe, M., Lowary, T.L., Reynolds, E., Walters-Morgan, H., Bhatt, A., Lovering, A., Besra, G.S., and Alderwick, L.J. (2016). Lcp1 is a phosphotransferase responsible for ligating arabinogalactan to peptidoglycan in *Mycobacterium tuberculosis*. *mBio.* **7**, e00972–16.
- Harz, H., Burgdorf, K., and Höltje, J.V. (1990). Isolation and separation of the glycan strands from murein of *Escherichia coli* by reversed-phase high-performance liquid chromatography. *Anal Biochem.* **190**, 120–128.
- Hayhurst, E.J., Kailas, L., Hobbs, J.K., and Foster, S.J. (2008). Cell wall peptidoglycan architecture in *Bacillus subtilis*. *Proc. Natl. Acad. Sci. U.S.A.* **105**, 14603–14608.
- Higgins, P.G., Dammhayn, C., Hackel, M., and Seifert, H. (2010). Global spread of carbapenem-resistant *Acinetobacter baumannii*. *J. Antimicrob. Chemother.* **65**, 233–238.
- Holkenbrink, A., Koester, D.C., Kaschel, J., and Werz, D.B. (2011). Total synthesis of α -Linked Rha–Rha–Gal undecaprenyl diphosphate found in *Geobacillus stearothermophilus*. *Eur. J. Org. Chem.* **2011**, 6233–6239.
- Hong, S.J., Kim, S.K., Ko, E.B., Yun, C.-H., and Han, S.H. (2017). Wall teichoic acid is an essential component of *Staphylococcus aureus* for the induction of human dendritic cell maturation. *Mol. Immunol.* **81**, 135–142.

- Höltje, J.V. (1998). Growth of the stress-bearing and shape-maintaining murein sacculus of *Escherichia coli*. *Microbiol. Mol. Biol. Rev.* *62*, 181–203.
- Huang, S.-H., Wu, W.-S., Huang, L.-Y., Huang, W.-F., Fu, W.-C., Chen, P.-T., Fang, J.-M., Cheng, W.-C., Cheng, T.-J.R., and Wong, C.-H. (2013). New continuous fluorometric assay for bacterial transglycosylase using Förster resonance energy transfer. *J. Am. Chem. Soc.* *135*, 17078–17089.
- Hübscher, J., Lüthy, L., Berger-Bächi, B., and Stutzmann Meier, P. (2008). Phylogenetic distribution and membrane topology of the LytR-CpsA-Psr protein family. *BMC Genomics* *9*, 617–16.
- Hübscher, J., McCallum, N., Sifri, C.D., Majcherczyk, P.A., Entenza, J.M., Heusser, R., Berger-Bächi, B., and Stutzmann Meier, P. (2009). MsrR contributes to cell surface characteristics and virulence in *Staphylococcus aureus*. *FEMS Microbiol. Lett.* *295*, 251–260.
- Hyams, C., Camberlein, E., Cohen, J.M., Bax, K., and Brown, J.S. (2010). The *Streptococcus pneumoniae* capsule inhibits complement activity and neutrophil phagocytosis by multiple mechanisms. *Infect. Immun.* *78*, 704–715.
- Karamata, D., Pooley, H.M., and Monod, M. (1987). Expression of heterologous genes for wall teichoic acid in *Bacillus subtilis*. *Mol. Gen. Genet.* *207*, 73–81.
- Kawai, Y., Marles-Wright, J., Cleverley, R.M., Emmins, R., Ishikawa, S., Kuwano, M., Heinz, N., Bui, N.K., Hoyland, C.N., Ogasawara, N., Lewis, R.J., Vollmer, W., Canel, R.A., and Errington, J. (2011). A widespread family of bacterial cell wall assembly proteins. *EMBO J.* *30*, 4931–4941.
- Koch, A.L., and Doyle, R.J. (1985). Inside-to-outside growth and turnover of the wall of gram-positive rods. *J. Theor. Biol.* *117*, 137–157.
- Kojima, N., Araki, Y., and Ito, E. (1983). Structure of linkage region between ribitol teichoic acid and peptidoglycan in cell walls of *Staphylococcus aureus* H. *J. Biol. Chem.* *258*, 9043–9045.
- Kojima, N., Araki, Y., and Ito, E. (1985). Structure of the linkage units between ribitol teichoic acids and peptidoglycan. *J. Bacteriol.* *161*, 299–306.
- Kovács, M., Halfmann, A., Fedtke, I., Heintz, M., Peschel, A., Vollmer, W., Hakenbeck, R., and Brückner, R. (2006). A functional *dlt* operon, encoding proteins required for incorporation of d-Alanine in teichoic acids in Gram-positive bacteria, confers resistance to cationic antimicrobial peptides in *Streptococcus pneumoniae*. *J. Bacteriol.* *188*, 5797–5805.

- Köster, S., Upadhyay, S., Chandra, P., Papavinasasundaram, K., Yang, G., Hassan, A., Grigsby, S.J., Mittal, E., Park, H.S., Jones, V., Hsu, F-F., Jackson, M., Sasseti, C.M., and Philips, J.A. (2017). *Mycobacterium tuberculosis* protected from NADPH oxidase and LC3-associated phagocytosis by the LCP protein CpsA. *Proc. Natl. Acad. Sci.* **374**, 201707792–10.
- Kuk, A.C.Y., Mashalidis, E.H., and Lee, S.-Y. (2017). Crystal structure of the MOP flippase MurJ in an inward-facing conformation. *Nat. Struct. Mol. Biol.* **24**, 171–176.
- Lange, R.P., Locher, H.H., Wyss, P.C., and Then, R.L. (2007). The targets of currently used antibacterial agents: Lessons for drug discovery. *Curr. Pharm. Des.* **13**, 3140-3154.
- Larson, T.R., and Yother, J. (2017). *Streptococcus pneumoniae* capsular polysaccharide is linked to peptidoglycan via a direct glycosidic bond to β -D-N-acetylglucosamine. *Proc. Natl. Acad. Sci. U.S.A.* 201620431.
- Lazarevic, V., and Karamata, D. (1995). The tagGH operon of *Bacillus subtilis* 168 encodes a two-component ABC transporter involved in the metabolism of two wall teichoic acids. *Mol. Microbiol.* **16**, 345–355.
- Lazarevic, V., Abellan, F.-X., Möller, S.B., Karamata, D., and Mauël, C. (2002). Comparison of ribitol and glycerol teichoic acid genes in *Bacillus subtilis* W23 and 168: identical function, similar divergent organization, but different regulation. *Microbiology (Reading, Engl.)* **148**, 815–824.
- Lazarevic, V., Margot, P., Soldo, B., and Karamata, D. (1992). Sequencing and analysis of the *Bacillus subtilis* lytRABC divergon: A regulatory unit encompassing the structural genes of the N-acetylmuramoyl-L-alanine amidase and its modifier. *Microbiology.* **138**, 1949–1961.
- Lebar, M.D., Lupoli, T.J., Tsukamoto, H., May, J.M., Walker, S., and Kahne, D. (2013). Forming cross-linked peptidoglycan from synthetic Gram-negative Lipid II. *J. Am. Chem. Soc.* **135**, 4632–4635.
- Lee, K., Campbell, J., Swoboda, J.G., Cuny, G.D., and Walker, S. (2010). Development of improved inhibitors of wall teichoic acid biosynthesis with potent activity against *Staphylococcus aureus*. *Bioorg. Med. Chem. Lett.* **20**, 1767–1770.
- Lee, S.H., Wang, H., Labroli, M., Koseoglu, S., Zuck, P., Mayhood, T., Gill, C., Mann, P., Sher, X., Ha, S., Yang, S.W., Mandal, M., Yang, C., Liang, L., Tan, Z.,

Tawa, P., Hou, Y., Kuvelkar, R., DeVito, K., Wen, X., Xiao, J., Batchlett, M., Balibar, C.J., Liu, J., Xiao, J., Murgolo, N., Garlisi, C.G., Sheth, P.R., Flattery, A., Su, J., Tan, C., and Roemer, T. (2016). TarO-specific inhibitors of wall teichoic acid biosynthesis restore β -lactam efficacy against methicillin-resistant staphylococci. *Sci. Transl. Med.* **8**, 329ra32.

Lewis, K. (2017). New approaches to antimicrobial discovery. *Biochem. Pharmacol.* **134**, 87–98.

Li, L., Woodward, R.L., Han, W., Qu, J., Song, J., Ma, C., and Wang, P.G. (2016). Chemoenzymatic synthesis of the bacterial polysaccharide repeating unit undecaprenyl pyrophosphate and its analogs. *Nat. Protoc.* **11**, 1280–1298.

Li, L., Woodward, R., Ding, Y., Liu, X.-W., Yi, W., Bhatt, V.S., Chen, M., Zhang, L.-W., and Wang, P.G. (2010). Overexpression and topology of bacterial oligosaccharyltransferase PglB. *Biochem. Biophys. Res. Commun.* **394**, 1069–1074.

Ligozzi, M., Pittaluga, F., and Fontana, R. (1993). Identification of a genetic element (psr) which negatively controls expression of *Enterococcus hirae* penicillin-binding protein 5. *J. Bacteriol.* **175**, 2046–2051.

Ling, L.L., Schneider, T., Peoples, A.J., Spoering, A.L., Engels, I., Conlon, B.P., Mueller, A., Schäberle, T.F., Hughes, D.E., Epstein, S., Jones, M., Lazarides, L., Steadman, V.A., Cohen, D.R., Felix, C.R., Fetterman, K.A., Millett, W.P., Nitti, A.G., Zullo, A.M., Chen, C., and Lewis, K. (2015). A new antibiotic kills pathogens without detectable resistance. *Nature.* **517**, 455–459.

Liszewski Zilla, M., Lunderberg, J.M., Schneewind, O., and Missiakas, D. (2015). *Bacillus anthracis* lcp genes support vegetative growth, envelope assembly, and spore formation. *J. Bacteriol.* **197**, 3731–3741.

Luepke, K.H., Suda, K.J., Boucher, H., Russo, R.L., Bonney, M.W., Hunt, T.D., and Mohr, J.F. (2017). Past, present, and future of antibacterial economics: Increasing bacterial resistance, limited antibiotic pipeline, and societal implications. *Pharmacotherapy.* **37**, 71–84.

Maadani, A., Fox, K.A., Mylonakis, E., and Garsin, D.A. (2007). *Enterococcus faecalis* mutations affecting virulence in the *Caenorhabditis elegans* model host. *Infect. Immun.* **75**, 2634–2637.

Maréchal, M., Amoroso, A., Morlot, C., Vernet, T., Coyette, J., and Joris, B. (2016). *Enterococcus hirae* LcpA (Psr), a new peptidoglycan-binding protein

localized at the division site. *BMC Microbiol.* **16**, 239.

Matano, L.M., Morris, H.G., Hesser, A.R., Martin, S.E.S., Lee, W., Owens, T.W., Laney, E., Nakaminami, H., Hooper, D., Meredith, T.C., Walker, S. (2017). Antibiotic that inhibits the ATPase activity of an ATP-binding cassette transporter by binding to a remote extracellular site. *J. Am. Chem. Soc.* **139**, 10597–10600.

Meeske, A.J., Sham, L.-T., Kimsey, H., Koo, B.-M., Gross, C.A., Bernhardt, T.G., and Rudner, D.Z. (2015). MurJ and a novel lipid II flippase are required for cell wall biogenesis in *Bacillus subtilis*. *Proc. Natl. Acad. Sci. U.S.A.* **112**, 6437–6442.

Moynihan, P.J., and Clarke, A.J. (2011). O-Acetylated peptidoglycan: controlling the activity of bacterial autolysins and lytic enzymes of innate immune systems. *Int. J. Biochem. Cell Biol.* **43**, 1655–1659.

Moynihan, P.J., Sychantha, D., and Clarke, A.J. (2014). Chemical biology of peptidoglycan acetylation and deacetylation. *Bioorg. Chem.* **54**, 44–50.

Munch, D., Muller, A., Schneider, T., Kohl, B., Wenzel, M., Bandow, J.E., Maffioli, S., Sosio, M., Donadio, S., Wimmer, R., and Sahl, H.-G. (2014). The lantibiotic NAI-107 binds to bactoprenol-bound cell wall precursors and impairs membrane functions. *J. Biol. Chem.* **289**, 12063–12076.

Musumeci, M.A., Hug, I., Scott, N.E., Ielmini, M.V., Foster, L.J., Wang, P.G., and Feldman, M.F. (2013). *In vitro* activity of *Neisseria meningitidis* PglL O-oligosaccharyltransferase with diverse synthetic lipid donors and a UDP-activated sugar. *J. Biol. Chem.* **288**, 10578–10587.

Müller, A., Klöckner, A., and Schneider, T. (2017). Targeting a cell wall biosynthesis hot spot. *Nat. Prod. Rep.* **34**, 909–932.

Müller, A., Ulm, H., Reder-Christ, K., Sahl, H.-G., and Schneider, T. (2012). Interaction of Type A lantibiotics with undecaprenol-bound cell envelope precursors. *Microb. Drug Resist.* **18**, 261–270.

Münch, D., Engels, I., Müller, A., Reder-Christ, K., Falkenstein-Paul, H., Bierbaum, G., Grein, F., Bendas, G., Sahl, H.-G., and Schneider, T. (2015). Structural variations of the cell wall precursor Lipid II and their influence on binding and activity of the lipoglycopeptide antibiotic Oritavancin. *Antimicrob. Agents Chemother.* **59**, 772–781.

Myers, C.L., Li, F.K.K., Koo, B.-M., El-Halfawy, O.M., French, S., Gross, C.A., Strynadka, N.C.J., and Brown, E.D. (2016). Identification of two phosphate starvation-induced wall teichoic acid hydrolases provides first insights into the

degradative pathway of a key bacterial cell wall component. *J. Biol. Chem.* **291**, 26066–26082.

Navarre, W.W., and Schneewind, O. (1999). Surface proteins of Gram-positive bacteria and mechanisms of their targeting to the cell wall envelope. *Microbiol. Mol. Biol. Rev.* **63**, 174–229.

Neuhaus, F.C., and Baddiley, J. (2003). A continuum of anionic charge: Structures and functions of d-Alanyl-teichoic acids in Gram-positive bacteria. *Microbiol. Mol. Biol. Rev.* **67**, 686–723.

Over, B., Heusser, R., McCallum, N., Schulthess, B., Kupferschmied, P., Gaiani, J.M., Sifri, C.D., Berger-Bächi, B., and Meier, P.S. (2011). LytR-CpsA-Psr proteins in *Staphylococcus aureus* display partial functional redundancy and the deletion of all three severely impairs septum placement and cell separation. *FEMS Microbiol. Lett.* **320**, 142–151.

Pasquina, L.W., Maria, J.P.S., and Walker, S. (2013). Teichoic acid biosynthesis as an antibiotic target. *Curr. Opin. Microbiol.* **16**, 531–537.

Payne, D.J., Gwynn, M.N., Holmes, D.J., and Pompliano, D.L. (2007). Drugs for bad bugs: confronting the challenges of antibacterial discovery. *Nat. Rev. Drug Discov.* **6**, 29–40.

Pereira, M.P., D’Elia, M.A., Troczynska, J., and Brown, E.D. (2008). Duplication of teichoic acid biosynthetic genes in *Staphylococcus aureus* leads to functionally redundant poly(ribitol phosphate) polymerases. *J. Bacteriol.* **190**, 5642–5649.

Pereira, M.P., Schertzer, J.W., D’Elia, M.A., Koteva, K.P., Hughes, D.W., Wright, G.D., and Brown, E.D. (2008). The wall teichoic acid polymerase TagF efficiently synthesizes poly(glycerol phosphate) on the TagB product Lipid III. *Chembiochem.* **9**, 1385–1390.

The Pew Charitable Trusts (2016). A scientific roadmap for antibiotic discovery. <http://www.pewtrusts.org/~media/assets/2016/06/ascientificroadmapforantibioticdiscoveryjune2016.pdf>

The Pew Charitable Trusts (2017). Antibiotics currently in clinical development. <http://www.pewtrusts.org/~media/assets/2017/05/antibiotics-currently-in-clinical-development-03-2017.pdf>

Pieters, J. (2008). *Mycobacterium tuberculosis* and the macrophage: Maintaining a balance. *Cell Host Microbe.* **3**, 399–407.

Projan, S.J. (2002). New (and not so new) antibacterial targets – from where and when will the novel drugs come? *Curr. Opin.Pharmacol.* 2, 513-522.

Public Health Agency of Canada (2014). Antimicrobial resistance and use in Canada. A federal framework for action. HP40-126/2014E-PDF

Public Health Agency of Canada (2015). Federal action plan on antimicrobial resistance and use in Canada. HP40-141/2015E-PDF

Qiao, Y., Lebar, M.D., Schirner, K., Schaefer, K., Tsukamoto, H., Kahne, D., and Walker, S. (2014). Detection of lipid-linked peptidoglycan precursors by exploiting an unexpected transpeptidase reaction. *J. Am. Chem. Soc.* 136, 14678–14681.

Rajagopal, M., and Walker, S. (2015). Envelope structures of Gram-positive bacteria. *Curr. Top. Microbiol. Immunol.* 404, 1–44.

Rossi, J., Bischoff, M., Wada, A., and Berger-Bächi, B. (2003). MsrR, a putative cell envelope-associated element involved in *Staphylococcus aureus* sarA attenuation. *Antimicrob. Agents Chemother.* 47, 2558–2564.

Rowe, H.M., Hanson, B.R., Runft, D.L., Lin, Q., Firestine, S.M., and Neely, M.N. (2015). Modification of the CpsA protein reveals a role in alteration of the *Streptococcus agalactiae* cell envelope. *Infect. Immun.* 83, 1497–1506.

Schäffer, C., and Messner, P. (2005). The structure of secondary cell wall polymers: how Gram-positive bacteria stick their cell walls together. *Microbiology (Reading, Engl.)* 151, 643–651.

Schertzer, J.W., and Brown, E.D. (2003). Purified, recombinant TagF protein from *Bacillus subtilis* 168 catalyzes the polymerization of glycerol phosphate onto a membrane acceptor in vitro. *J. Biol. Chem.* 278, 18002–18007.

Schlag, M., Biswas, R., Krismer, B., Kohler, T., Zoll, S., Yu, W., Schwarz, H., Peschel, A., and Götz, F. (2010). Role of staphylococcal wall teichoic acid in targeting the major autolysin Atl. *Mol. Microbiol.* 75, 864–873.

Schneider, T., Senn, M.M., Berger-Bächi, B., Tossi, A., Sahl, H.-G., and Wiedemann, I. (2004). *In vitro* assembly of a complete, pentaglycine interpeptide bridge containing cell wall precursor (lipid II-Gly5) of *Staphylococcus aureus*. *Mol. Microbiol.* 53, 675–685.

Schwartz, B., Markwalder, J.A., and Wang, Y. (2001). Lipid II: Total synthesis of the bacterial cell wall precursor and utilization as a substrate for glycosyltransfer

and transpeptidation by penicillin binding protein (PBP) 1b of *Eschericia coli*. J. Am. Chem. Soc. 123, 11638–11643.

Sewell, E.W.C., Pereira, M.P., and Brown, E.D. (2009). The wall teichoic acid polymerase TagF is non-processive *in vitro* and amenable to study using steady state kinetic analysis. J. Biol. Chem. 284, 21132–21138.

Sewell, E.W., and Brown, E.D. (2013). Taking aim at wall teichoic acid synthesis: new biology and new leads for antibiotics. J. Antibiot. (Tokyo). 67, 43–51.

Sham, L.-T., Butler, E.K., Lebar, M.D., Kahne, D., Bernhardt, T.G., and Ruiz, N. (2014). MurJ is the flippase of lipid-linked precursors for peptidoglycan biogenesis. Science. 345, 220–222.

Sigle, S., Steblau, N., Wohleben, W., and Muth, G. (2016). Polydiglycosylphosphate transferase PdtA (SCO2578) of *Streptomyces coelicolor* A3(2) is crucial for proper sporulation and apical tip extension under stress conditions. Appl. Environ. Microbiol. 82, 5661–5672.

Silhavy, T.J., Kahne, D., and Walker, S. (2010). The bacterial cell envelope. Cold Spring Harb. Perspect. Biol. 2, a000414.

Silver, L.L. (2007). Multi-targeting by monotherapeutic antibacterials. Nat. Rev. Drug Discov. 6, 41–55.

Silver, L.L. (2012). Viable screening targets related to the bacterial cell wall. Ann. N. Y. Acad. Sci. 1277, 29–53.

Silver, L.L. (2016). Appropriate targets for antibacterial drugs. Cold Spring Harb. Perspect. Med. 6, a030239–8.

Silver, L.L. (2017). The antibiotic future. (Berlin, Heidelberg: Springer Berlin Heidelberg), pp. 589–37.

Singh, M., Chang, J., Coffman, L., and Kim, S.J. (2017). Hidden mode of action of glycopeptide antibiotics: Inhibition of wall teichoic acid biosynthesis. J. Phys. Chem. B. 121, 3925–3932.

Singh, S.B., Young, K., and Silver, L.L. (2017). What is an “ideal” antibiotic? Discovery challenges and path forward. Biochem. Pharmacol. 133, 63–73.

Soldo, B., Lazarevic, V., and Karamata, D. (2002). tagO is involved in the synthesis of all anionic cell-wall polymers in *Bacillus subtilis* 168. Microbiology 148, 2079–2087.

Spellberg, B. (2014). The future of antibiotics. *Critical Care*. 18, 228.

Sutterlin, H.A., Malinverni, J.C., Lee, S.H., Balibar, C.J., and Roemer, T. (2017). Antibacterial new target discovery: Sentinel examples, strategies, and surveying success. In: *Topics in Medicinal Chemistry*. Springer, Berlin, Heidelberg. pp. 1–29.

Swoboda, J.G., Meredith, T.C., Campbell, J., Brown, S., Suzuki, T., Bollenbach, T., Malhowski, A.J., Kishony, R., Gilmore, M.S., and Walker, S. (2009). Discovery of a small molecule that blocks wall teichoic acid biosynthesis in *Staphylococcus aureus*. *ACS Chem. Biol.* 4, 875–883.

Tommasi, R., Brown, D.G., Walkup, G.K., Manchester, J.I., and Miller, A.A. (2015). ESKAPEing the labyrinth of antibacterial discovery. *Nat. Rev. Drug Discov.* 14, 529-542.

Turner, R.D., Vollmer, W., and Foster, S.J. (2014). Different walls for rods and balls: the diversity of peptidoglycan. *Mol. Microbiol.* 91, 862–874.

Ulm, H., and Schneider, T. (2016). Targeting bactoprenol-coupled cell envelope precursors. *Appl. Microbiol. Biotechnol.* 100, 7815-7825.

Umbreit, J.N., and Strominger, J.L. (1973). d-Alanine carboxypeptidase from *Bacillus subtilis* membranes I. Purification and characterization. *J. Biol. Chem.* 248, 6759–6766.

Unemo, M., and Nicholas, R.A. (2012). Emergence of multidrug-resistant, extensively drug-resistant and untreatable gonorrhea. *Future Microbiol.* 7, 1401–1422.

Van Boeckel, T.P., Gandra, S., Ashok, A., Caudron, Q., Grenfell, B.T., Levin, S.A., and Laxminarayan, R. (2014). Global antibiotic consumption 2000 to 2010: an analysis of national pharmaceutical sales data. *Lancet Infect. Dis.* 14, 742–750.

van Heijenoort, Y., Gómez, M., Derrien, M., Ayala, J., and van Heijenoort, J. (1992). Membrane intermediates in the peptidoglycan metabolism of *Escherichia coli*: possible roles of PBP 1b and PBP 3. *J. Bacteriol.* 174, 3549–3557.

VanNieuwenhze, M.S., Mauldin, S.C., Zia-Ebrahimi, M., Aikins, J.A., and Blaszcak, L.C. (2001). The total synthesis of Lipid I. *J. Am. Chem. Soc.* 123, 6983–6988.

VanNieuwenhze, M.S., Mauldin, S.C., Zia-Ebrahimi, M., Winger, B.E., Hornback,

- W.J., Saha, S.L., Aikins, J.A., and Blaszczyk, L.C. (2002). The First Total Synthesis of Lipid II: The final monomeric intermediate in bacterial cell wall biosynthesis. *J. Am. Chem. Soc.* *124*, 3656–3660.
- Vollmer, W., Blanot, D., and de Pedro, M.A. (2008). Peptidoglycan structure and architecture. *FEMS Microbiol. Rev.* *32*, 149–167.
- Wang, H., Gill, C.J., Lee, S.H., Mann, P., Zuck, P., Meredith, T.C., Murgolo, N., She, X., Kales, S., Liang, L., Liu, L., Wu, J., Santa Maria, J., Su, J., Pan, J., Hailey, J., McGuinness, D., Tan, C.M., Flattery, A., Walker, S., Black, T., and Roemer, T. (2013). Discovery of wall teichoic acid inhibitors as potential anti-MRSA β -lactam combination agents. *Chem. Biol.* *20*, 272–284.
- Wang, Q., Zhu, L., Jones, V., Wang, C., Hua, Y., Shi, X., Feng, X., Jackson, M., Niu, C., and Gao, Q. (2015). CpsA, a LytR-CpsA-Psr family protein in *Mycobacterium marinum*, is required for cell wall integrity and virulence. *Infect. Immun.* *83*, 2844–2854.
- Wanner, S., Schade, J., Keinhörster, D., Weller, N., George, S.E., Kull, L., Bauer, J., Grau, T., Winstel, V., Stoy, H., Kretschmer, D., Kolata, J., Wolz, C., Bröker, B.M. and Weidenmaier, C. (2017). Wall teichoic acids mediate increased virulence in *Staphylococcus aureus*. *Nat. Microbiol.* *2*, 16257.
- Ward, J.B. (1981). Teichoic and teichuronic acids: biosynthesis, assembly, and location. *Microbiol. Rev.* *45*, 211–243.
- Weerapana, E., Glover, K.J., Chen, M.M., and Imperiali, B. (2005). Investigating Bacterial N-linked glycosylation: Synthesis and glycosyl acceptor activity of the undecaprenyl pyrophosphate-linked bacillosamine. *J. Am. Chem. Soc.* *127*, 13766–13767.
- Weidenmaier, C., Kokai-Kun, J.F., Kristian, S.A., Chanturiya, T., Kalbacher, H., Gross, M., Nicholson, G., Neumeister, B., Mond, J.J., and Peschel, A. (2004). Role of teichoic acids in *Staphylococcus aureus* nasal colonization, a major risk factor in nosocomial infections. *Nature Medicine* *10*, 243–245.
- Wen, Z.T., Baker, H.V., and Burne, R.A. (2006). Influence of BrpA on critical virulence attributes of *Streptococcus mutans*. *J. Bacteriol.* *188*, 2983–2992.
- Winstel, V., Kühner, P., Salomon, F., Larsen, J., Skov, R., Hoffmann, W., Peschel, A., and Weidenmaier, C. (2015). Wall teichoic acid glycosylation governs *Staphylococcus aureus* nasal colonization. *MBio* *6*, e00632.
- Woodward, R., Yi, W., Li, L., Zhao, G., Eguchi, H., Sridhar, P.R., Guo, H., Song,

J.K., Motari, E., Cai, L., Kelleher, P., Liu, X., Han, W., Zhang, W., Ding, Y., Li, M., and Wang, P.G. (2010). *In vitro* bacterial polysaccharide biosynthesis: defining the functions of Wzy and Wzz. *Nat. Chem. Biol.* 6, 418–423.

World Health Organization (2017a). Prioritization of pathogens to guide discovery, research and development of new antibiotics for drug resistant bacterial infections, including tuberculosis. WHO/EMP/IAU/2017.12

World Health Organization (2017b). Antibacterial agents in clinical development: an analysis of the antibacterial clinical development pipeline, including tuberculosis. WHO/EMP/IAU/2017.11

Wu, C., Huang, I.-H., Chang, C., Reardon-Robinson, M.E., Das, A., and Ton-That, H. (2014). Lethality of sortase depletion in *Actinomyces oris* caused by excessive membrane accumulation of a surface glycoprotein. *Mol. Microbiol.* 94, 1227–1241.

Xu, H., Wang, L., Huang, J., Zhang, Y., Ma, F., Wang, J., Xu, W., Zhang, X., Yin, Y., and Wu, K. (2015). Pneumococcal wall teichoic acid is required for the pathogenesis of *Streptococcus pneumoniae* in murine models. *J. Microbiol.* 53, 147–154.

Ye, X.-Y., Lo, M.-C., Brunner, L., Walker, D., Kahne, D., and Walker, S. (2001). Better substrates for bacterial transglycosylases. *J. Am. Chem. Soc.* 123, 3155–3156.

Zhang, Y.-H., Ginsberg, C., Yuan, Y., and Walker, S. (2006). Acceptor substrate selectivity and kinetic mechanism of *Bacillus subtilis* TagA. *Biochemistry* 45, 10895–10904.

Zilla, M.L., Chan, Y.G.Y., Lunderberg, J.M., Schneewind, O., and Missiakas, D. (2015). LytR-CpsA-Psr enzymes as determinants of *Bacillus anthracis* secondary cell wall polysaccharide assembly. *J. Bacteriol.* 197, 343–353.

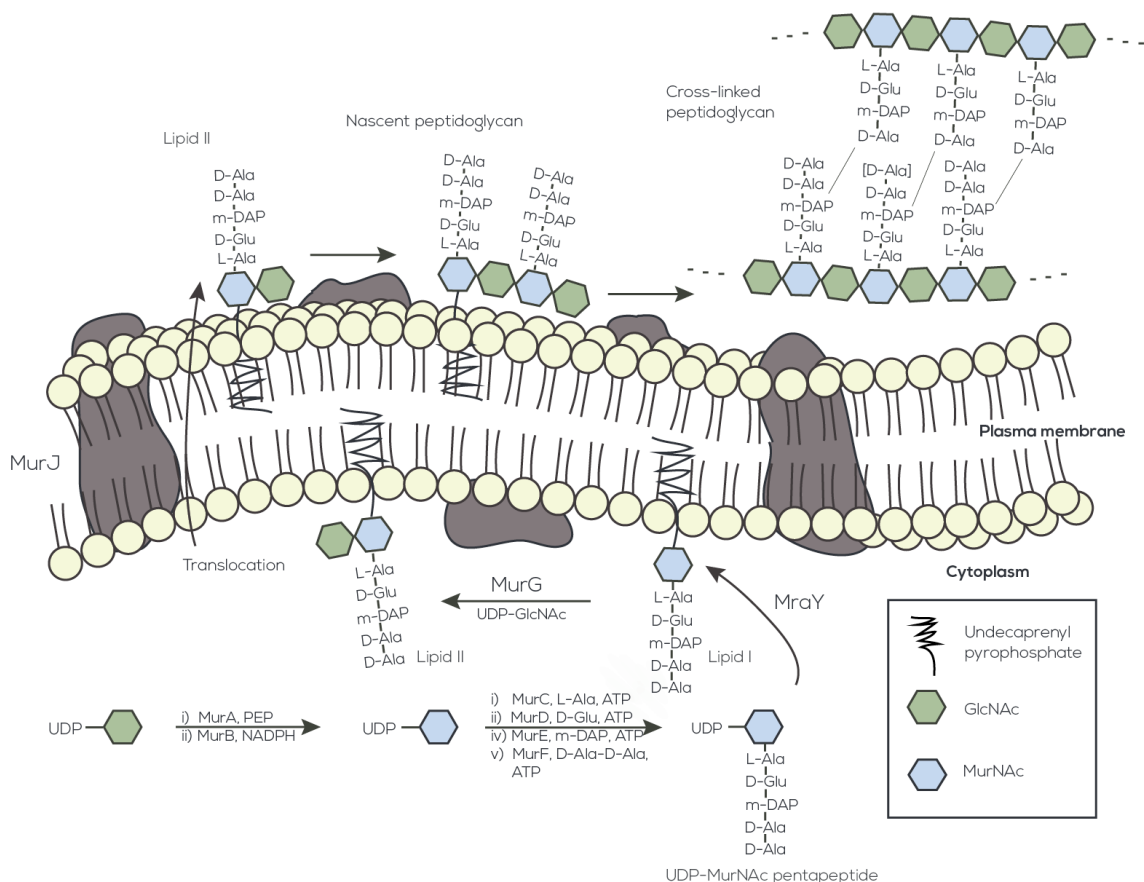


Figure 1. *B. subtilis* peptidoglycan biosynthesis. The pathway begins with the cytoplasmic generation of UDP-MurNac pentapeptide from precursor UDP-GlcNAc. MurA modifies UDP-GlcNAc by addition of an enolpyruvyl residue onto the C(3) hydroxyl moiety of GlcNAc. The NADPH-dependent enolpyruvyl reductase MurB reduces the resulting molecule to yield UDP-MurNac. ATP-dependent amino acid ligases (MurC-MurF) incorporate the stem peptide side chain on the lactate handle of UDP-MurNac to produce UDP-MurNac pentapeptide (Barreteau et al., 2008). MraY mediates a pyrophosphate exchange reaction that couples the MurNac pentapeptide moiety of this molecule to a membrane-embedded (C₅₅-P) undecaprenyl phosphate lipid carrier, yielding Lipid I. MurG transforms Lipid I to Lipid II via the addition of GlcNAc to the C(4) hydroxyl group of MurNac (Bouhss et al., 2008). MurJ translocates this intermediate to the extracellular leaflet of the cytoplasmic membrane (Kuk et al., 2017; Meeske et al., 2015; Sham et al., 2014). Penicillin-binding proteins (PBPs) polymerize, cross-link, and process Lipid II intermediates and derivatives thereof using transglycosylase, transpeptidase, and carboxypeptidase activities (Egan and Vollmer, 2012; Umbreit and Strominger, 1973; Vollmer et al., 2008). The remaining undecaprenyl diphosphate lipid carrier is de-phosphorylated and shuttled back into the cell to recycle precious undecaprenyl phosphate material (Bernard et al., 2005).

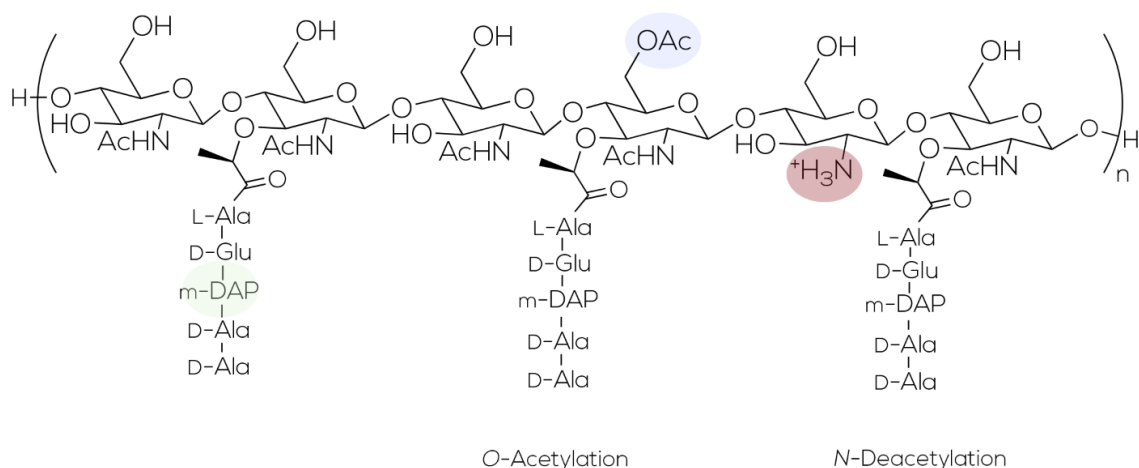


Figure 2. *B. subtilis* peptidoglycan structure and chemical diversity. Almost all bacteria synthesize peptidoglycan chains composed of GlcNAc-MurNAc disaccharides. The lactyl group of MurNAc contains the stem pentapeptide. Most Gram-positive bacteria contain L-Lysine at position 3 within the stem-peptide. *B. subtilis*, like almost all Gram-negative bacteria, contains meso-diaminopimelic acid at this position (green). Most cross-links occur between residues/substituents at position three of one peptide and position four of another (Vollmer and Bertsche, 2008). Enzyme-mediated reactions modify peptidoglycan through N-deacetylation at the C(2) position of GlcNAc (red) and O-acetylation at the C(6) hydroxyl group of MurNAc (blue) (Moynihan et al., 2014). The C(6) hydroxyl group of MurNAc is also the point of attachment for WTAs (see also Figure 3). Adapted from Rajagopal and Walker, 2015.

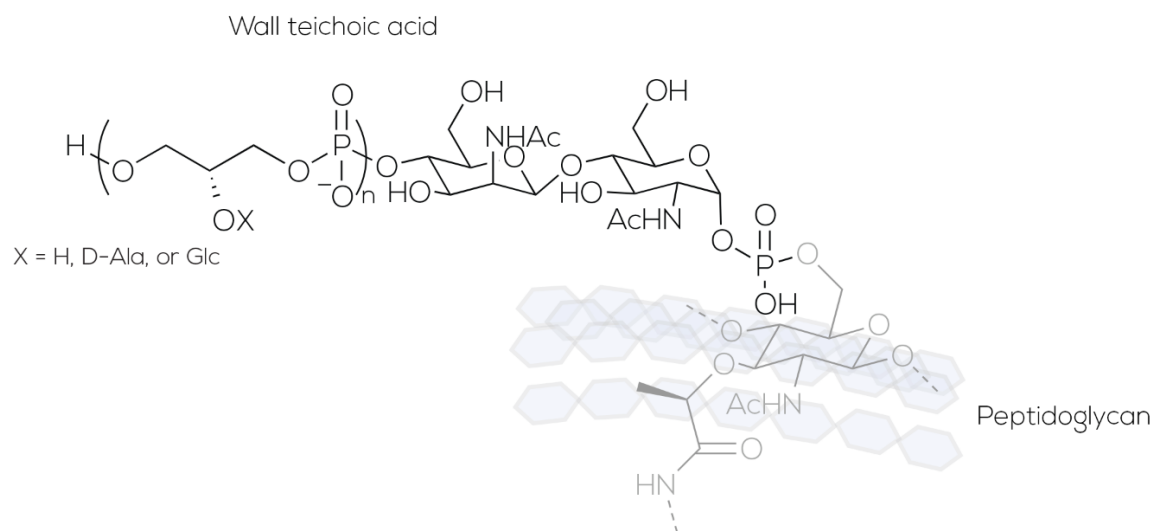


Figure 3. *B. subtilis* 168 wall teichoic acid structure. Phosphodiester bonds anchor poly(glycerol phosphate) WTAs of *B. subtilis* to the C(6) hydroxyl group of peptidoglycan *N*-acetylmuramic acid.

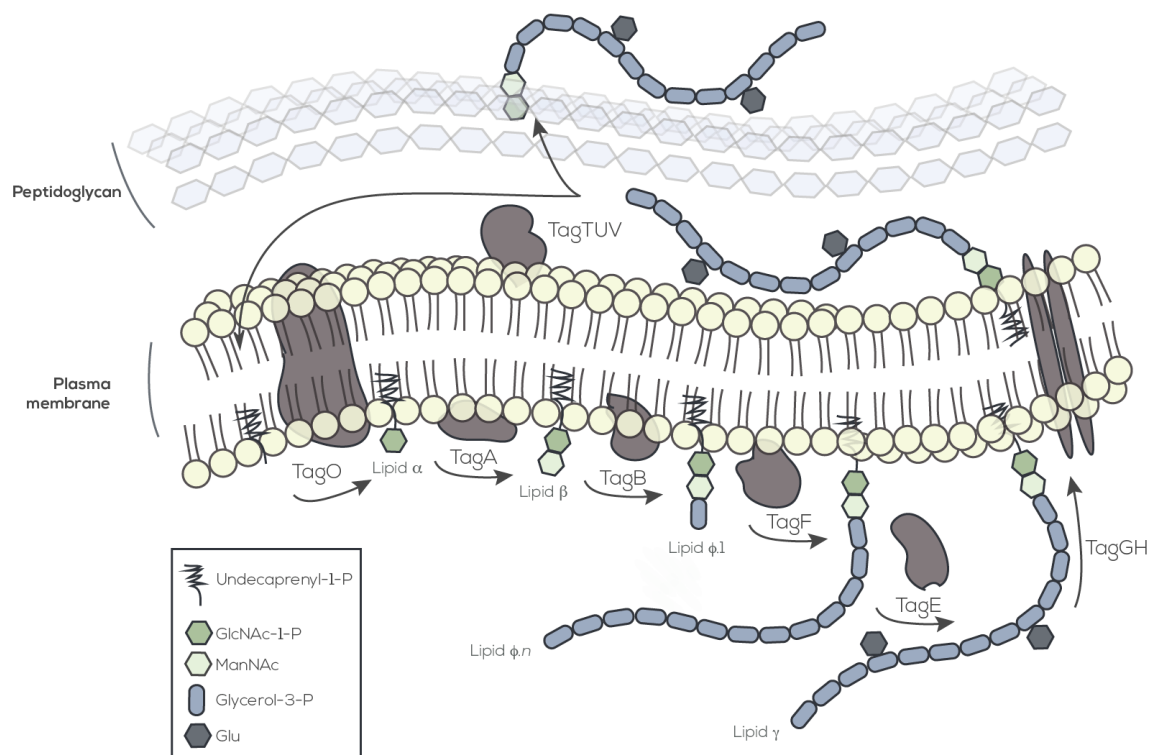


Figure 4. *B. subtilis* 168 wall teichoic acid biosynthesis. (Re-stated from thesis text) The first step of this pathway involves the transfer of *N*-acetylglucosamine-1-phosphate to the undecaprenyl phosphate lipid carrier in a reaction catalyzed by the transmembrane protein TagO, producing intermediate Lipid α. Lipid α is also an intermediate in the biosynthesis of minor teichoic acids poly(glycosyl *N*-acetylgalactosamine-1-phosphate) and teichuronic acids poly(glucuronyl *N*-acetylgalactosamine) (Soldo et al., 2002). TagA catalyzes the first committed step of the pathway with the addition of *N*-acetylmannosamine to the C(4) hydroxyl group of the Lipid α GlcNAc moiety to yield Lipid β (D'Elia et al., 2009). TagB catalyzes the incorporation of a single *sn*-glycerol-3-phosphate residue to the lipid-linked disaccharide to form Lipid φ.1 (Bhavsar et al., 2005). TagF then polymerizes roughly 50 glycerol-3-phosphate monomers on Lipid φ.1 (Pereira et al., 2008; Schertzer and Brown, 2003). TagE modifies these polymers with α-linked glucose residues, generating Lipid γ. The ABC transporter TagGH transports Lipid γ to the extracellular leaflet of the plasma membrane (Allison et al., 2011; Lazarevic and Karamata, 1995). Uncharacterized enzymes likely modify these lipid-linked glycopolymers with D-alanyl substituents (Kovács et al., 2006). The recently characterized TagTUV enzymes (Gale et al., 2017) transfer WTAs from their lipid anchors to the C(6) hydroxyl group of peptidoglycan *N*-acetylmuramic acid – as demonstrated in Chapter 3.

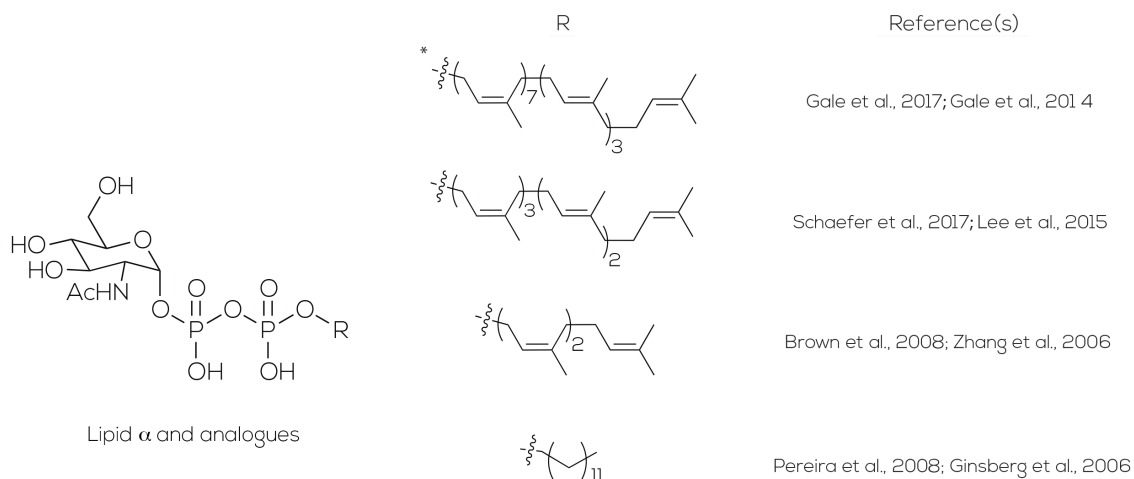


Figure 5. Structure of the wall teichoic acid biosynthetic intermediate Lipid α and analogs thereof. The chemical composition of lipid α is GlcNAc-1-P-P-Und. An asterisk indicates the authentic undecaprenyl-linked Lipid α molecule. The last two analogs have been used for the last decade as more soluble solutions to authentic substrates in biochemical assays of WTA glycosyltransferases. Shown are references detailing the preparation of Lipid α and its analogues.

**CHAPTER II – Reconstituting poly(glycerol phosphate) wall teichoic acid
biosynthesis *in vitro* using authentic substrates**

Preface

The work presented in this chapter was previously published in:

Gale, R.T., Sewell, E.W., Garrett, T.A., and Brown, E.D. (2014). Reconstituting poly(glycerol phosphate) wall teichoic acid biosynthesis *in vitro* using authentic substrates. Chem. Sci. 5, 3823–3830.

Permission has been granted by the publisher to reproduce the material herein.

I performed all experiments with the exception of mass spectrometry, which was conducted by Garrett, T.A. Sewell E.W. assisted with the preparation of undecaprenyl-phosphate. I wrote and edited the manuscript with input from all authors.

Summary

Wall teichoic acids (WTAs) are phosphate-rich anionic polymers that constitute a substantial portion of the Gram-positive cell wall. Recent work has demonstrated the importance of WTAs in cell shape, virulence, and antibiotic resistance. These findings highlight WTA biosynthetic enzymes as attractive targets for novel antimicrobial agents. Due to challenges involved in the isolation of natural substrates, *in vitro* studies of the recombinant enzymes have largely employed soluble substrate analogues. Herein we present a semisynthetic approach to obtain the authentic precursor for WTA biosynthesis, Lipid α , complete with its polyisoprenoid lipid moiety. We show that this material can be used to reconstitute the activities of four enzymes involved in poly(glycerol phosphate) WTA biosynthesis in a detergent micelle. This work enables the creation of chemically defined and realistic systems for the study of interfacial catalysis by WTA biosynthetic machinery, which could aid efforts to discover and develop novel agents against WTA biosynthesis.

Introduction

The bacterial cell wall has been targeted with spectacular success in the development of antibiotics. Indeed, β -lactams and glycopeptides that inhibit cell wall biosynthesis are the most widely used chemotherapeutic agents to treat bacterial infections (Koch, 2003). Nevertheless, increasing resistance to these agents is a serious threat to their continued use and to public health (Boucher et al., 2009). Thus, the search is on for new agents of unique chemical class that are unsusceptible to existing resistance mechanisms and are effective perturbants of this celebrated and well-validated target.

In addition to peptidoglycan, the Gram-positive bacterial cell wall is largely composed of long, phosphate-rich, anionic polymers called wall teichoic acids

(WTAs) (Burger and Glaser, 1964). These polymers are typically comprised of repeating polyol phosphate residues modified with D-alanyl and glycosyl substituents (Neuhaus and Baddiley, 2003). WTAs have emerged as attractive antibacterial targets (Sewell and Brown, 2013) due to their important roles in cell shape determination (D'Elia et al., 2006), virulence (Atilano et al., 2011; Weidenmaier et al., 2004) and antibiotic resistance (Brown et al., 2012; Farha et al., 2013). While studies of the genetics and physiology of WTA biosynthesis have provided strong validation for this biosynthetic pathway as a target for new antibiotics, a lack of tools and understanding of the biochemistry of WTA synthesis remains an obstacle to its effective utility in modern antibiotic drug discovery.

Despite ready access to recombinant enzymes involved in WTA biosynthesis, challenges in the isolation of natural substrates from bacterial sources have hindered detailed studies. Efforts to date have involved the synthesis of soluble analogues of the substrates to study WTA biosynthesis *in vitro* (Ginsberg et al., 2006; Pereira et al., 2008; Sewell and Brown, 2013; Zhang et al., 2006). These soluble analogues substitute a short aliphatic or prenyl chain for the C₅₅ undecaprenyl moiety of the authentic precursor glycolipid, GlcNAc-PP-undecaprenol. These analogues provided ready access to pure substrates for the functional characterization of several WTA biosynthetic enzymes (Allison et al., 2011; Ginsberg et al., 2006; Pereira et al., 2008; Sewell et al., 2009; Zhang et al., 2006), and have largely underpinned our current understanding of the biosynthetic pathway. These soluble analogues, however, fail to recapitulate the interfacial nature of catalysis of WTA glycolipids. Indeed, the many glycosyltransferase enzymes and the flippase transporter involved in WTA synthesis are membrane-bound and thus the membrane interface is central to synthesis and assembly of WTA (Sewell and Brown, 2013).

Here we present a semisynthetic strategy to obtain the authentic WTA glycolipid precursor GlcNAc-PP-undecaprenol, also known as Lipid α (Table 1 outlines the nomenclature for WTA intermediates). Further we show that this molecule, in a detergent micelle, is a capable substrate for the activities of four consecutive recombinant enzymes - TagA, the ManNAc transferase, TagB, the poly(glycerol phosphate) primase, TagF, the poly(glycerol phosphate) polymerase and TagE, the poly(glycerol phosphate) glucosyltransferase - in the synthesis of poly(glycerol phosphate) WTA *in vitro*. This work provides an important new avenue for the characterization of WTA enzymes at interfaces using authentic and chemically defined substrates.

Results and discussion

Semisynthetic preparation of Lipid α

WTA biosynthesis utilizes undecaprenyl phosphate (**4**) as a lipid carrier to build glycosyl intermediates (**Figure 1** details the biosynthetic pathway). This lipid carrier is essential for the transport of oligosaccharides across the bacterial membrane during synthesis of many other important polysaccharides including lipopolysaccharides (Trent, 2001), peptidoglycans (Bouhss et al., 2008) and capsular polysaccharides (Masson and Holbein, 1985). Undecaprenyl phosphate (**4**) was required in quantity for use in chemical transformations to generate Lipid α (**5**) and, while this molecule is commercially available, its cost is prohibitive for purchase in useful quantities. It can be obtained from bacterial sources, however, it represents a relatively minor species relative to other membrane lipids (Barreteau et al., 2009) and thus it is challenging to isolate and purify. Compound **4** is also available through total synthesis. But, the methodology involves a cumbersome multistep procedure (Lee et al., 2009). Thus, we elected to obtain undecaprenyl phosphate (**4**) through a semisynthetic approach, whereby the precursor undecaprenol (**3**) was obtained from a plant source,

namely from *Laurus nobilis* leaves (bay leaves), according to published methodology (Breukink et al., 2003). Subsequent phosphorylation of the polyprenol was achieved with tetra-*n*-butylammonium dihydrogen phosphate and trichloroacetonitrile according to published methods (Danilov et al., 1989), to afford undecaprenyl phosphate (**4**) in 40% yield over the phosphorylation step.

Lipid α (**5**) represents a challenging synthetic target due to the acid sensitivity of the anomeric diphosphate linkage. For this reason, our synthetic strategy to the undecaprenyl-linked glycosyl diphosphate involved a late stage introduction of the diphosphate linkage and use of base-cleavable protecting groups that allowed for a final global deprotection step. Thus, our strategy involved (a) peracetylation of commercially available *N*-acetylglucosamine (**1**), (b) anomeric acetate deprotection, (c) hemiacetal α -phosphorylation, (d) undecaprenyl phosphate (**4**) coupling, and (e) base-mediated global deprotection (**Scheme 1**). The synthesis began with the preparation of α -phosphate **2** in 25% yield over five steps following published methodology (Ginsberg et al., 2006; Pereira et al., 2008). Coupling of undecaprenyl phosphate (**4**) with the α -phosphate **2** was conducted with 1,1'-carbonyldiimidazole (CDI) and tin(II) chloride. Global acetate deprotection using sodium methoxide in methanol transformed the resulting peracetyl diphosphate intermediate to desired target Lipid α (**5**) in 20% yield over coupling and deprotection steps and in 5% yield over the entire synthetic procedure. We found that yields of the coupling reaction were higher with the use of tin(II) chloride, which agrees with recent findings highlighting the effectiveness of this agent for promoting phosphate-phosphate coupling (Holkenbrink et al., 2011). In addition, our modest yield is commensurate with those reported for other CDI-mediated coupling reactions yielding lipid-linked glycosyl diphosphates (Holkenbrink et al., 2011; Woodward et al., 2010). Detailed synthetic procedures and chemical characterization can be found in the ESI.

***In vitro* reconstitution of TagA and TagB activities**

Access to Lipid α (**5**) allowed us to begin studying WTA biosynthesis using authentic substrates. We first reconstituted the activities of two *B. subtilis* 168 enzymes involved in poly(glycerol phosphate) biosynthesis *in vitro*. These enzymes, TagA and TagB, transform Lipid α (GlcNAc-PP-Und) to Lipid β (ManNAc-GlcNAc-PP-Und) and Lipid β to Lipid $\phi.1$ (GroP-ManNAc-GlcNAc-PP-Und), respectively (Bhavsar et al., 2005; Ginsberg et al., 2006).

We reconstituted Lipid α (**5**) into detergent micelles containing Triton-X100 to prevent substrate aggregation and to provide an interface for catalysis. This approach has previously proved effective for reconstituting functional enzyme activities in assays containing undecaprenyl-linked substrates (Woodward et al., 2010; Zapun et al., 2013). We assessed the ability of TagA and TagB to make their respective products in this system through a combination of analytical TLC and high-resolution mass spectrometry (HRMS) (**Figure 2**). The radioactive precursor UDP-[^{14}C]ManNAc was used to incorporate radioactivity into products after TagA-mediated catalysis (**Figure 2a**). This allowed us to monitor product formation following lipid extraction (Farha et al., 2013; Schaffer et al., 2002) by analytical TLC autoradiography (**Figure 2b**). Overnight incubation of Lipid α -containing micelles with TagA and UDP-[^{14}C]ManNAc led to the formation of a radioactive lipid species more polar than a radiolabelled Lipid α standard derived from a bacterial membrane source (Farha et al., 2013) as visualized by normal-phase TLC. LC/MS analysis of this species showed a peak at $m/z = 1331.789$ corresponding to the $[\text{M}-\text{H}^+]$ ion of Lipid β (**Figure S1a**). Negative ion collision-induced dissociation mass spectrometry (MS/MS) analysis of the *in vitro* product (m/z 1331.8, **Figure S1a**) showed the formation of two predominant product ions at m/z 485.116 and 907.601, which corresponds to the ManNAc-GlcNAc-P and

undecaprenyl diphosphate (Guan et al., 2005) respectively from Lipid β (**Figure S2a**, inset).

Incubation of Lipid α mixed-micelles with TagA, TagB, UDP-[^{14}C]ManNAc and CDP-glycerol produced a radioactive lipid species more polar than both Lipid α and Lipid β (**Figure 2b**). LC/MS analysis of this species showed a peak at $m/z = 742.382$ corresponding to the $[\text{M}-2\text{H}^+]^{2-}$ ion of Lipid $\phi.1$ (**Figure S1b**). MS/MS analysis of this $[\text{M}-2\text{H}^+]^{2-}$ ion (**Figure S2b**) showed the formation of several predominant product ions consistent with the structure of Lipid $\phi.1$. The ion at m/z 152.996 corresponds to $\text{C}_3\text{H}_6\text{O}_5\text{P}^-$ and is typical of lipids containing glycerol phosphate (Pulfer and Murphy, 2003). The product ions at m/z 639.123, 577.157 and 359.043 correspond to ions derived from the GroP-ManNAc-GlcNAc-P portion of Lipid $\phi.1$ as indicated in **Figure S2b** inset. The ion at m/z 907.614 is indicative of undecaprenyl diphosphate (Guan et al., 2005).

***In vitro* reconstitution of TagF and TagE activities**

The formation of Lipid β and Lipid $\phi.1$ intermediates in our *in vitro* assays demonstrated that semisynthetic Lipid α was a capable substrate for the WTA machinery. Therefore, using Lipid $\phi.1$ generated *in vitro*, we sought to reconstitute the remaining steps involved in the intracellular biosynthesis of poly(glycerol phosphate) WTA. To accomplish this, Lipid $\phi.1$ was further transformed to Lipid $\phi.n$ ([GroP] $_n$ -ManNAc-GlcNAc-PP-Und) using the poly(glycerol phosphate) polymerase TagF (Schertzer and Brown, 2003). We then tailored this polymer with α -linked glucose residues using the glucosyltransferase TagE (Allison et al., 2011) to generate Lipid γ ([GroP*] $_n$ -ManNAc-GlcNAc-PP-Und) (**Figure 3a**). We developed a radioactive anion exchange HPLC-based assay to monitor product formation during enzyme-mediated reactions (see Experimental). Radioactive precursors CDP-

[¹⁴C]glycerol and UDP-[¹⁴C]GlcNAc were used to incorporate radioactivity into products following incubation with TagF and TagE respectively. Our initial attempts with this approach failed to reveal radioactive products that could be detected by HPLC after incubation of TagF with non-radioactive Lipid ϕ .1 and CDP-[¹⁴C]glycerol (data not shown). We hypothesized that the lipid moiety of the TagF product may have interfered with effective chromatographic separation, likely through aggregation and resulting heterogeneity. Accordingly, we treated the reaction products with mild alkali conditions (0.5 M NaOH, 37°C, 25 min), well known to liberate poly(glycerol phosphate) polymers from their disaccharide anchors (**Figure S4a**) (Kojima et al., 1985). Anion exchange HPLC analysis of this sample revealed a broad peak with a greater retention time than its radioactive precursor (**Figure 3b**). This result suggested that the TagF product was highly anionic. To confirm this, we synthesized previously characterized poly(glycerol phosphate) polymers (Pereira et al., 2008; Schertzer and Brown, 2008; Sewell et al., 2009) (**Figure S3a**) of distinct chemical composition and compared their elution profiles to the alkali-treated TagF reaction. We found that all polymers had a similar retention time to the TagF product (**Figure S3b**).

Treatment of poly(glycerol phosphate) WTAs with mild acid conditions is known to hydrolyze phosphodiester linkages between glycerol phosphate residues (**Figure S4a**) (Kojima et al., 1985; Schertzer and Brown, 2003). Thus, we further subjected the alkali-treated TagF reaction mixture to mild acid conditions (1 N HCl, 100°C, 3 hr) and monitored hydrolysis by anion exchange HPLC. Under these conditions, we observed a complete loss of signal from the polyanionic species (**Figure S4b**). Hydrolytic products coincided with the retention time of [³H]glycerol (**Figure S5**), a well-known product of WTA hydrolysis (Schertzer and Brown, 2003). Indeed, we subjected a previously characterized poly(glycerol phosphate) polymer (Sewell et al., 2009) to these treatments and observed

similar degradation (**Figure S4**). Taken together, the characteristic WTA lability patterns of the TagF product demonstrate TagF's ability to make Lipid $\phi.n$ in this interfacial system.

We have previously shown that recombinant TagE can glucosylate soluble poly(glycerol phosphate) polymers (Allison et al., 2011). Likewise, using the authentic Lipid $\phi.n$ substrate and UDP-[^{14}C]glucose, we observed a TagE-dependent signal at a longer retention time than the radioactive precursor using anion exchange HPLC (**Figure 3b**). This retention time was similar to that of other well-characterized WTA polymers and alkali-treated Lipid $\phi.n$ produced from TagF (**Figure S3**). These findings are consistent with the conclusion that TagE is able to α -glucosylate poly(glycerol phosphate) polymers assembled on the authentic undecaprenyl-linked substrate.

Conclusions

WTAs constitute a significant component of the Gram-positive bacterial cell wall and have emerged as attractive antibiotic targets owing to the crucial roles they play in *Staphylococcus aureus* host colonization (Weidenmaier et al., 2004), peptidoglycan synthesis co-ordination (Atilano et al., 2010) and β -lactam resistance (Brown et al., 2012; Farha et al., 2013). These structures have been targeted with success recently in both academe (Farha et al., 2013; 2014) and the pharmaceutical sector (Wang et al., 2013), where biosynthetic inhibitors have been shown to restore the efficacy of β -lactams against methicillin-resistant *S. aureus* (MRSA). While progress in the discovery of inhibitors using cell-based approaches has been promising, many biochemical details of WTA synthesis remain obscure.

Biochemical study of WTA enzymes has been hampered by the limited availability of natural substrates. Recent use of soluble substrate analogues of WTA biosynthetic intermediates has facilitated the study of WTA enzymes *in vitro*, away from the membrane. These studies have culminated in defining the functions of WTA enzymes (Allison et al., 2011; Ginsberg et al., 2006; Pereira et al., 2008); obtaining kinetic parameters for enzyme-mediated reactions (Allison et al., 2011; Ginsberg et al., 2006; Pereira et al., 2008; Sewell et al., 2009; Zhang et al., 2006); discerning substrate preferences (Zhang et al., 2006); elucidating steps involved in WTA assembly (Brown et al., 2010; 2008); describing mechanism (Allison et al., 2011; Sewell et al., 2009) and mode (Sewell et al., 2009) of catalysis; and helping to unveil WTAs unique role in antibiotic resistance (Brown et al., 2012). Despite the utility these analogues have displayed in enhancing understanding of WTA biosynthesis, they are unable to mimic the natural membrane environment where WTA biosynthetic enzymes function (Bhavsar et al., 2007; 2005; Schertzer and Brown, 2003). Thus, even basic features of interfacial WTA synthesis and assembly have eluded characterization.

In the work presented here, we detail a robust strategy to obtain in quantity both undecaprenyl phosphate (**4**) and a valuable intermediate in WTA biosynthesis, Lipid α (**5**). We show that Lipid α is a capable substrate for poly(glycerol phosphate) WTA by reconstituting the activities of WTA enzymes TagA, TagB, TagF, and TagE *in vitro*. This work contributes to other efforts broadly focused on the application of authentic undecaprenyl-linked substrates for the *in vitro* study of bacterial cell envelope biosynthesis, namely O-polysaccharide biosynthesis in *Escherichia coli* (Woodward et al., 2010) and peptidoglycan assembly in pathogenic *Streptococcus pneumonia* (Zapun et al., 2013). Studies of this nature may provide new mechanistic information that is otherwise unobtainable through the employment of soluble analogues and significantly

enhance our limited understanding of the synthesis and assembly of bacterial cell surface structures.

Access to Lipid α and other WTA intermediates reported here lays an important foundation to probe the molecular details of interfacial WTA biosynthesis. We envision the employment of these compounds in mixed-micelle or unilamellar vesicle systems to properly assess the influence of the membrane interface on catalytic efficiency, substrate binding/dissociation, processivity and length regulation by WTA enzymes. Further, our methods are not limited to the model Gram-positive bacterium *B. subtilis*. The synthetic approach described here could be used to study WTA biosynthesis in MRSA and other pathogens, as Lipid α is a common precursor for the assembly of WTA. These authentic substrates could also be used in crystallographic studies to further understand the molecular structures and interactions between lipid acceptors and the WTA machinery. Indeed, the recent crystal structure of the TagF polymerase from *Staphylococcus epidermidis* was obtained for the apo-enzyme (Lovering et al., 2010). Finally, synthetic poly(glycerol phosphate) WTA may well be of utility for the study of uncharacterized enzyme(s), for example, those responsible for anchoring WTA to the peptidoglycan meshwork (Kawai et al., 2011).

Experimental

General methods

Chemicals and solvents were purchased from Sigma-Aldrich (Oakville, ON, Canada) or Fisher Scientific (Whitby, ON, Canada) unless otherwise stated. Analytical thin layer chromatography (TLC) was carried out on silica gel 60 F254 aluminum-backed plates from EMD Chemicals (Gibbstown, NJ, USA) or glass-backed C18 plates from Silicycle (Quebec City, QC, Canada). TLC plates were visualized by exposure to ultraviolet light and/or exposure to iodine vapour (I₂) or

an acidic solution of *p*-anisaldehyde. UDP-[¹⁴C]GlcNAc (0.1 mCi/mL) was purchased from American Radiolabeled Chemicals (St. Louis, MO, USA). *Sn*-[U-¹⁴C]glycerol-3-phosphate (0.05 mCi/mL), UDP-[¹⁴C]glucose (0.02 mCi/mL) and Ultima Gold liquid scintillation cocktail were purchased from PerkinElmer (Woodbridge, ON, Canada). [2-³H]glycerol (1 mCi/mL) was purchased from Amersham Biosciences (Piscataway, NJ, USA). Recombinant TagA, TagB, TagF, TagE, TarD and MnaA were prepared as previously described (Allison et al., 2011; Badurina et al., 2003; Bhavsar et al., 2005; Pereira et al., 2008; Schertzer and Brown, 2003). Anion exchange HPLC was conducted on a Waters (Mississauga, ON, Canada) ACQUITY UPLC H-Class using a ThermoScientific (Waltham, MA, USA) DNAPac PA 200 column. Radioactive components were separated using a linear gradient from 0->100% 1.25 M NaCl in 20 mM Tris (pH 8) and visualized with in-line scintillation counting using a PerkinElmer Radiomatic 150TR.

Semisynthetic preparation of Lipid α (5)

Full synthetic procedures and product characterization can be found in the ESI.

Compound synthesis

UDP-ManNAc and UDP-[¹⁴C]ManNAc were prepared enzymatically from UDP-GlcNAc and UDP-[¹⁴C]GlcNAc respectively using MnaA (Soldo et al., 2002). CDP-glycerol and CDP-[U-¹⁴C]glycerol were synthesized enzymatically using *Staphylococcus aureus* TarD following previously described methods (Badurina et al., 2003). Lipid ϕ .1 analogue was prepared chemoenzymatically as described previously (Pereira et al., 2008) and subsequently purified over a Waters Sep-Pak C18 Plus Cartridge using 95% MeCN in 0.1% aqueous NH₄OH for compound elution. [¹⁴C]Lipid ϕ .10 analogue was prepared through incubation of Lipid ϕ .1 analogue (3.6 μ M) with TagF (2.4 μ M) and CDP-[U-¹⁴C]glycerol (32.4

μM , 0.3 μCi) for 4 hours in 50 mM Tris-HCl (pH 8) and 30 mM MgCl_2 at ambient temperature (Sewell et al., 2009). [^{14}C]Lipid $\phi.40$ analogue was prepared in a similar manner using 140 μM CDP-[U- ^{14}C]glycerol (0.3 μCi). [^{14}C]CDP-glycerol-linked polymer was prepared enzymatically through incubation of TagF (2.4 μM) and CDP-[U- ^{14}C]glycerol (36 μM , 0.3 μCi) for 4 hours in 50 mM Tris-HCl (pH 8), 30 mM MgCl_2 and 0.13% (v/v) Triton X-100 at ambient temperature (Schertzer and Brown, 2008). [^{14}C]-Lipid α standard was prepared following previously described TarO activity assays of *E. coli* cell membranes (Farha et al., 2013). Briefly, TarO-enriched membranes (500 μg protein) were incubated with UDP-GlcNAc (300 μM), UDP-[^{14}C]GlcNAc (0.1 μCi), 0.1% (v/v) TritonX-100 and Reaction Buffer (50 mM Tris pH = 8, 10 mM MgCl_2 , 1 mM EDTA) for 2 hours at ambient temperature. Lipid-linked products were extracted following known methods (Farha et al., 2013), and analyzed by TLC.

High-resolution mass spectrometry

High-resolution mass spectra and collision-induced dissociation mass spectra (MS/MS) were collected on an Agilent 6520 quadrupole time-of-flight (Q-TOF) mass spectrometer following previously described methods (Bulat and Garrett, 2011). All compounds were lyophilized and resuspended in $\text{CHCl}_3/\text{CH}_3\text{OH}$ (2:1) prior to analysis.

TagA and TagB *in vitro* reconstitution

To reconstitute the activity of TagA, dried semisynthetic Lipid α (0.22 mM) was resuspended in a buffer containing 0.13% (v/v) Triton X-100, 50 mM Tris (pH 8.0) and 220 mM NaCl. The mixture was vortexed vigorously and sonicated for 5 min at ambient temperature. TagA (11.2 μM), MnaA (6 μM) and UDP-[^{14}C]GlcNAc (1 mM, 0.1 μCi) were added to initiate the reaction. The reaction mixture incubated at ambient temperature for 4 hours then overnight at 5°C. TagB reconstitution

assays were performed identically, with the exception that CDP-glycerol (2 mM) and TagB (6 μ M) were added to the reaction mixture after 4 hours of incubation. A control reaction containing no Lipid α was also set up under these conditions. Reactions were quenched using $\text{CHCl}_3/\text{CH}_3\text{OH}$ (3:2) and lipid-linked products were extracted according to published methods (Farha et al., 2013; Schaffer et al., 2002). Reaction extracts and [^{14}C]-Lipid α standard were separated by normal phase TLC using a $\text{CHCl}_3/\text{CH}_3\text{OH}/\text{H}_2\text{O}$ (65:25:4) solvent system. The plates were dried and exposed overnight at ambient temperature to a storage phosphor screen (GE Healthcare). Radioactive compounds were visualized using a Typhoon Trio Variable Mode Imager (GE Healthcare). Identical TagA and TagB reconstitution reactions were set up using nonradioactive UDP-GlcNAc for MS analysis.

TagF and TagE *in vitro* reconstitution

Lipid $\phi.1$ was obtained from lipid extracts of non-radioactive TagB reconstitution reactions. To reconstitute the activity of TagF, dried Lipid $\phi.1$ was resuspended in a buffer containing 0.13% (v/v) Triton X-100, 50 mM Tris (pH 8.0) and 30 mM MgCl_2 . This solution was vortexed vigorously and sonicated for 5 minutes at ambient temperature. TagF (2.4 μ M) and CDP- ^{14}C glycerol (36 μ M, 0.3 μ Ci) were added to initiate the reaction. The reaction mixture incubated at room temperature for 4 hours. An identical reaction was set up using CDP-glycerol in place of CDP- ^{14}C glycerol to generate non-radioactive Lipid $\phi.n$ for TagE reconstitution assays. To reconstitute the activity of TagE, UDP- ^{14}C glucose (36 μ M, 0.4 μ Ci) and TagE (1 μ M) were added to a non-radioactive TagF reaction after 4 hours of incubation. The reaction mixture proceeded for an additional 4 hours at ambient temperature. TagF and TagE reactions were treated with mild alkali conditions to liberate poly (glycerol phosphate) polymers from disaccharide anchors (Kojima et al., 1985) for anion exchange HPLC analysis. Briefly, each

reaction mixture was treated to 0.5 M NaOH for 25 min at 37°C. The reaction mixtures were neutralized with the addition of 0.5 M HCl prior to anion exchange HPLC analysis. For WTA lability experiments, these reactions underwent further treatment in 1 N HCl for 3 hours at 100°C (Kojima et al., 1985) prior to anion exchange HPLC analysis.

Acknowledgements

We thank Dr. Kalinka Koteva and Dr. Mehdi Keramane for assistance in chemical synthesis. We also thank Soumaya Zlitni and Dr. Sebastian Gehrke for helpful discussions in the preparation of this manuscript. We are grateful for the guidance provided by Dr. Eefjan Breukink for the preparation of undecaprenyl phosphate. Support to EDB for this work included a salary award (Canada Research Chair) and an operating grant from the Canadian Institutes of Health Research (MOP-15496). This work was also supported by National Science Foundation Major Research Instrumentation Award 1039659 to TAG.

References

- Allison, S.E., D'Elia, M.A., Arar, S., Monteiro, M.A., and Brown, E.D. (2011). Studies of the genetics, function, and kinetic mechanism of TagE, the wall teichoic acid glycosyltransferase in *Bacillus subtilis* 168. *J. Biol. Chem.* **286**, 23708–23716.
- Atilano, M.L., Pereira, P.M., Yates, J., Reed, P., Veiga, H., Pinho, M.G., and Filipe, S.R. (2010). Teichoic acids are temporal and spatial regulators of peptidoglycan cross-linking in *Staphylococcus aureus*. *Proc. Natl. Acad. Sci. U.S.A.* **107**, 18991–18996.
- Atilano, M.L., Yates, J., Glittenberg, M., Filipe, S.R., and Ligoxygakis, P. (2011). Wall teichoic acids of *Staphylococcus aureus* limit recognition by the *Drosophila* peptidoglycan recognition protein-SA to promote pathogenicity. *PLoS Pathog.* **7**, e1002421–13.
- Badurina, D.S., Zolli-Juran, M., and Brown, E.D. (2003). CTP: glycerol 3-

phosphate cytidylyltransferase (TarD) from *Staphylococcus aureus* catalyzes the cytidylyl transfer via an ordered Bi–Bi reaction mechanism with micromolar K_m values. *Biochim. Biophys. Acta, Proteins Proteomics* 1646, 196–206.

Barreteau, H., Magnet, S., Ghachi, M.E., Touzé, T., Arthur, M., Mengin-Lecreulx, D., and Blanot, D. (2009). Quantitative high-performance liquid chromatography analysis of the pool levels of undecaprenyl phosphate and its derivatives in bacterial membranes. *J. Chromatogr. B. Analyt. Technol. Biomed. Life Sci.* 877, 213–220.

Bhavsar, A.P., D'Elia, M.A., Sahakian, T.D., and Brown, E.D. (2007). The Amino Terminus of *Bacillus subtilis* TagB possesses separable localization and functional properties. *J. Bacteriol.* 189, 6816–6823.

Bhavsar, A.P., Truant, R., and Brown, E.D. (2005). The TagB protein in *Bacillus subtilis* 168 is an intracellular peripheral membrane protein that can incorporate glycerol phosphate onto a membrane-bound acceptor in vitro. *J. Biol. Chem.* 280, 36691–36700.

Boucher, H.W., Talbot, G.H., Bradley, J.S., Edwards, J.E., Gilbert, D., Rice, L.B., Scheld, M., Spellberg, B., and Bartlett, J. (2009). Bad bugs, no drugs: No ESKAPE! An update from the Infectious Diseases Society of America. *Clin. Infect. Dis.* 48, 1–12.

Bouhss, A., Trunkfield, A.E., Bugg, T.D.H., and Mengin-Lecreulx, D. (2008). The biosynthesis of peptidoglycan lipid-linked intermediates. *FEMS Microbiol. Rev.* 32, 208–233.

Breukink, E., van Heusden, H.E., Vollmerhaus, P.J., Swiezewska, E., Brunner, L., Walker, S., Heck, A.J.R., and de Kruijff, B. (2003). Lipid II is an intrinsic component of the pore induced by nisin in bacterial membranes. *J. Biol. Chem.* 278, 19898–19903.

Brown, S., Xia, G., Luhachack, L.G., Campbell, J., Meredith, T.C., Chen, C., Winstel, V., Gekeler, C., Irazoqui, J.E., Peschel, A., and Walker, S. (2012). Methicillin resistance in *Staphylococcus aureus* requires glycosylated wall teichoic acids. *Proc. Natl. Acad. Sci. U.S.A.* 109, 18909–18914.

Brown, S., Meredith, T., Swoboda, J., and Walker, S. (2010). *Staphylococcus aureus* and *Bacillus subtilis* W23 make polyribitol wall teichoic acids using different enzymatic pathways. *Chem. Biol.* 17, 1101–1110.

Brown, S., Zhang, Y.-H., and Walker, S. (2008). A revised pathway proposed for

Staphylococcus aureus wall teichoic acid biosynthesis based on *in vitro* reconstitution of the intracellular steps. *Chem. Biol.* **15**, 12–21.

Bulat, E., and Garrett, T.A. (2011). Putative N-Acylphosphatidylethanolamine Synthase from *Arabidopsis thaliana* is a lysoglycerophospholipid acyltransferase. *J. Biol. Chem.* **286**, 33819–33831.

Burger, M.M., and Glaser, L. (1964). The synthesis of teichoic acids. I. Polyglycerophosphate. *J. Biol. Chem.* **239**, 3168–3177.

Danilov, L.L. (1989). Polyprenyl phosphates: synthesis and structure-activity relationship for a biosynthetic system of *Salmonella anatum* O-specific polysaccharide. *Chem. Phys. Lipids* **51**, 191–203.

D'Elia, M.A., Millar, K.E., Beveridge, T.J., and Brown, E.D. (2006). Wall teichoic acid polymers are dispensable for cell viability in *Bacillus subtilis*. *J. Bacteriol.* **188**, 8313–8316.

Farha, M.A., Koteva, K., Gale, R.T., Sewell, E.W., Wright, G.D., and Brown, E.D. (2014). Designing analogs of ticlopidine, a wall teichoic acid inhibitor, to avoid formation of its oxidative metabolites. *Bioorg. Med. Chem. Lett.* **24**, 905–910.

Farha, M.A., Leung, A., Sewell, E.W., D'Elia, M.A., Allison, S.E., Ejim, L., Pereira, P.M., Pinho, M.G., Wright, G.D., and Brown, E.D. (2013). Inhibition of WTA synthesis blocks the cooperative action of PBPs and sensitizes MRSA to β -lactams. *ACS Chem. Biol.* **8**, 226–233.

Ginsberg, C., Zhang, Y.-H., Yuan, Y., and Walker, S. (2006). *In vitro* reconstitution of two essential steps in wall teichoic acid biosynthesis. *ACS Chem. Biol.* **1**, 25–28.

Holkenbrink, A., Koester, D.C., Kaschel, J., and Werz, D.B. (2011). Total synthesis of α -linked Rha–Rha–Gal undecaprenyl diphosphate found in *Geobacillus stearothermophilus*. *Eur. J. Org. Chem.* **2011**, 6233–6239.

Kawai, Y., Marles-Wright, J., Cleverley, R.M., Emmins, R., Ishikawa, S., Kuwano, M., Heinz, N., Bui, N.K., Hoyland, C.N., Ogasawara, N., Lewis, R.J., Vollmer, W., Daniel, R.A., and Errington, J. (2011). A widespread family of bacterial cell wall assembly proteins. *EMBO J.* **30**, 4931–4941.

Khidyrova, N.K., and Shakhidoyatov, K.M. (2002). Plant polyprenols and their biological activity. *Chem. Nat. Compd.* **38**, 107–121.

Koch, A.L. (2003). Bacterial wall as target for attack: Past, present, and future

research. Clin. Microbiol. Rev. 16, 673–687.

Kojima, N., Araki, Y., and Ito, E. (1985). Structure of the linkage units between ribitol teichoic acids and peptidoglycan. J. Bacteriol. 161, 299–306.

Lazarevic, V., and Karamata, D. (1995). The tagGH operon of *Bacillus subtilis* 168 encodes a two-component ABC transporter involved in the metabolism of two wall teichoic acids. Mol. Microbiol. 16, 345–355.

Lee, Y.J., Ishiwata, A., and Ito, Y. (2009). Synthesis of undecaprenyl pyrophosphate-linked glycans as donor substrates for bacterial protein N-glycosylation. Tetrahedron 65, 6310–6319.

Neuhaus, F.C., and Baddiley, J. (2003). A continuum of anionic charge: structures and functions of D-alanyl-teichoic acids in Gram-positive bacteria. Microbiol. Mol. Biol. Rev. 67, 686–723.

Pereira, M.P., Schertzer, J.W., D’Elia, M.A., Koteva, K.P., Hughes, D.W., Wright, G.D., and Brown, E.D. (2008). The wall teichoic acid polymerase TagF efficiently synthesizes poly(glycerol phosphate) on the TagB product Lipid III. ChemBioChem. 9, 1385–1390.

Schäffer, C., Wugeditsch, T., Messner, P., and Whitfield, C. (2002). Functional expression of enterobacterial O-polysaccharide biosynthesis enzymes in *Bacillus subtilis*. Appl. Environ. Microbiol. 68, 4722–4730.

Schertzer, J.W., and Brown, E.D. (2003). Purified, recombinant TagF protein from *Bacillus subtilis* 168 catalyzes the polymerization of glycerol phosphate onto a membrane acceptor *in vitro*. J. Biol. Chem. 278, 18002–18007.

Schertzer, J.W., and Brown, E.D. (2008). Use of CDP-glycerol as an alternate acceptor for the teichoic acid polymerase reveals that membrane association regulates polymer length. J. Bacteriol. 190, 6940–6947.

Sewell, E.W.C., Pereira, M.P., and Brown, E.D. (2009). The wall teichoic acid polymerase TagF is non-processive *in vitro* and amenable to study using steady state kinetic analysis. J. Biol. Chem. 284, 21132–21138.

Sewell, E.W. and Brown, E.D. (2014). Taking aim at wall teichoic acid synthesis: new biology and new leads for antibiotics. J. Antibiot. 67, 43–51.

Sim, M.M., Kondo, H., and Wong, C.-H. (1993). Synthesis of dibenzyl glycosyl

phosphites using dibenzyl N,N-diethylphosphoramidite as phosphitylating reagent: an effective route to glycosyl phosphates, nucleotides, and glycosides. *J. Am. Chem. Soc.* **115**, 2260–2267.

Swiezewska, E., Sasak, W., Mańkowski, T., Jankowski, W., Vogtman, T., Krajewska, I., Hertel, J., Skoczylas, E., and Chojnacki, T. (1994). The search for plant polyprenols. *Acta Biochim. Pol.* **41**, 221–260.

Soldo, B., Lazarevic, V., Pooley, H.M., and Karamata, D. (2002). Characterization of a *Bacillus subtilis* thermosensitive teichoic acid-deficient mutant: Gene *mnaA* (*yvyH*) encodes the UDP-N-acetylglucosamine 2-epimerase. *J. Bacteriol.* **184**, 4316–4320.

Trent, M.S. (2001). An inner membrane enzyme in *Salmonella* and *Escherichia coli* that transfers 4-Amino-4-deoxy-L-arabinose to Lipid A. Induction in polymyxin-resistant mutants and role of a novel lipid-linked donor. *J. Biol. Chem.* **276**, 43122–43131.

Wang, H., Gill, C.J., Lee, S.H., Mann, P., Zuck, P., Meredith, T.C., Murgolo, N., She, X., Kales, S., Liang, L., Liu, J., Wu, J., Santa Maria, J., Su, J., Pan, J., Hailey, J., McGuinness, D., Tan, C.M., Flattery, A., Walker, S., Black, T., and Roemer, T. (2013). Discovery of wall teichoic acid inhibitors as potential anti-MRSA β -lactam combination agents. *Chem. Biol.* **20**, 272–284.

Weidenmaier, C., Kokai-Kun, J.F., Kristian, S.A., Chanturiya, T., Kalbacher, H., Gross, M., Nicholson, G., Neumeister, B., Mond, J.J., and Peschel, A. (2004). Role of teichoic acids in *Staphylococcus aureus* nasal colonization, a major risk factor in nosocomial infections. *Nat. Med.* **10**, 243–245.

Woodward, R., Yi, W., Li, L., Zhao, G., Eguchi, H., Sridhar, P.R., Guo, H., Song, J.K., Motari, E., Cai, L., Kelleher, P., Liu, X., Han, W., Zhang, W., Ding, Y., Li, M., and Wang, P.G. (2010). *In vitro* bacterial polysaccharide biosynthesis: defining the functions of Wzy and Wzz. *Nat. Chem. Biol.* **6**, 418–423.

Zapun, A., Philippe, J., Abrahams, K.A., Signor, L., Roper, D.I., Breukink, E., and Vernet, T. (2013). *In vitro* reconstitution of peptidoglycan assembly from the Gram-positive pathogen *Streptococcus pneumoniae*. *ACS Chem. Biol.* **8**, 2688–2696.

Zhang, Y.-H., Ginsberg, C., Yuan, Y., and Walker, S. (2006). Acceptor substrate selectivity and kinetic mechanism of *Bacillus subtilis* TagA. *Biochemistry* **45**, 10895–10904

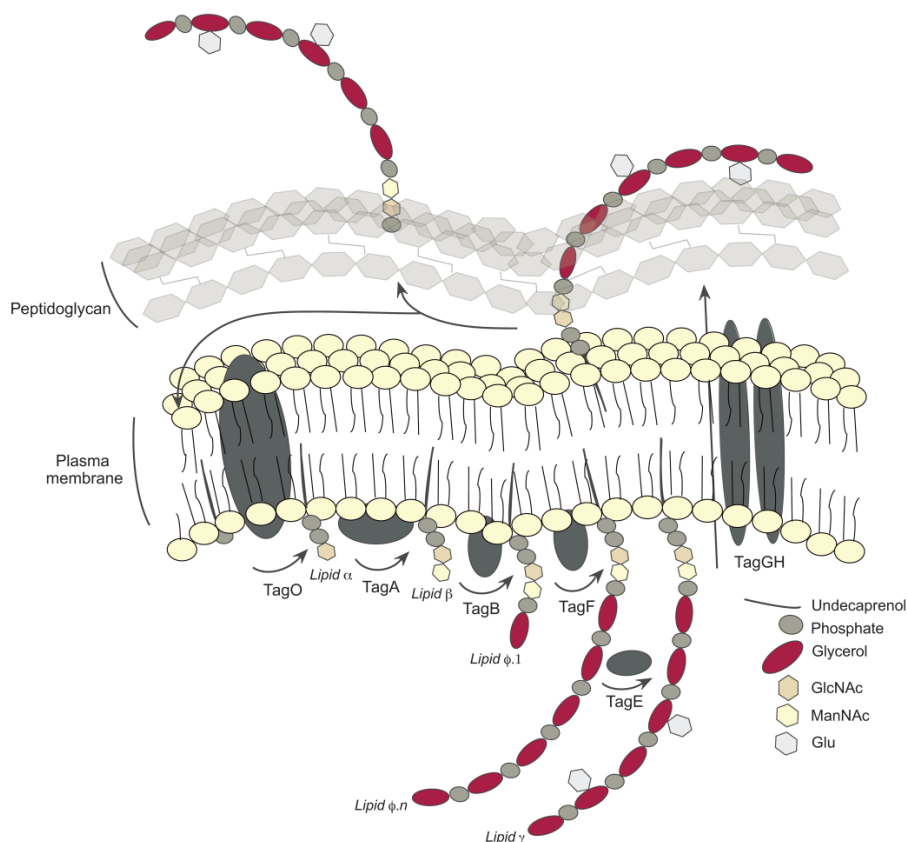


Figure 1. Poly(glycerol phosphate) WTA biosynthesis in *B. subtilis* 168. WTA biosynthesis takes place at the inner leaflet of the cytoplasmic membrane. The first reaction in the pathway is mediated by the transmembrane protein TagO, wherein a UDP-GlcNAc precursor is coupled to a membrane-anchored undecaprenyl lipid carrier to produce undecaprenylpyrophosphoryl-GlcNAc, also known as Lipid α (Soldo et al., 2002). In a second reaction, TagA catalyzes the transfer of ManNAc from a UDP-ManNAc precursor to the C(4) hydroxyl group of the lipid-linked GlcNAc, forming Lipid β (Ginsberg et al., 2006). TagB catalyzes the transfer of glycerol phosphate from a CDP-glycerol precursor to the lipid-linked disaccharide (Bhavsar et al., 2005; Ginsberg et al., 2006). An additional 25-35 glycerol phosphate monomers are added to this product, Lipid $\phi.1$ by the polymerase TagF utilizing CDP-glycerol precursors (Bhavsar et al., 2005; Pereira et al., 2008; Schertzer and Brown, 2003; Sewell et al., 2009). The polymer, Lipid $\phi.n$, is tailored with α -linked Glu residues by the glycosyltransferase TagE through use of UDP-Glu precursors, forming Lipid γ (Allison et al., 2011). The polymer is translocated to the extracellular leaflet through the action of the two-component ABC transporter TagGH (Lazarevic and Karamata, 1995). The last step in *B. subtilis* 168 poly(glycerol phosphate) WTA biosynthesis is mediated by currently uncharacterized transferases, which are predicted to cleave the polymer from its lipid anchor and attach it to the C(6) hydroxyl group of peptidoglycan muramic acid (Kawai et al., 2011). Abbreviations: GlcNAc, *N*-acetylglucosamine; ManNAc, *N*-acetylmannosamine; Glu, glucose; UDP, uridine diphosphate; CDP, cytidine diphosphate.

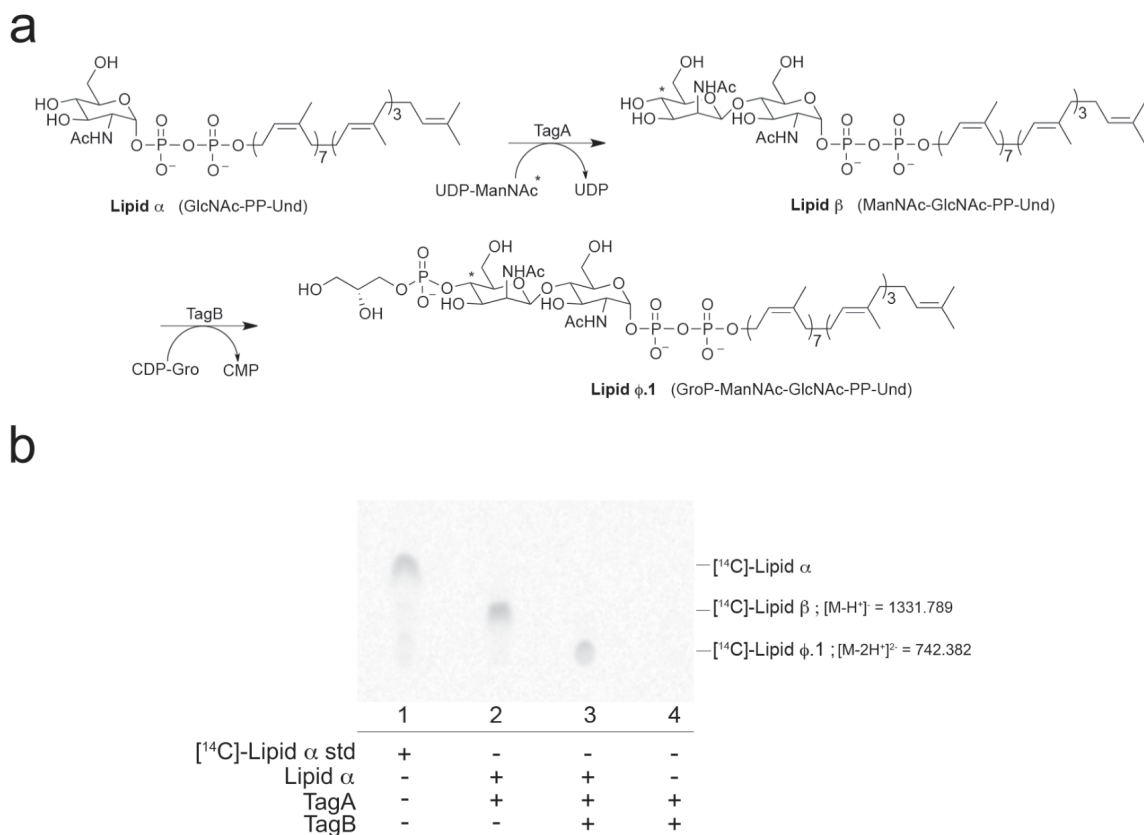


Figure 2. Semisynthetic Lipid α (5) can be used to reconstitute the activities of pure, recombinant WTA biosynthetic enzymes TagA and TagB *in vitro*. (a) Reactions catalyzed by TagA and TagB in our *in vitro* system. The asterisk (*) denotes ^{14}C -labelled compounds in assays employing semisynthetic Lipid α (5). Nomenclature and chemical composition for each WTA intermediate are shown in bold and in brackets respectively. (b) Product characterization by TLC autoradiography and ESI-MS of WTA intermediates synthesized *in vitro*. Relevant reaction components are indicated (+/-) below the appropriate lane and reaction products confirmed by ESI-MS are indicated to the right of the frame with experimental m/z values shown (for associated MS spectra, see **Figure S1**). In reactions involving semisynthetic derived Lipid α (5) (lanes 2-4), radioactivity was incorporated into reaction products from a UDP- $[^{14}\text{C}]$ ManNAc precursor (see panel a). Lipid-linked reaction products were extracted according to published methodology (Farha et al., 2013). Lane 1, $[^{14}\text{C}]$ -Lipid α standard prepared from membranes of *E. coli* cells expressing recombinant TarO from *S. aureus* following known methods (Farha et al., 2013); lane 2, TagA-mediated reaction of semisynthetic Lipid α (5) to Lipid β; lane 3, TagA and TagB-mediated reaction of semisynthetic Lipid α (5) to Lipid φ.1; lane 4, control reaction without either sources of Lipid α (5).

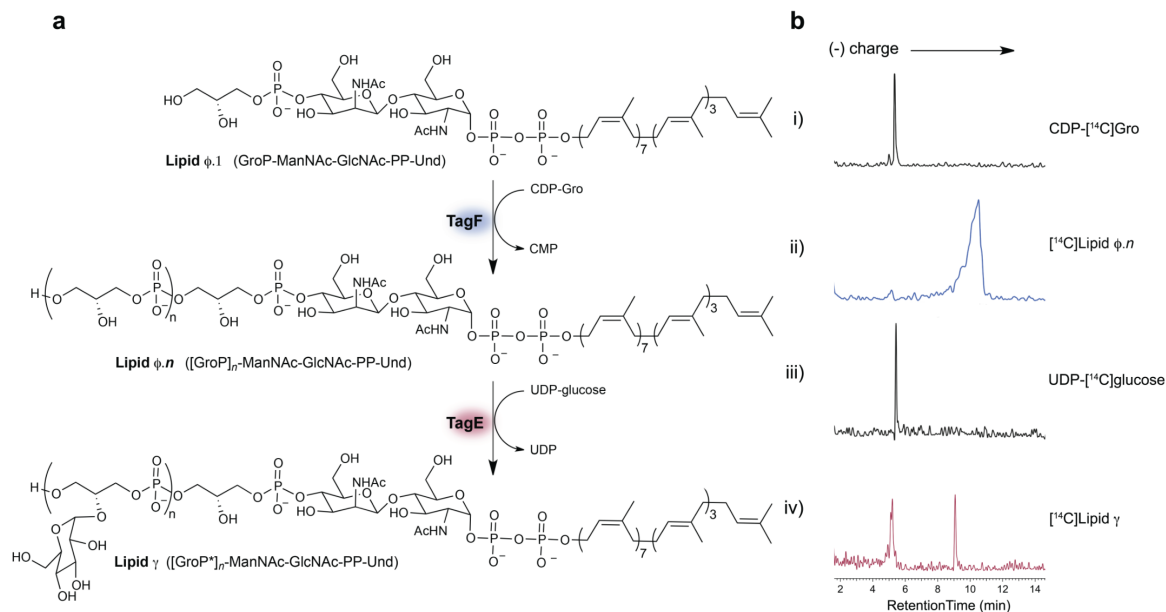
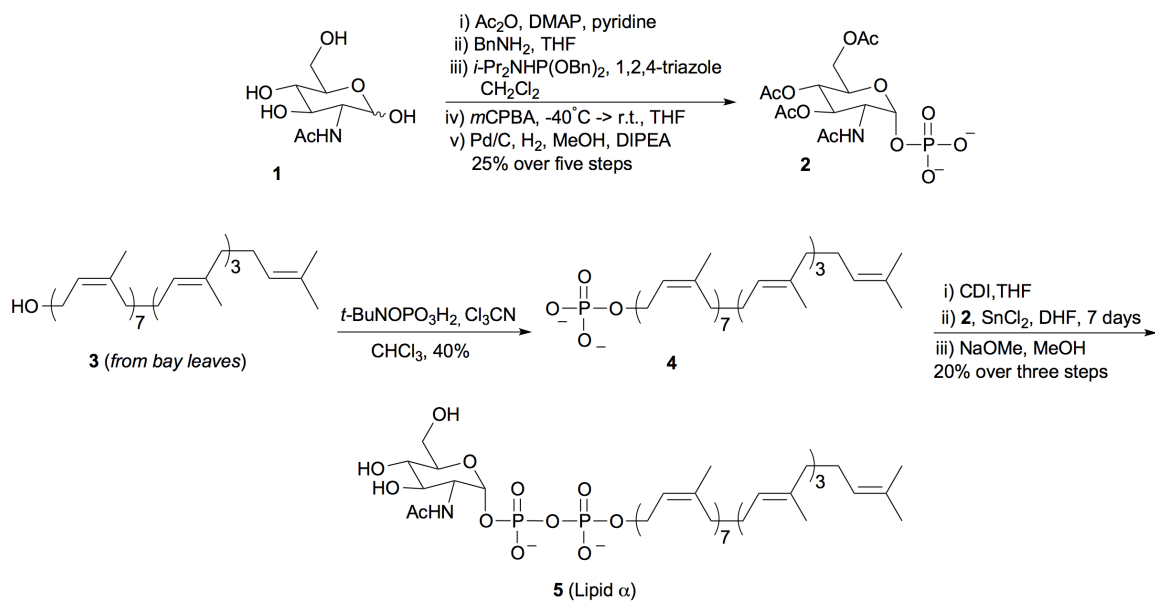


Figure 3. Authentic late-stage WTA intermediates are substrates for polymerization and glucosylation. (a) *In vitro* reactions mediated by the poly(glycerol phosphate) polymerase TagF and the glucosyltransferase TagE. Nomenclature and chemical composition for each late-stage wall teichoic acid intermediate is shown in bold and in brackets respectively. (b) Product characterization by anion exchange HPLC of late-stage WTA intermediates synthesized *in vitro*. In reactions involving TagF (shown in blue), Lipid $\phi.1$ was prepared through TagA and TagB-mediated reactions starting with semisynthetic Lipid α (5) and purified by lipid extraction. Radioactivity was incorporated into polymeric products using a CDP-[14 C]Gro precursor. In reactions involving TagE (shown in red), Lipid $\phi.n$ polymer was prepared in a non-radioactive assay using Lipid $\phi.1$ and TagF. Radioactivity was incorporated into this substrate following incubation with TagE and UDP-[14 C]glucose. Radioactive reaction components were separated by anion exchange HPLC and visualized with in-line scintillation counting. i) TagF reaction mixture prior to the addition of enzyme (T=0); ii) NaOH-treated (0.5M NaOH, 37°C, 25 min) TagF reaction mixture after 4 hours of incubation with enzyme; iii) TagE reaction mixture prior to addition of enzyme (T=0); iv) NaOH-treated (0.5 M NaOH, 37°C, 25 min) TagE reaction mixture after 4 hours of incubation with enzyme. Predicted radioactive components prior to mild alkali treatment are indicated to the right of the panel.



Scheme 1. Semisynthetic preparation of Lipid α (**5**).

Table 1. Nomenclature for undecaprenyl-linked WTA intermediates^a

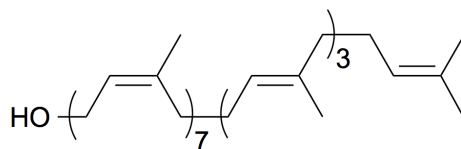
| Intermediate | Chemical composition |
|----------------|---|
| Lipid α | GlcNAc-1-P-P-Und |
| Lipid β | ManNAc- β -(1-4)-GlcNAc-1-P-P-Und |
| Lipid $\phi.n$ | (GroP) _n -ManNAc- β -(1-4)-GlcNAc-1-P-P-Und |
| Lipid γ | (GroP*) _n -ManNAc- β -(1-4)-GlcNAc-1-P-P-Und |

^aWTA intermediates are named according to the enzyme utilizing the molecule as a substrate. *n* represents the number of repeating *sn*-glycerol-3-phosphate units. The asterisk (*) denotes oligomeric and polymeric species bearing α -linked glucose residues. Abbreviations: GlcNAc, *N*-acetylglucosamine; ManNAc, *N*-acetylmannosamine; GroP, *sn*-glycerol-3-phosphate; P, phosphate; Und, undecaprenol.

Supplementary methods

General. Chemicals and solvents were purchased from Sigma-Aldrich (Oakville, ON) or Fisher Scientific (Whitby, ON) unless otherwise stated. Flash column chromatography was performed using silica, C18, and SAX pre-packed columns from Teledyne Isco (Lincoln, NE) or Silicycle (Quebec City, QC) on a CombiFlash Rf system (Teledyne ISCO Inc.). Analytical thin layer chromatography (TLC) was carried out on silica gel 60 F254 aluminum-backed plates from EMD Chemicals (Gibbstown, NJ) or glass-backed C18 plates from Silicycle. TLC plates were visualized by exposure to ultraviolet light and/or exposure to iodine vapor (I_2) or an acidic solution of *p*-anisaldehyde. 1H , ^{13}C , and ^{31}P NMR spectra were obtained using a Bruker AVIII 700 MHz spectrometer. Spectra are reported in parts per million on the δ scale and are referenced to internal methanol (Methanol- d_4 : 1H , δ = 3.31 and ^{13}C , δ = 49.0). 1H data are reported as follows: chemical shift (δ , ppm) (multiplicity, coupling constant (Hz), integration), ^{13}C and ^{31}P data are reported as follows: chemical shift (δ , ppm) (multiplicity, coupling constant (Hz)). Multiplicity abbreviations are as follows: s = singlet, d = doublet, dd = doublet of doublets, t = triplet, m = multiplet, b = broad. High-resolution mass spectra and collision-induced dissociation mass spectra (MS/MS) were collected on an Agilent 6520 quadrupole time-of-flight (Q-TOF) mass spectrometer. All compounds were lyophilized and resuspended in $CHCl_3/CH_3OH$ (2:1) prior to analysis following previously described methods (Bulat and Garrett, 2011).

Extraction and isolation of undecaprenol (**3**)



3 (from bay leaves)

Undecaprenol (**3**) was prepared loosely following published methodology for obtaining polyprenols from plant sources (Breukink et al., 2003; Khidyrova and Shakhidoyatov, 2002; Swiezewska et al., 1994). Our procedure was the following: Commercially available leaves of the *Laurus nobilis* tree (bay leaves) (42 g) were granulated and extracted in a Soxhlet apparatus with acetone/hexane (9:1) (500 mL) for 48 hours. The extract was set aside and the procedure was repeated. The combined extracts were evaporated to dryness, dissolved in 500 mL of hexane/EtOH/15% aqueous KOH (w/v) (3:15:2), and refluxed for 1 hour at 90°C. The mixture was cooled and extracted with H₂O/diethyl ether (1:1) (500 mL). The unsaponifiable extract was dried over Na₂SO₄, evaporated to dryness and purified by silica normal-phase chromatography (hexane/diethyl ether, 100:0 -> 95:5 -> 85:15). Polyisoprenol-enriched fractions were identified by mass spectrometry, combined, evaporated to dryness and further purified by C18 reverse-phase chromatography (H₂O/Acetone, 5:95). Undecaprenol (**3**) enriched fractions were identified by mass spectrometry, combined, evaporated to dryness and used for phosphorylation reactions without further purification (158 mg, colourless oil).

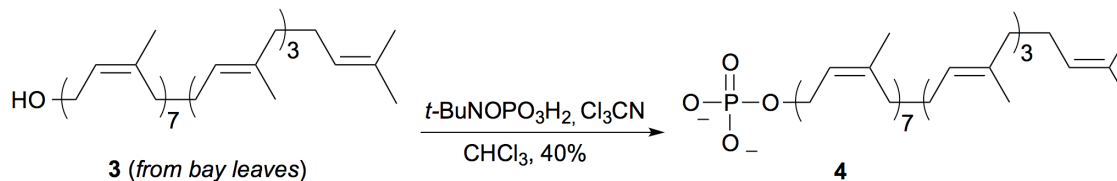
HRMS (ESI) (*m/z*):

calc'd for C₅₅H₉₀ClO, [M+Cl]⁻: 801.669
observed: 801.668

TLC (H₂O/Acetone, 5:95, Silica), R_f:

0.29 (I₂)

Preparation of undecaprenyl phosphate (4)



Undecaprenyl phosphate (**4**) was prepared from *Laurus nobilis*-derived undecaprenol (**3**) (122 mg, 0.16 mmol) following previously described methodology for phosphorylation of polyprenols (Danilov, 1989). Our modifications to the procedure were the following: anion exchange chromatography was conducted using a pre-packed RediSep®Rf SAX column (5.7 g) from Teledyne ISCO. Compound elution was achieved using NH₄Ac (0 mM -> 30 mM -> 150 mM) in CHCl₃/MeOH (2:1). Lipid-linked products were extracted away from salts using a previously published CHCl₃/MeOH/H₂O extraction technique (Farha et al., 2013; Schaffer et al., 2002). The lipid extract was concentrated under reduced pressure and further purified by silica normal-phase chromatography (CHCl₃/MeOH/H₂O in 0.1% aqueous NH₄OH, 97:3:0 -> 65:25:4) to afford **4** (54 mg, 40%) as a white powder.

¹H NMR (700 MHz, MeOH-*d*₄): δ ppm 1.60 (s, 9H), 1.61 (s, 3H), 1.68 (s, 21H), 1.73 (s, 3H), 1.99-2.09 (m, 40H), 4.40 (t, *J* = 6.3 Hz, 2H), 5.10-5.16 (m, 11H), 5.42 (t, *J* = 6.3 Hz, 1H)

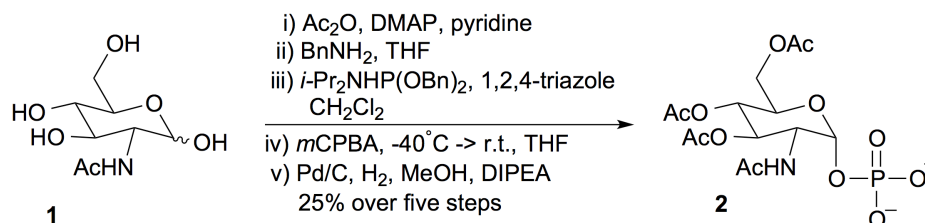
¹³C NMR (176 MHz, MeOH-*d*₄): δ ppm 16.17, 16.19, 17.81, 23.72, 23.76, 23.81, 23.86, 23.88, 25.94, 27.54, 27.58, 27.60, 27.61, 27.63, 27.67, 27.70, 27.75, 27.85, 32.92, 33.25, 33.26, 33.29, 33.33, 40.83, 40.88, 40.90, 62.69 (d, *J*_{C-P} = 5.28 Hz), 124.13 (d, *J*_{C-P} = 8.8 Hz), 125.46, 125.49, 125.50, 125.52, 125.92, 126.16, 126.18, 126.20, 132.03, 135.81, 135.82, 136.02, 136.19, 136.22, 136.24, 136.27, 136.29, 136.41, 139.67.

³¹P NMR (283 MHz, MeOH-*d*₄): δ ppm 1.37
HRMS (ESI) (*m/z*): calc'd for C₅₅H₉₀O₄P, [M-H⁺]: 845.658
observed: 845.661

TLC (CHCl₃/MeOH/H₂O, 65:25:5, Silica), R_f: 0.38 (I₂)

*Our spectral characterization of **4** provides additional information to incomplete ¹H and ¹³C spectra previously reported in the literature (Lee et al., 2009).

Preparation of (2*R*,3*R*,4*R*,5*S*,6*R*)-3-acetamido-4,5-diacetoxy-6-(acetoxymethyl)tetrahydro-2*H*-pyran-2-yl phosphate (2**)**



The α-phosphate (**2**) was synthesized from commercially available *N*-acetyl-D-glucosamine (**1**) according to known methods (Ginsberg et al., 2006; Pereira et al., 2008; Sim et al., 1993; Woodward et al., 2010). In addition to referenced methods, **2** was further purified by C18 reverse-phase chromatography (H₂O/MeCN in 0.1% aqueous NH₄OH, 95:5 → 5:95) to afford **2** (25%) as a brown/yellow film.

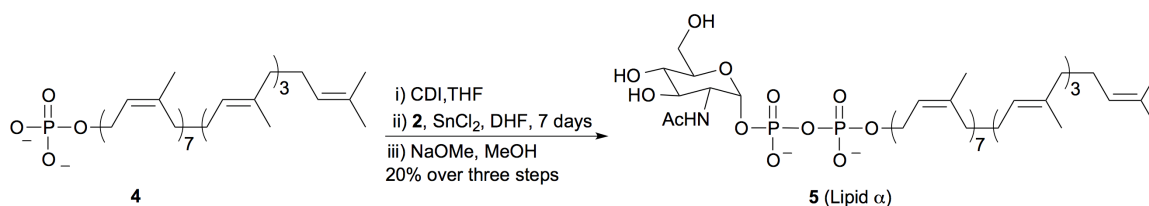
¹H NMR (700 MHz, MeOH-*d*₄): δ ppm 1.94 (s, 3H), 1.96 (s, 3H), 2.00 (s, 3H), 2.05 (s, 3H), 4.18 (d, *J* = 11.9 Hz, 1H), 4.24 (d, *J* = 10.5 Hz, 1H), 4.28 (d, *J* = 11.9 Hz, 1H), 4.33 (d, *J* = 9.8 Hz, 1H), 5.09 (t, *J* = 9.8 Hz, 1H), 5.32 (t, *J* = 9.8 Hz, 1H), 5.48 (bs, 1H)

¹³C NMR (176 MHz, MeOH-*d*₄): δ ppm 20.63, 20.69, 22.60, 53.48, 62.96, 69.46, 69.84, 73.00, 94.91 (d, *J*_{C-P} = 5.63 Hz), 171.35, 172.01, 172.60, 173.61

³¹P NMR (283 MHz, MeOH-*d*₄): δ ppm -0.80

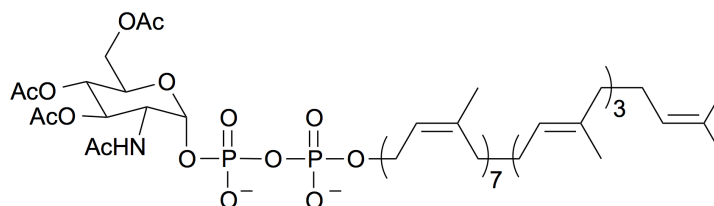
HRMS (ESI) (*m/z*): calc'd for C₁₄H₂₁NO₁₂P, [M-H]⁺: 426.081
observed: 426.080

* Our spectral characterization of **2** provides additional information to ¹H spectra reported for the dibenzylated precursor of **2** (Sim et al., 1993)

Preparation of GlcNAc-PP-undecaprenol (Lipid α) (5)

All steps of the synthesis were performed in oven-dried glassware under argon atmosphere. The ammonium salts of **2** (5 mg, 10.8 μmol , 1.0 equiv) and **4** (10 mg, 11.8 μmol , 1.1 equiv) were placed in separate vessels and co-evaporated three times with anhydrous toluene. The vessels were dried under high vacuum for 3 hours. The ammonium salt of **4** was dissolved in anhydrous THF (2.4 mL) and CDI (9.2 mg, 56 μmol , 5.5 equiv) was added to initiate activation. Reaction progress was monitored by MS showed incomplete activation after 18 hours incubation at ambient temperature. Therefore, an additional amount of CDI (11.6 mg, 72 μmol , 6.1 equiv) was added. Reaction completion was observed after overnight incubation at ambient temperature. The reaction was quenched with anhydrous methanol (20 μL) and stirred for 30 min. The solvents were evaporated and the residue was dried under high vacuum for two hours. Activated **4** was dissolved in DHF (1.5 mL) and transferred to the vessel containing the α -phosphate **2**, after which anhydrous tin(II) chloride (4 mg, 22 μmol , 2 equiv) was added. The reaction mixture was stirred at ambient temperature for one week and quenched with ethylenediaminetetraacetic acid (EDTA) (10 mM, 2.2 mL). Solvents were evaporated and the lipid-linked products were extracted using a previously published $\text{CHCl}_3/\text{MeOH}/\text{H}_2\text{O}$ extraction technique (Farha et al., 2013; Schaffer et al., 2002). The lipid extract was concentrated under reduced pressure and purified by silica normal-phase chromatography ($\text{CHCl}_3/\text{MeOH}$ in 0.2% aqueous NH_4OH , 95:5 \rightarrow 50:50) to afford the peracetylated form of Lipid α (**5**) (3.2 mg, 22%) as a white powder.

Structure of peracetylated form:



Precursor to **5**

^1H NMR (700 MHz, $\text{MeOH-}d_4$): δ ppm 1.60 (s, 9H), 1.61 (s, 3H), 1.65-1.70 (m, 21H), 1.74 (s, 3H), 1.95 (s, 3H), 1.97-1.99 (m, 6H), 1.99 (s, 3H), 1.99-2.17 (m, 40H) 4.20 (dd, $J_a = 2.1$ Hz, $J_b = 12.6$ Hz, 1H), 4.30 (d, $J = 10.5$ Hz, 1H), 4.33 (dd, $J_a = 2.8$ Hz, $J_b = 12.6$ Hz, 1H), 4.41 (d, $J = 9.8$ Hz, 1H), 4.53 (t, $J = 6.3$ Hz, 2H), 5.07-5.18 (m, 12H), 5.34 (t, $J = 10.5$ Hz, 1H), 5.47 (t, $J = 6.3$ Hz, 1H), 5.59 (dd, $J_a = 3.5$ Hz, $J_b = 7$ Hz, 1H)

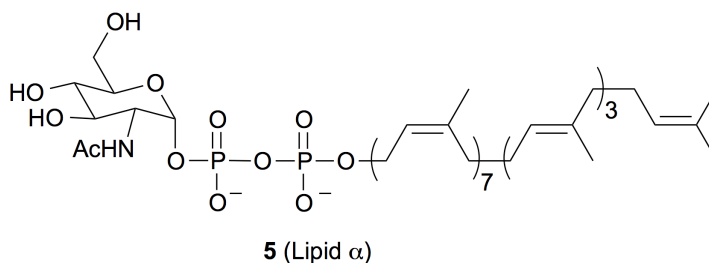
^{31}P NMR (283 MHz, $\text{MeOH-}d_4$): δ ppm -10.17 (d, $J_{P-P} = 21.2$ Hz), -13.21 (d, $J_{P-P} = 20.9$ Hz)

HRMS (ESI) (m/z): calc'd for $\text{C}_{69}\text{H}_{109}\text{NO}_{15}\text{P}_2$, $[\text{M}-2\text{H}]^{2-}$: 626.864
observed: 626.864

TLC ($\text{CHCl}_3/\text{MeOH}/\text{H}_2\text{O}$, 65:25:5, Silica), R_f : 0.36 (I_2)

The peracetylated form of **5** (3.2 mg, 2.6 μmol) was evaporated three times with anhydrous methanol and placed under high vacuum for two hours. The residue was then dissolved in anhydrous methanol (4 mL) and a 23% (v/v) NaOCH_3 in methanol solution (0.9 mL) was added dropwise to initiate deacetylation. The reaction mixture was stirred at ambient temperature for one hour, quenched with ammonium acetate (1.2 mL, 0.5 M in H_2O) and stirred again at ambient temperature for 30 min. The solvents were evaporated and the residue was dried under high vacuum for 3 hours. Lipid α (**5**) was isolated from reaction components following known lipid extraction methods (Farha et al., 2013; Schaffer et al., 2002) to afford **5** (2.7 mg, 92%) as a white powder. Lipid α (**5**)

was thus obtained in 5% yield over the entire synthetic procedure when considering overall yields during the preparation of α -phosphate **2**, and over the final coupling and deprotection steps.



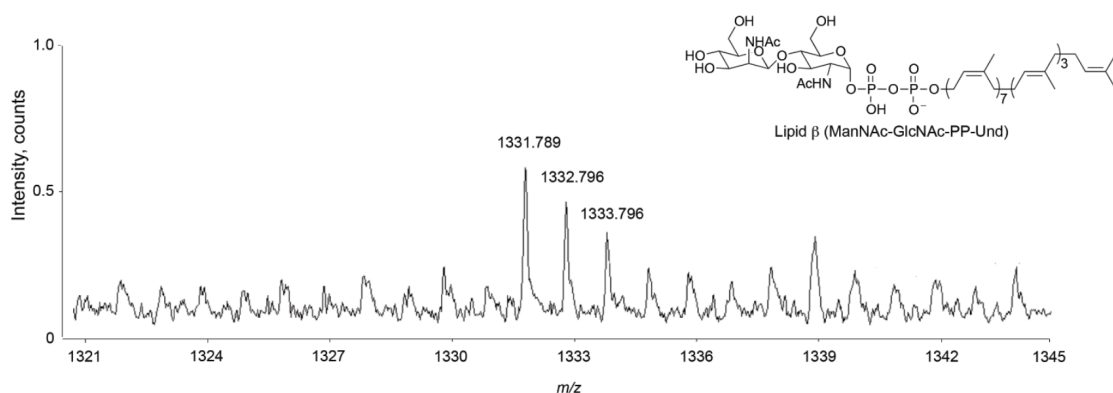
*The final product proved too insoluble to obtain suitable spectral data, as has been reported for other undecaprenyl-linked glycosyl diphosphates. (Holkenbrink et al., 2011; Woodward et al., 2010)

HRMS (ESI) (m/z): calc'd for $C_{63}H_{103}NO_{12}P_2$, $[M-2H^+]^{2-}$: 563.849
observed: 563.848

TLC ($CHCl_3/MeOH/H_2O$, 65:25:5, Silica), R_f : 0.3 (I_2)

Supplementary figures

a



b

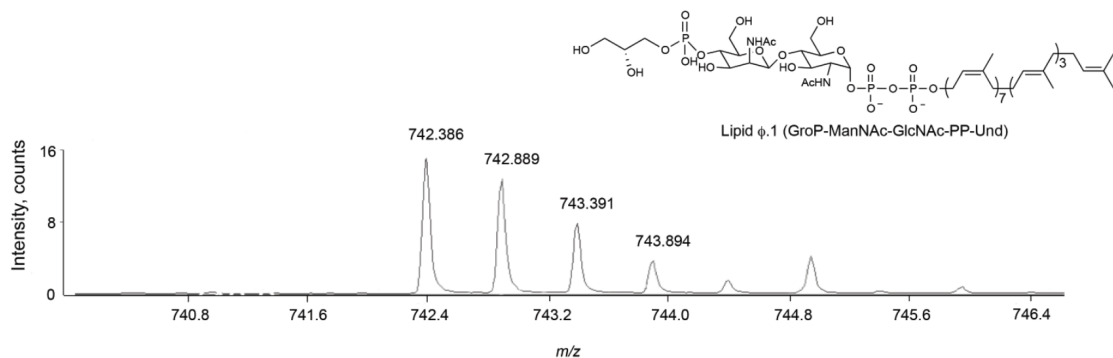


Figure S1. HRMS of WTA intermediates produced *in vitro*. Negative-ion electrospray ionization mass spectrum (ESI-MS) of lipid extracted products from: **(a)** Non-radioactive reaction involving TagA, semi-synthesized Lipid α , and UDP-ManNAc; **(b)** Non-radioactive reaction involving TagA, TagB, semi-synthesized Lipid α , UDP-ManNAc, and CDP-glycerol. The exact m/z of the $[M-H]^+$ for Lipid β is 1331.783. The exact m/z of the $[M-2H]^2-$ for Lipid $\phi.1$ is 742.389.

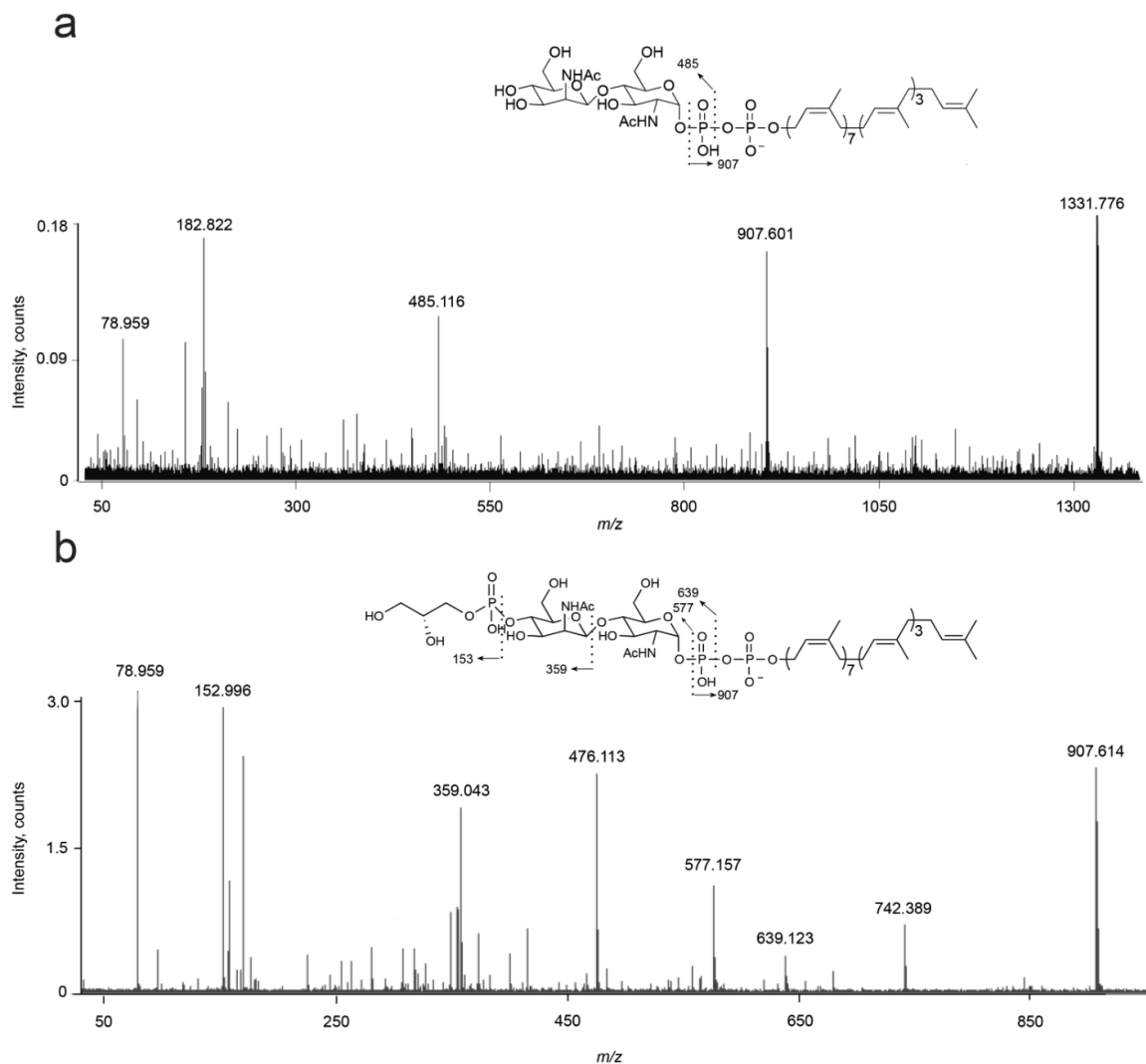
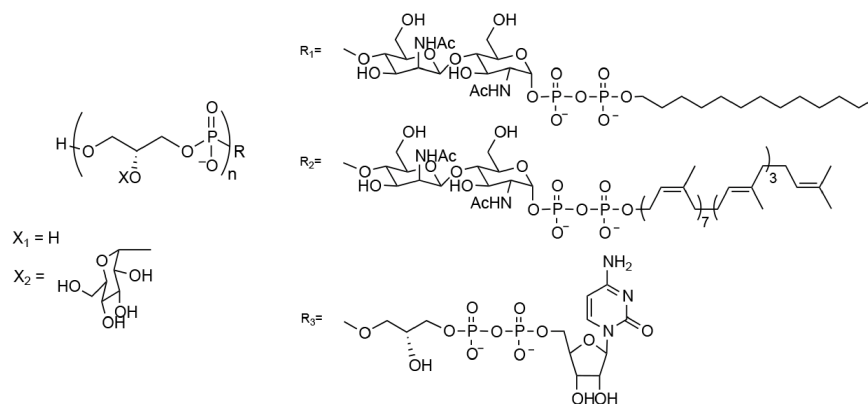


Figure S2. Negative-ion collision-induced dissociation mass spectra (MS/MS) of WTA intermediates produced *in vitro*. MS/MS spectra were obtained for the ions corresponding to **(a)** Lipid β (m/z 1331.783) and **(b)** Lipid $\phi.1$ (m/z 742.389). The inset shows the predicted product ions for each.

a



b

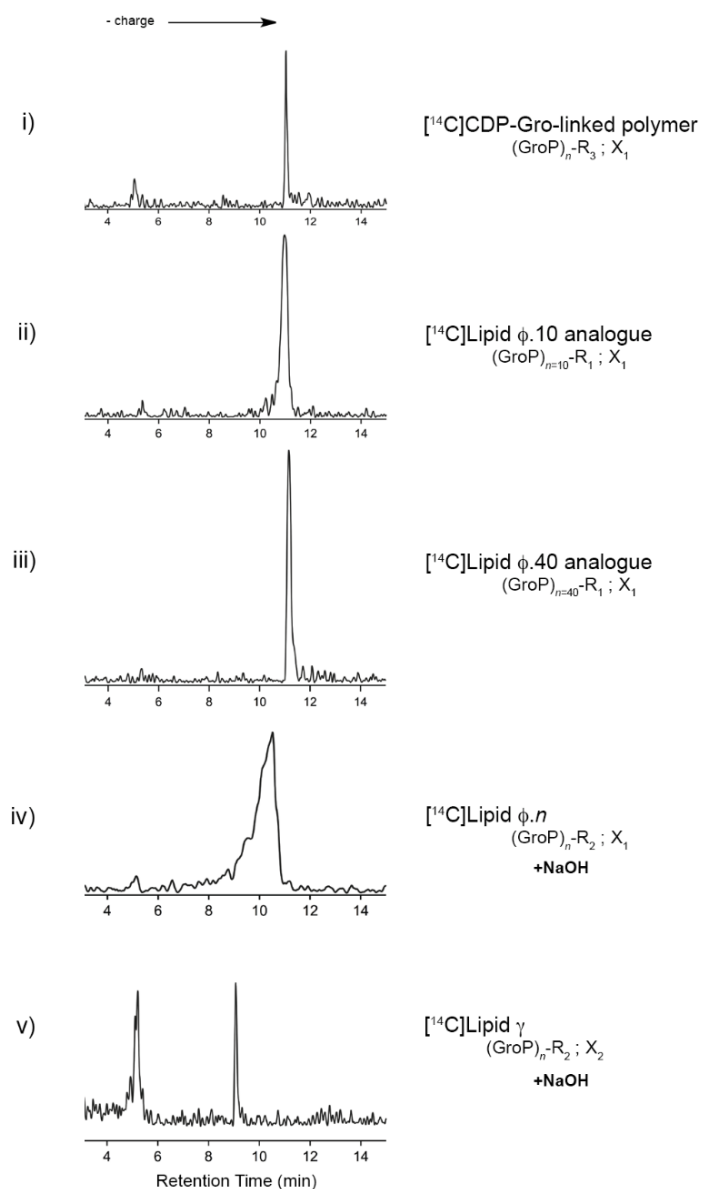


Figure S3. TagF and TagE reaction products are polyanionic. (a) A depiction of poly(glycerol phosphate) polymers synthesized for anion exchange HPLC analysis. Polymers were built on: tridecyl-linked substrates (R_1) bearing 10 and 40 glycerol phosphate repeats ($n=10,40$); native undecaprenyl-linked substrates (R_2) through enzymatic elaboration of semisynthetic Lipid α (**5**); and CDP-Gro (R_3). In addition, some polymers were chemically tailored with α -linked glucose (X_2). **(b)** Anion exchange HPLC profile of chemically distinct radioactive WTA polymers. Radioactivity was incorporated into polymers during synthesis from either CDP- $[^{14}\text{C}]$ Gro (profiles i-iv) or UDP- $[^{14}\text{C}]$ glucose (profile v) precursors. Polymer nomenclature and composition of reaction products following synthesis are indicated to the right of the frame. '+ NaOH' indicates reaction products further subjected to mild alkaline conditions (0.5 M NaOH, 37°C, 25 min) prior to anion exchange HPLC analysis. Elution profiles for the following are shown: i) CDP-Gro-linked polymer; ii) Lipid ϕ .10 analogue; iii) Lipid ϕ .40 analogue; iv) mild alkali-treated TagF reaction mixture after 4 hours of incubation with enzyme and Lipid ϕ .1; and v) mild alkali-treated TagE reaction mixture after 4 hours of incubation with enzyme and Lipid ϕ . n .

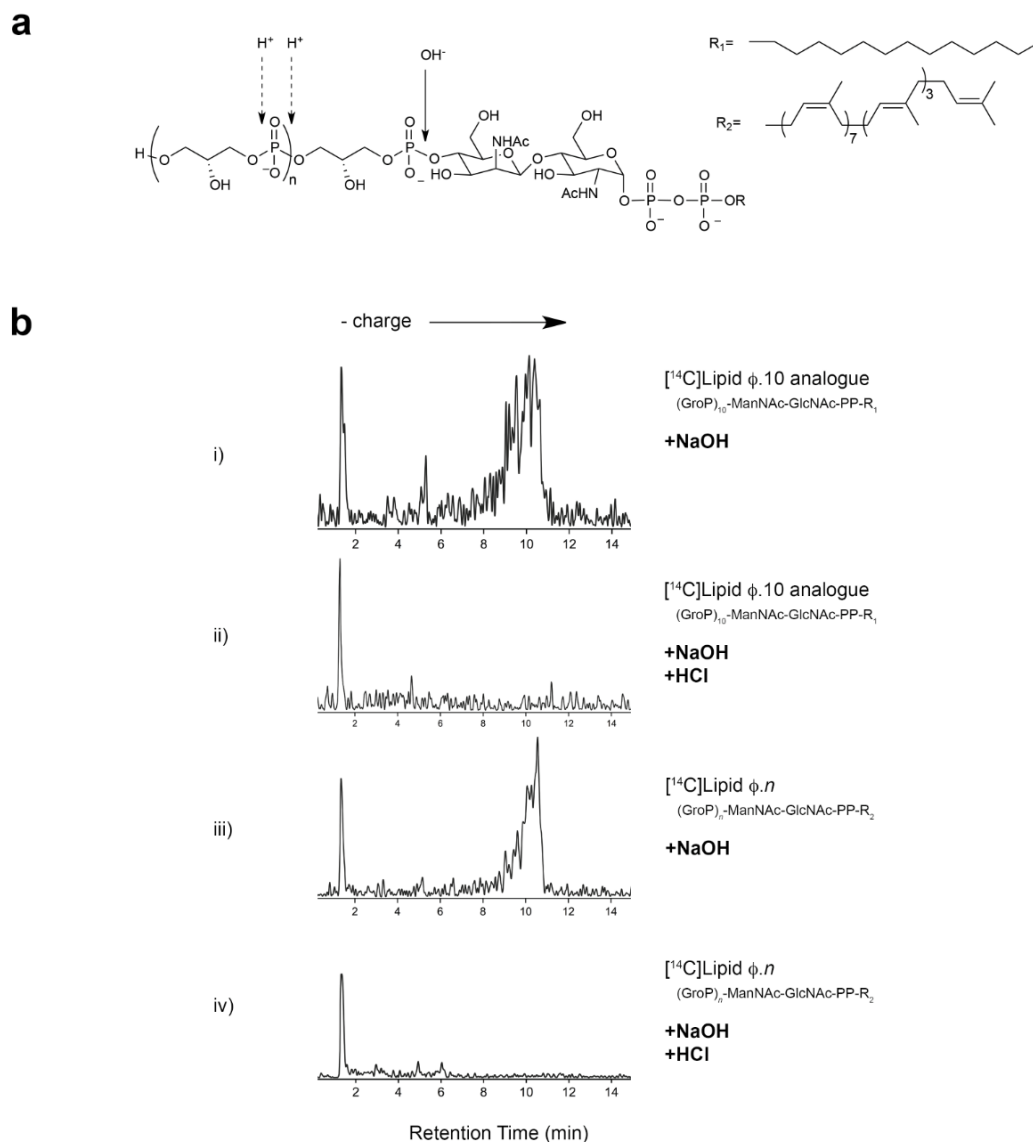


Figure S4. The TagF reaction product shows typical WTA lability patterns. (a) Chemical structure of WTAs prepared for anion exchange HPLC analysis. Poly(glycerol phosphate) polymers were built on tridecyl (R₁) and undecaprenyl (R₂) lipid chains. Relevant linkages that are labile under mild acid (H⁺) and mild alkali (OH⁻) conditions during *in vitro* assays are shown with dashed and solid arrows respectively. **(b)** Anion exchange HPLC profile of hydrolyzed WTA polymers. Radioactivity was incorporated into synthesized polymers from a CDP-[¹⁴C]Gro precursor. Polymer nomenclature and composition prior to acid/base treatment are indicated to the right of the frame. In addition, treatment of polymers to mild alkali (0.5 M NaOH, 37°C, 25 min) and/or mild acid (1N HCl, 100°C, 3 hours) conditions are indicated with '+NaOH' and '+HCl' labels respectively. Elution profiles for the following are shown: i) Lipid $\phi.10$ analogue treated with NaOH; ii) Lipid $\phi.10$ analogue treated with NaOH then HCl; iii) TagF reaction mixture after 4 hours of incubation with enzyme and Lipid $\phi.1$ treated with NaOH; iv) same as iii) with subsequent HCl treatment.

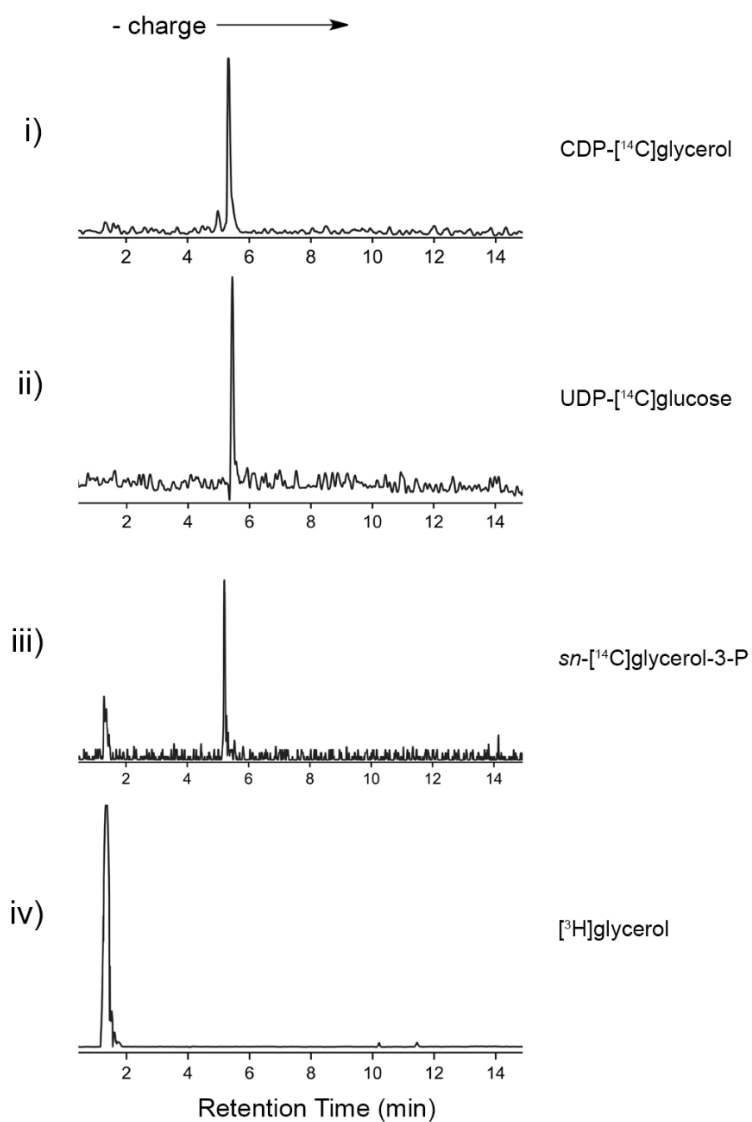


Figure S5. Radioactive standards for anion exchange HPLC analysis. Standards subject to anion exchange HPLC analysis are indicated to the right of the frame. Elution profiles for the following compounds are shown: i) CDP-[U- ^{14}C]glycerol; ii) UDP-[^{14}C]glucose; iii) *sn*-[U- ^{14}C]glycerol-3-phosphate; and iv) [2- ^3H]glycerol.

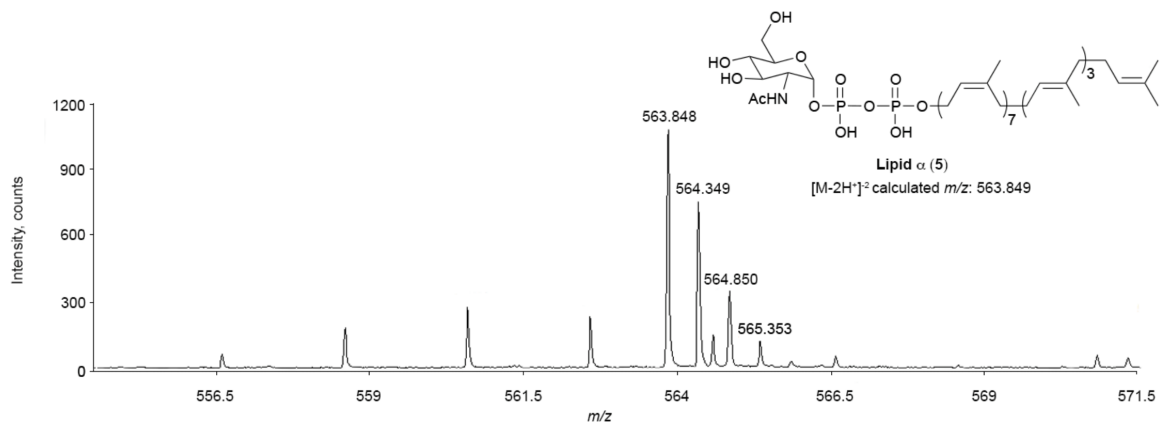
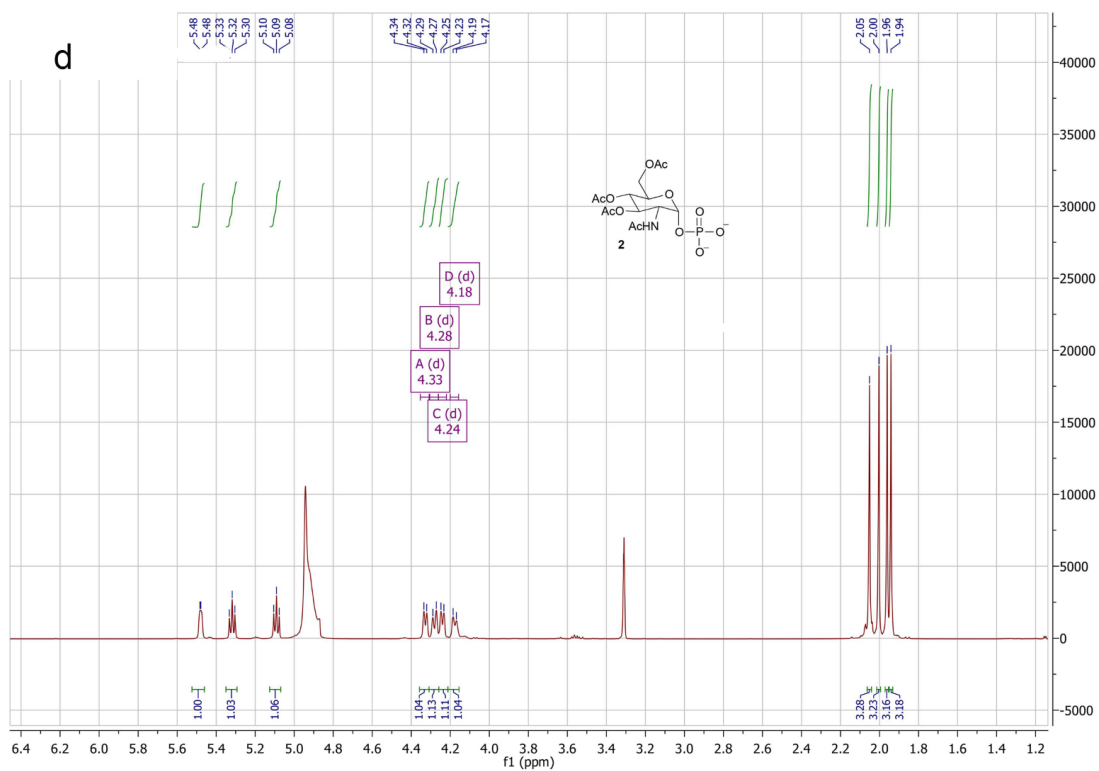
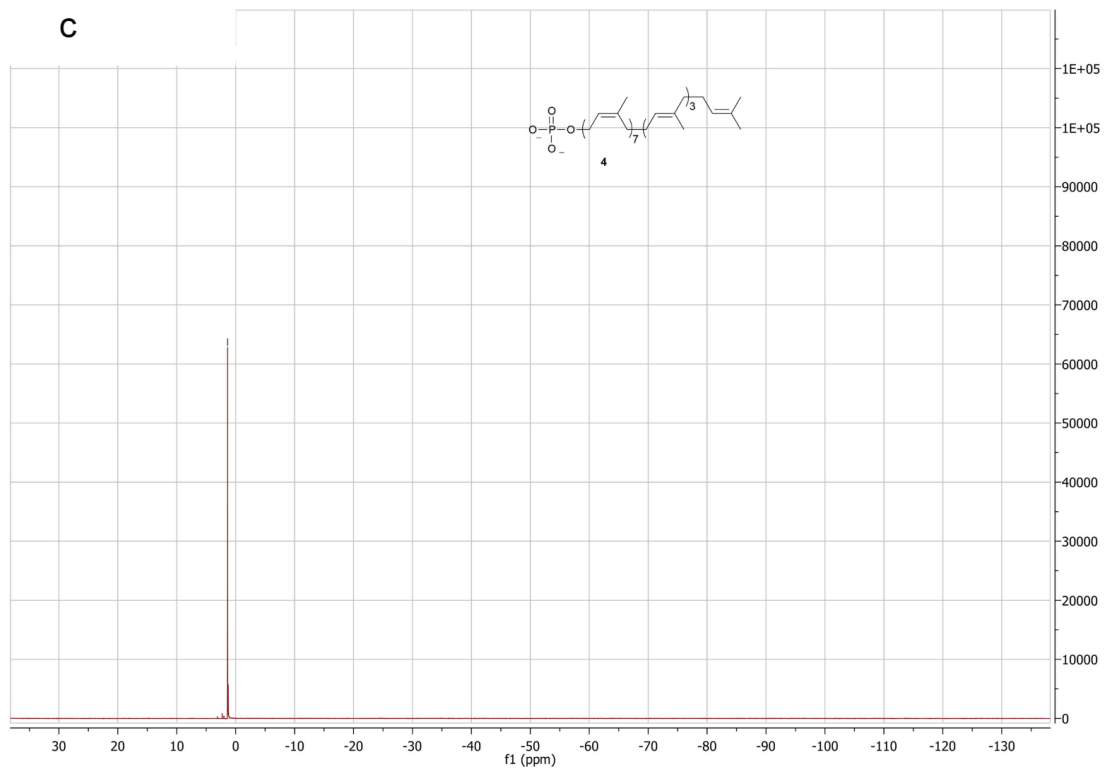
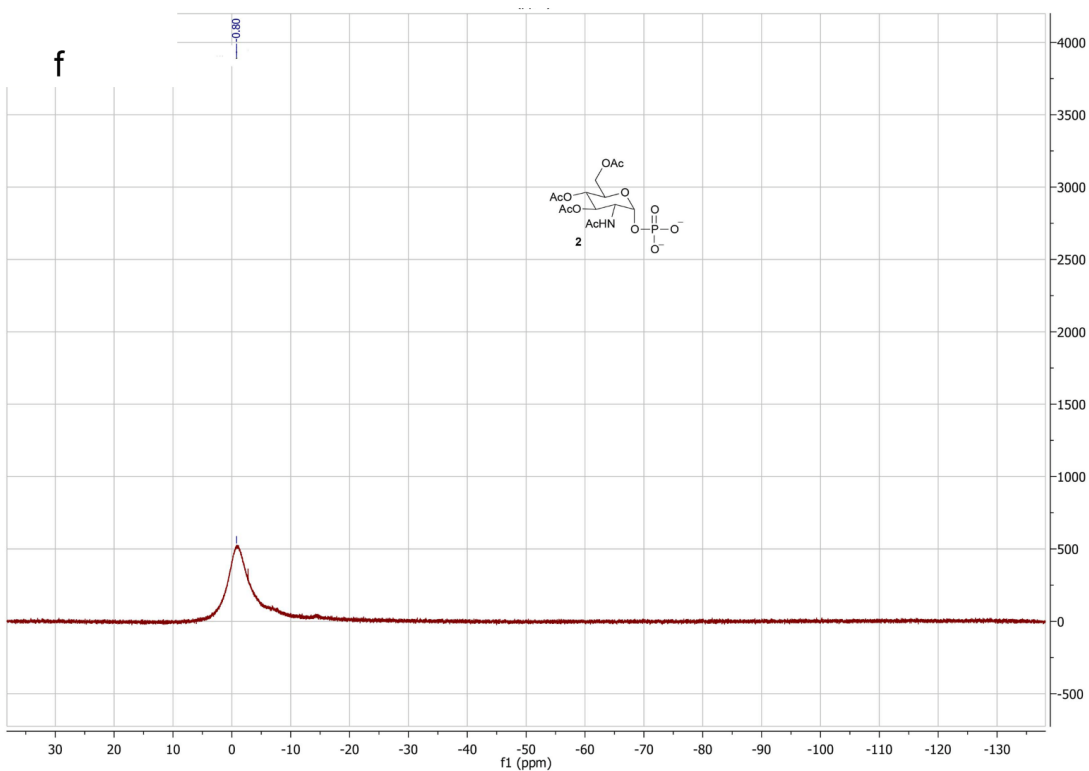
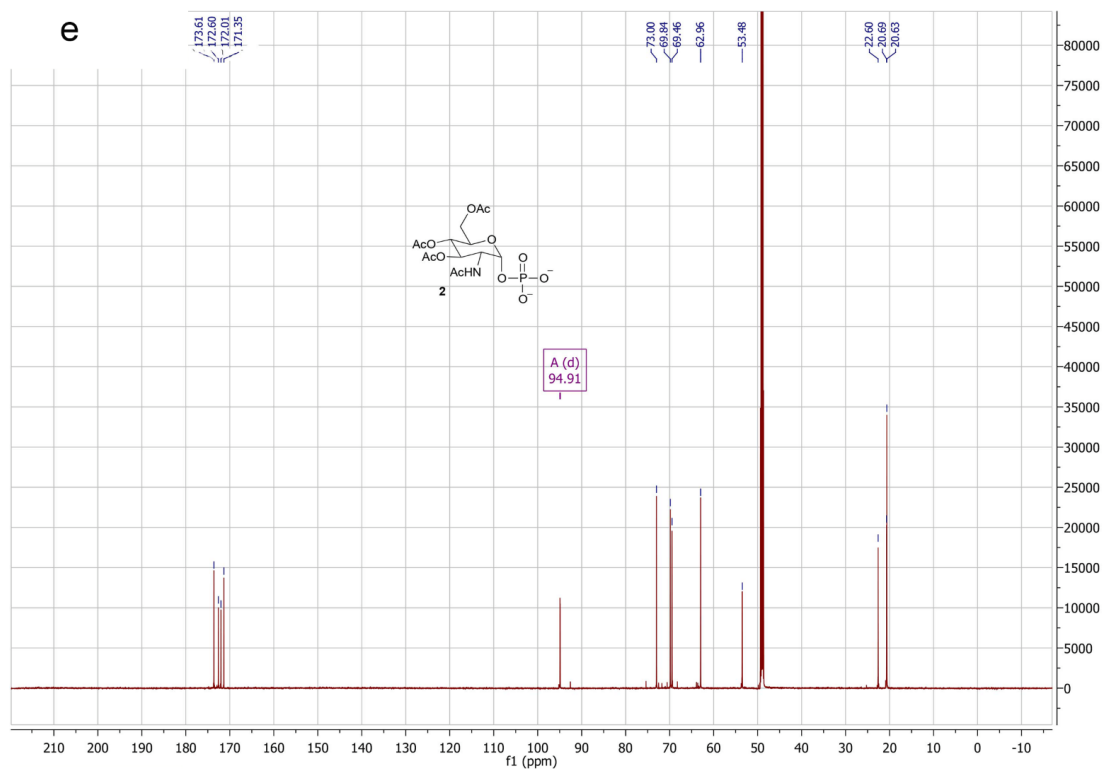
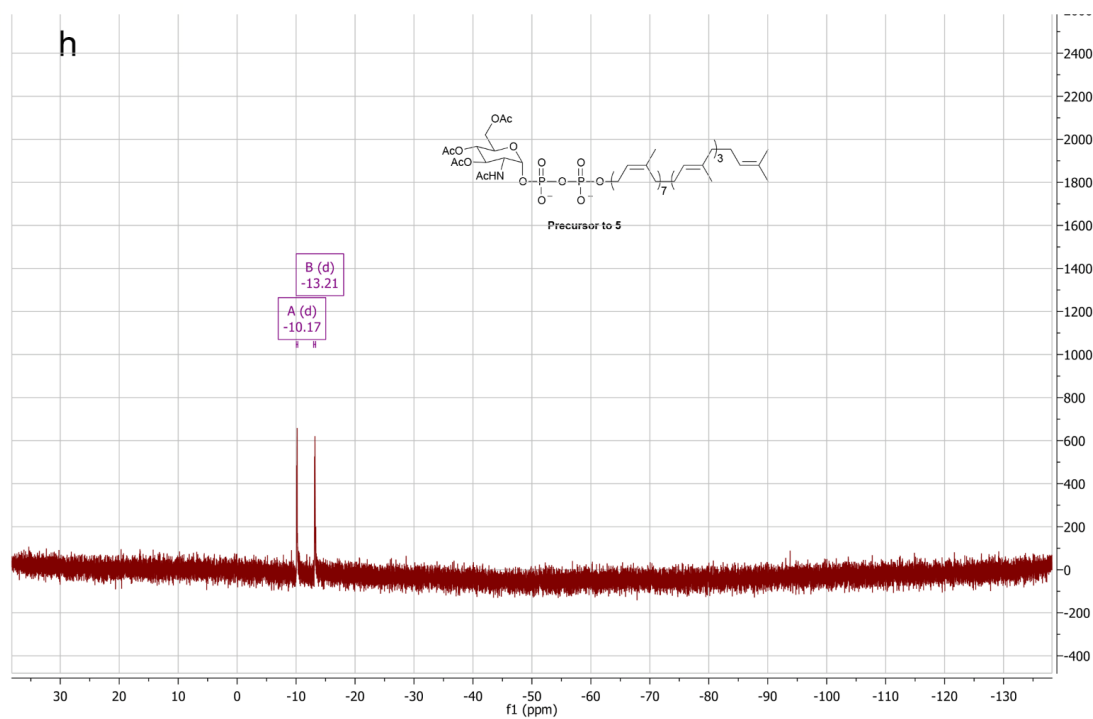
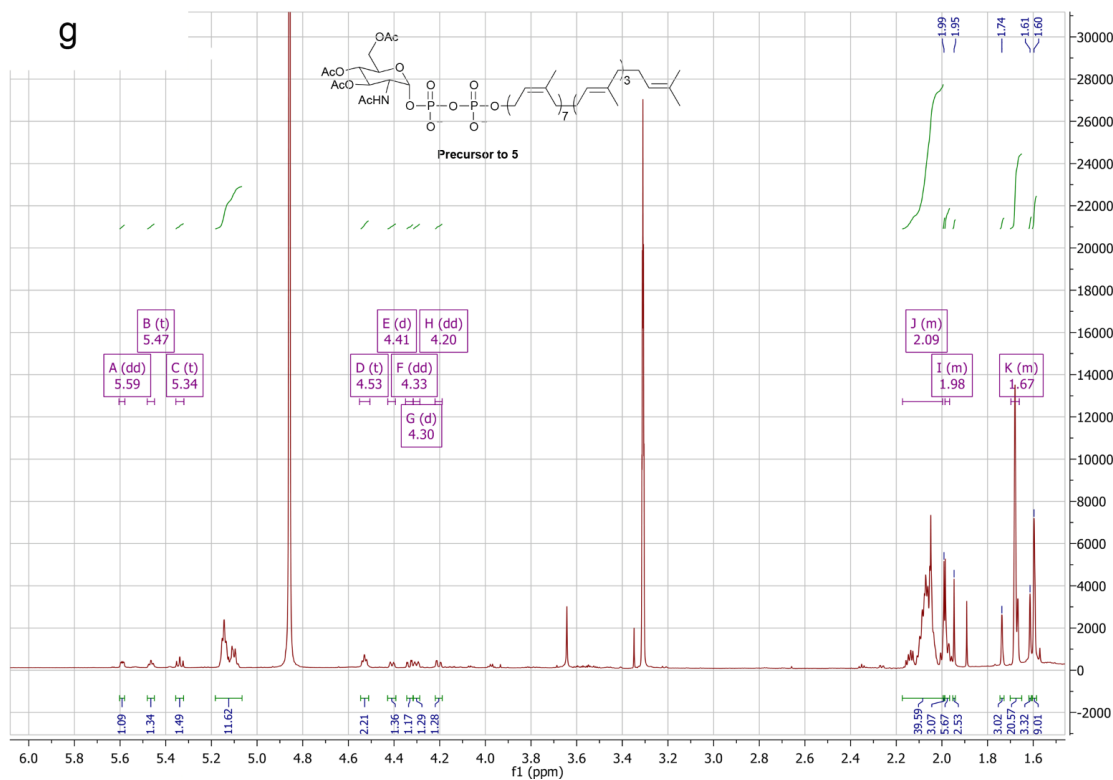


Figure S6. HRMS of synthesized materials. Negative-ion electrospray ionization mass spectrum (ESI-MS) of compounds 2-5 and the peracetylated form of 5. Chemical structure and calculated m/z are provided for each molecule.









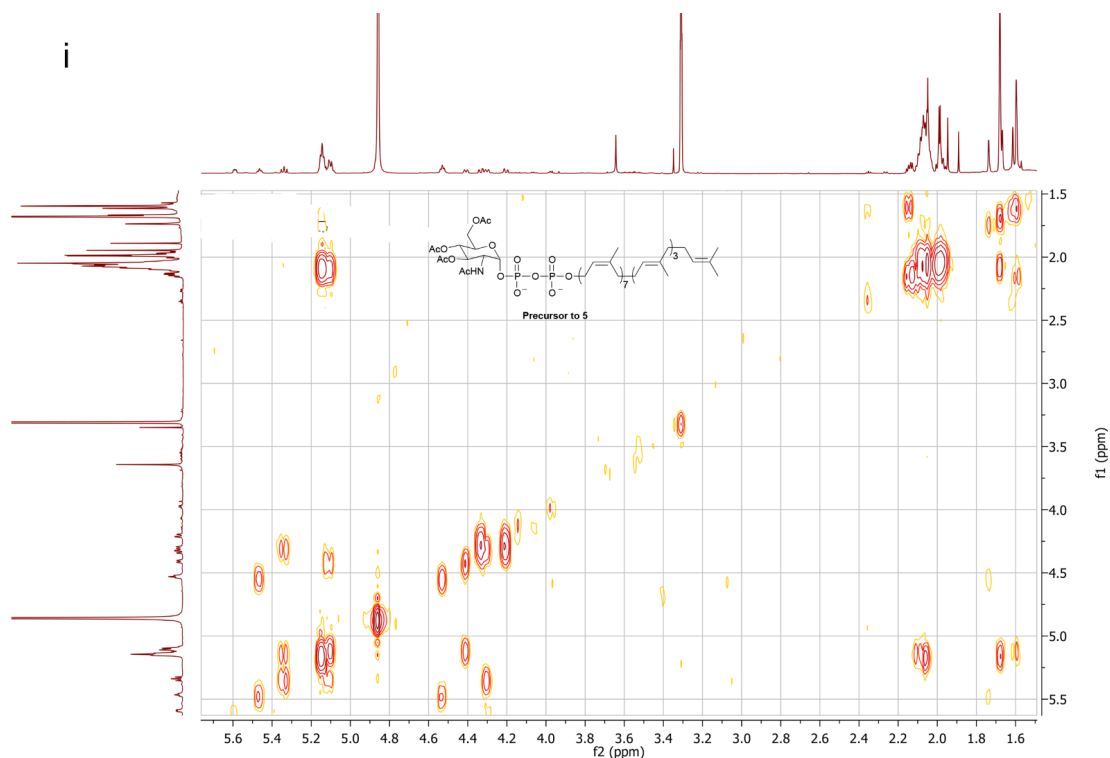


Figure S7. NMR analysis of synthesized materials. Compounds **2** (d-f), **4** (a-c), and peracetylated **5** (g-i) were analyzed. ^1H NMR (a,d, and g); ^{13}C NMR (b and e); ^{31}P NMR (c,f, and h); ^1H - ^1H COSY (i).

CHAPTER III – *B. subtilis* LytR-CpsA-Psr enzymes transfer wall teichoic acids from authentic lipid-linked substrates to mature peptidoglycan *in vitro*

Preface

The work presented in this chapter was previously published in:

Gale, R.T., Li, F.K.K., Sun, T., Strynadka, N.C.J., and Brown, E.D. (2017). *B. subtilis* LytR-CpsA-Psr enzymes transfer wall teichoic acids from authentic lipid-linked substrates to mature peptidoglycan *in vitro*. *Cell Chem. Biol.* **24**, 1537-1546

Permission has been granted by the publisher to reproduce the material herein.

I performed all experiments. Li, F.K.K. and Sun, T. provided *S. aureus* LCP enzymes. I wrote and edited the manuscript with input from all authors.

Summary

Gram-positive bacteria endow their peptidoglycan with glycopolymers that are crucial for viability and pathogenesis. However, the cellular machinery that executes this function is not well understood. While decades of genetic and phenotypic work have highlighted the LytR-CpsA-Psr (LCP) family of enzymes as cell wall glycopolymer transferases, their *in vitro* characterization has been elusive, largely due to a paucity of tools for functional assays. In this report, we synthesized authentic undecaprenyl diphosphate-linked wall teichoic acid (WTA) intermediates and built an assay system capable of monitoring LCP-mediated glycopolymer transfer. We report that all *B. subtilis* LCP enzymes anchor WTAs to peptidoglycan *in vitro*. Furthermore, we probed the catalytic requirements and substrate preferences for these LCP enzymes and elaborated *in vitro* conditions for facile tests of enzyme function. This work sheds light on the molecular features of glycopolymer transfer and aims to aid drug discovery and development programs exploiting this promising antibacterial target.

Introduction

Bacteria commonly synthesize a cell wall peptidoglycan composed of glycan hetero-polymers bridged by short peptides (Bugg and Walsh, 1992). In addition to providing protection from environmental challenges, this structure specifies cell shape, resists turgor pressure, and scaffolds numerous proteins and glycopolymers (Höltje, 1998). Peptidoglycan is synthesized in several distinct stages: i) cytoplasmic generation of a soluble building block UDP-*N*-acetylmuramic acid pentapeptide, ii) preparation and translocation of polyisoprenoid-linked intermediate Lipid II at the cytoplasmic membrane, iii) polymerization of Lipid II to form glycan strands and iv) incorporation of nascent strands into the existing peptidoglycan layer via peptide cross-linking (for a review see Egan and Vollmer, 2012). This meshwork-like structure is constantly

being built, modified and hydrolyzed as cells grow and divide (Egan and Vollmer, 2012; Johnson et al., 2013). In addition, its composition, organization, and architecture can drastically vary across bacteria (Turner et al., 2014).

Recent discoveries, due in part to a surge of novel chemical tools (reviewed in Gale and Brown, 2015), have begun to challenge the conventional understanding of peptidoglycan assembly. *In situ* labeling of peptidoglycan has identified peptidoglycan in organisms long-thought to be devoid of the structures and has enabled the real-time study of assembly and dynamics (Liechti et al., 2016; 2015). Furthermore, members of the SEDS (shape, elongation, division, and sporulation) family are now thought to perform crucial peptidoglycan glycosyltransferase functions (Leclercq et al., 2017; Meeske et al., 2016; 2015). These findings are encouraging at a time when we have witnessed a dramatic erosion in the utility of antibiotic drugs once successful at interfering with peptidoglycan formation. Indeed, antibacterial drug discovery has declined precipitously and has failed to subvert the alarming rise of resistance to cell-wall targeting antibiotics like β -lactams and glycopeptides (Brown and Wright, 2016). Unveiling novel features surrounding peptidoglycan wall assembly may provide new therapeutic targets for modern antibacterial drug discovery programs.

The covalent attachment of glycopolymers to peptidoglycan is an enigmatic feature of cell wall assembly. Gram-positive bacteria, in particular, enhance their peptidoglycan sacculus with a repertoire of glycopolymers. For instance: pathogens attach long-chain capsular polysaccharides as a means to evade host immunity (O'Riordan and Lee, 2004); mycobacteria anchor a rigid and highly antibiotic-resistant arabinogalactan-mycolic acid complex (Marrakchi et al., 2014); and most Gram-positive bacteria tether several secondary polymers like wall teichoic acids (WTAs) that serve a myriad of crucial cellular functions

(Schäffer and Messner, 2005; Weidenmaier and Peschel, 2008). WTAs are phosphate-rich anionic polymers composed of repeating alditol phosphate residues. These polymers alone can account for up to 50% of the dry weight of cell wall in certain bacteria (Neuhaus and Baddiley, 2003). Importantly, WTAs are key determinants of virulence and antibiotic resistance and have thus been the target of numerous screening campaigns to find inhibitors (Lee et al., 2016; Sewell and Brown, 2014).

Genetic and phenotypic studies suggest that the LytR-CpsA-Psr (LCP) family of enzymes perform the glycopolymer transfer step. These proteins are found almost exclusively in Gram-positive bacteria (Hübscher et al., 2008).

Staphylococcus aureus and *B. subtilis* *lcp* gene deletion mutants display hallmark characteristics of cells devoid of glycopolymers, particularly WTAs. These include altered cell wall structures, increased susceptibility to antibiotics, and reduced virulence (Hübscher et al., 2009; Kawai et al., 2011; Over et al., 2011). While LCP enzymes are thought to be partially redundant *in vivo* (Over et al., 2011), certain members have been shown to be essential (Baumgart et al., 2016; Harrison et al., 2016). Despite over a decade's worth of investigations into this enzyme family, the *in vitro* biochemical characterization of glycopolymer transfer has largely been elusive. While there is ready access to recombinant LCP enzymes, challenges to reconstitute transferase activity arise from an incomplete understanding of biosynthetic events and in the acquisition of complex substrates; thus, even the most basic features of glycopolymer tethering remain obscure.

Here, we leveraged our recent success in preparing undecaprenyl diphosphate-linked WTAs (Gale et al., 2014) to provide authentic donor glycopolymers for transferase reactions. We report that all *B. subtilis* LCP members can transfer

WTAs to commercially available cross-linked peptidoglycan. This work contributes to very recent efforts focused on capturing LCP-mediated glycopolymer transfer *in vitro* (Harrison et al., 2016; Schaefer et al., 2017); however, our system is unique in its capacity to quantify activity. Thus, we were able to probe reaction requirements, compare activity between LCP enzymes, evaluate acceptor and donor substrate preferences and develop assay conditions for the ready evaluation of inhibitors of LCP-mediated catalysis. Taken together, this work provides new insights into the molecular details of glycopolymer transfer and serves to aid drug discovery and development programs targeting LCP enzymes.

Results

B. subtilis* LCP Enzymes Transfer WTA Intermediates to Mature Peptidoglycan *In Vitro

To reconstitute the WTA-peptidoglycan tethering reaction *in vitro*, we first purified truncated constructs of *B. subtilis* LCP enzymes TagT (YwtF), TagU (LytR), and TagV (YvhJ) (Figure S1). We found removing the conserved transmembrane domain - which anchors LCP proteins to the cytoplasmic membrane and orients the catalytic domain to the extramembrane region - greatly improved protein expression and subsequent purification. While LCP enzymes have been identified as likely glycopolymer transferases, their catalytic requirements have eluded characterization. This includes their preferences for glycopolymer donor and peptidoglycan acceptor substrates.

WTA biosynthesis in *B. subtilis* 168 culminates with the formation of polyisoprenoid-linked Lipid γ (Table 1; for a review, see Brown et al., 2013). The phosphoanhydride bond of this molecule is disrupted during LCP-mediated catalysis to facilitate the attachment of the glycosidic WTA polymer to peptidoglycan. Previous studies have shown that LCP enzymes bind

polyisoprenoid phosphate lipids when expressed and purified from heterologous hosts (Kawai et al., 2011). Thus, we reasoned that extensions beyond this moiety found in Lipid γ , particularly the polymeric components, may not be necessary for catalysis. Therefore, we synthesized an authentic early WTA intermediate Lipid β (Table 1; Figure S2), which contains only a disaccharide following the polyisoprenoid pyrophosphate anchor, to use in transferase assays (Gale et al., 2014). Radioactivity was incorporated in this molecule as a means to monitor reaction progression.

The identity of the peptidoglycan acceptor substrate has long been the subject of speculation. Analyses of bacterial cell wall preparations show that WTAs anchor to the C(6) hydroxyl group of peptidoglycan *N*-acetylmuramic acid (Kojima et al., 1985); however, this moiety is available for attachment throughout multiple stages of peptidoglycan biosynthesis (for a review see Egan and Vollmer, 2012). Given the extramembrane location of the LCP catalytic domain, the most plausible physiological peptidoglycan acceptor substrate(s) include Lipid II (Table S1), nascent glycan strands (non-crosslinked), and/or mature peptidoglycan (crosslinked). We failed in our attempts to reconstitute transfer of WTA intermediates to Lipid II (Lys) (data not shown). Therefore, it seemed likely that only the highly-ordered peptidoglycan structures could serve as acceptors for the transferase reaction. Advantageously, cell wall sacculi are easily prepared and lyophilized preparations are also available from commercial sources.

Harrison et al. (2016) recently designed a membrane-based assay that monitors LCP-mediated arabinogalactan-peptidoglycan tethering *in vitro*. We took inspiration from this work and built a membrane-free system to assess incorporation of [^{14}C]Lipid β into insoluble peptidoglycan by LCP enzymes (Figure 1A). If [^{14}C]Lipid β is affixed to the peptidoglycan sacculi in our assay system, the

radiolabel can be tracked as a disaccharide phosphate tether. The product peptidoglycan is purified from soluble reaction components via sedimentation. This material is then thoroughly washed with boiling SDS to remove any non-covalently associated proteins and lipids (Glauner et al., 1988). We looked for transfer in this membrane-free system, using only our defined substrates and recombinant LCP enzymes. As a first test, we set-up reactions with a mixture of all three truncated LCP enzymes from *B. subtilis*, synthetic [^{14}C]Lipid β and *B. subtilis* mature peptidoglycan. While there was less than 10% turnover of the total [^{14}C]Lipid β material in our assay system, we found significant amounts of the WTA glycopolymer to be covalently attached to peptidoglycan compared to negative reaction controls (Figure 1B, lanes 1-3; $p < 0.01$).

Having built an assay system capable of quantifying transferase activity across a variety of conditions, we were well-positioned to begin probing the requirements of LCP-mediated catalysis. Several crystal structures of LCP enzymes contain bound polyisoprenoid molecules and divalent cations (Eberhardt et al., 2012; Kawai et al., 2011); thus, it seemed likely that catalysis depended on these features. To test if efficient catalysis requires polyisoprenoid-linked molecules, we employed a soluble [^{14}C]Lipid β analog (Pereira et al., 2008) in transferase assays. This molecule contains a short aliphatic chain (C_{13}) in place of the undecaprenyl moiety (C_{55}) found in authentic Lipid β (Table 1). We observed a reduction in activity of ~95% with the use of this substrate analog (Figure 1B, lanes 1 and 4; $p < 0.01$). To test the thesis that transferase activity requires divalent cations, we added the metal-scavenging agent EDTA to our system that already contained Mg^{2+} . We found that EDTA abolished the *in vitro* transferase activity of *B. subtilis* LCP enzymes (Figure 1B, lane 5).

Gram-positive bacteria can encode anywhere from 1 to 11 LCP enzymes (Hübscher et al., 2008). *B. subtilis* and *S. aureus* both contain three LCP family members, and genetic and phenotypic studies suggest these proteins may be functionally redundant in their respective organisms (Kawai et al., 2011; Over et al., 2011). We were curious to test which *B. subtilis* LCP enzymes specifically had transferase activity in our *in vitro* system. Therefore, we set-up transferase assays with only one representative *B. subtilis* LCP member. We found that all truncated LCP proteins had the capacity to transfer [¹⁴C]Lipid β intermediates to *B. subtilis* peptidoglycan (Figure 1C). Interestingly, the *B. subtilis* LCP homologs displayed varying activities (Figure 1C); The truncated TagU protein showed close to 3-fold higher transferase activity compared to the other LCP proteins ($p < 0.01$). All truncated proteins showed significantly higher activity compared to their heat-inactivated negative controls ($p < 0.01$). We also prepared and assayed *S. aureus* LCP enzymes, but could not reconstitute activity in our *in vitro* system (data not shown).

Therefore, our *in vitro* transferase assay system yielded several key findings: (1) LCP enzymes can conduct transfer without auxiliary cofactors or a phospholipid-rich environment; (2) all truncated *B. subtilis* LCP enzymes transfer WTA glycopolymers; (3) both the polyisoprenoid moiety of the donor molecule and the divalent cation Mg^{2+} are required for catalysis; and (4) *B. subtilis* TagU displays the highest *in vitro* WTA glycopolymer transferase activity.

TagU-Mediated Activity Varies with Alternative Acceptor/Donor Substrates and is Linear with Time and Enzyme Concentration

We were intrigued by recent work demonstrating that *B. anthracis* LCP enzymes could act as surrogate WTA transferases when expressed in *S. aureus* (Liszewski Zilla et al., 2014). In *B. anthracis*, these enzymes likely transfer a

chemically distinct secondary polymer to a peptidoglycan structure that differs in composition to the glycine-rich *S. aureus* murein sacculus (Oh et al., 2016).

These experiments suggest that LCP enzymes have relaxed substrate preferences for both the peptidoglycan acceptor and the glycopolymer donor.

To evaluate the peptidoglycan acceptor preferences of LCP enzymes, we compared TagU-mediated [^{14}C]Lipid β transfer to commercially-available peptidoglycan sacculi derived from either *B. subtilis* or *Streptomyces* sp. While the glycan heteropolymers in these peptidoglycan structures are built from broadly conserved GlcNAc-MurNAc (GlcNAc, *N*-acetylglucosamine; MurNAc, *N*-acetylmuramic acid) disaccharides, the overall chemistry and architecture of each mature sacculus is highly variable (Vollmer, 2008; Turner et al., 2014). We found significant differences in TagU-mediated transferase activity between the two peptidoglycan sources (Figure 2A). Interestingly, the best acceptor substrate for *B. subtilis* TagU was its cognate peptidoglycan material, where $\sim 95\%$ higher transferase activity was observed ($p < 0.01$).

Our initial investigations of LCP-mediated glycopolymer transfer utilized the early WTA intermediate Lipid β . We were next interested in seeing if more physiologically relevant molecules would suffice as donor glycopolymers. Therefore, we synthesized late-stage WTA intermediates [^{14}C]Lipid $\phi.1$, [^{14}C]Lipid $\phi.n$, and [^{14}C]Lipid γ (Table 1) following previously established methods (Figure S2; Gale et al., 2014). Radioactivity was incorporated into the glycerol phosphate moieties of these molecules to make them trackable *in vitro*. Transferase reactions were conducted as before, using TagU and insoluble *B. subtilis* peptidoglycan. Our data show that TagU anchored all late-stage WTA biosynthetic intermediates onto mature *B. subtilis* peptidoglycan. We found that significantly higher transfer activity occurred with the use of Lipid $\phi.1$ compared to

the polymeric Lipid $\phi.n$ donor molecule when assayed at similar concentrations (Figure 2B; $p < 0.01$). We note here that difficulties with insolubility of polymeric intermediates Lipid $\phi.n$ and Lipid γ may have hampered their availability over the course of the reaction, thus lowering the observed incorporation rate.

LCP enzymes represent exciting targets for modern drug discovery programs. Thus, we endeavored to find reaction conditions under which transferase activity is linear with both time and enzyme concentration. In this reaction window, new chemical matter targeting LCP members can be assessed for *in vitro* efficacy. Employing our most active LCP enzyme, truncated TagU, we monitored [^{14}C]Lipid β incorporation into *B. subtilis* peptidoglycan and found conditions meeting the above criteria (Figure 2C). The apparent turnover by TagU was modest (~ 0.025 / hr), consistent with assay conditions lacking many physiological components. Nevertheless, the ready availability of cell wall sacculi provides for a facile platform to probe catalysis by these enzymes.

Hydrolysis and HPLC Analysis Confirm the Transfer of WTAs to Peptidoglycan by *B. subtilis* TagU

The sedimentation and thorough SDS washing steps in our transferase reaction work-up remove any non-covalently-linked sources of radioactivity from the product modified peptidoglycan sacculi. This indicated that the radioactivity detected in our insoluble fractions was derived from tethered WTA intermediates. As a further step, we wanted to probe the chemical composition of these tethered molecules and the nature of the covalent linkage to peptidoglycan. Since many believe LCP enzymes transfer a myriad of glycopolymers to peptidoglycan, we wished also to establish an analytical protocol whereby tethered products of any composition could be easily characterized.

A common method of analyzing the chemical composition of cross-linked peptidoglycan is to first cleave the structure using hydrolytic enzymes and then assess the subsequent muropeptide fragments using HPLC/UPLC (Desmarais et al., 2013). However, these hydrolytic enzymes produce a heterogeneous population of muropeptides. Since turnover was rather modest in our system, we felt it would be difficult to define single WTA-tethered fragments using such techniques and turned instead to decades old WTA hydrolysis experiments for inspiration (Armstrong et al., 1960; Kojima et al., 1985). We devised a strategy whereby various components of the anchored WTA molecule could be selectively liberated from peptidoglycan using mild alkali or mild acid conditions (Figure 3, top) and captured via HPLC. Together, these techniques inform on the covalent linkage, composition, and polymeric nature of peptidoglycan-linked glycopolymers.

To generate WTA-tethered peptidoglycan for characterization, we performed transferase assays employing truncated *B. subtilis* TagU, [^{14}C]Lipid $\phi.n$ and *B. subtilis* peptidoglycan. The hypothetical product, a poly(glycerol phosphate) disaccharide molecule anchored to the C(6) hydroxyl group of peptidoglycan *N*-acetylmuramic acid via a phosphodiester bond, is depicted in Figure 3 (top). We were first interested in a compositional analysis of the radiolabeled product molecule. Therefore, we selectively cleaved the poly(glycerol phosphate) moiety by treatment to mild alkali solution (0.5 M NaOH, 37°C, 30 min). These conditions solubilized greater than 95% of the radioactive signal from the peptidoglycan sacculi (data not shown). We further subjected the liberated WTA molecules to acidic conditions (1 N HCl, 100°C, 30 min) to completely decompose the poly(glycerol phosphate) moiety to building blocks glycerol and phosphoric acid. We found the hydrolytic products coincided with the retention

time of [^{14}C]glycerol when analyzed by HPLC using a column specifically suited for carbohydrate analysis (Figure 3A and 3B; see also Figure S3).

Our lab has previously published methods to analyze radiolabeled WTA polymers via anion-exchange HPLC (Gale et al., 2014; Myers et al., 2015; 2016).

Therefore, we sought to liberate intact WTAs from the same peptidoglycan product described above and capture it using these techniques. Fortunately, a gentle acid treatment exists (10% w/v TCA) that is capable of hydrolyzing WTAs from peptidoglycan specifically at the phosphodiester bond to *N*-acetylmuramic acid (Armstrong et al., 1960). We subjected our product peptidoglycan to these conditions and again found over 95% of radioactive material moved into the soluble aqueous fraction (data not shown). The elution profile of the hydrolysate using our anion-exchange method was similar to previously characterized WTA polymers (Pereira et al., 2008; Sewell et al., 2009) containing 10 or more glycerol phosphate repeats (Figure 3C&D; Figure S3). Taken together, the hydrolysis and HPLC experiments validate our conclusion that LCP enzymes catalyze the covalent attachment of WTA glycopolymers to mature peptidoglycan.

Discussion

LCP family members were first highlighted because of their importance in virulence and antibiotic resistance in several pathogens (Ligozzi et al., 1993; Rossi et al., 2003; Wen et al., 2006). Genetic and phenotypic studies subsequently led to their categorization as cell wall glycopolymer transferases in Gram-positive bacteria. These studies suggested that LCP enzymes transfer a repertoire of glycopolymers to peptidoglycan including capsule polysaccharides (Chan et al., 2014; Hanson et al., 2012), arabinogalactan (Baumgart et al., 2016; Grzegorzewicz et al., 2016; Harrison et al., 2016), and secondary cell wall polymers (Liszewski Zilla et al., 2015) like WTAs (Chan et al., 2013; Kawai et al.,

2011). Despite this enormous body of work, few reports have provided experimental evidence for LCP-mediated glycopolymer transfer *in vitro*. Challenges to reconstitute this activity arise from a poor understanding of reaction requirements, along with issues in the acquisition of complex donor and acceptor substrates.

Here, we leveraged our recent advances in the preparation of WTA intermediates (Gale et al., 2014) to provide authentic donor glycopolymers for transferase reactions. Our data show that *B. subtilis* LCP enzymes can conduct WTA transfer without the protein- and the phospholipid-rich environment they normally reside in during catalysis. Other groups have also reported cell-free and membrane-free glycopolymer transferase activity for LCP enzymes from *M. tuberculosis* (Harrison et al., 2016) and, most recently, *S. aureus* (Schaefer et al., 2017) respectively. Therefore, it seems likely that substrates/products are able to passively load/exit the soluble active site of LCP proteins during catalysis. How this feat is achieved, however, is still unknown. It could be that the conserved hydrophobic binding pocket (Kawai et al., 2011) and the transmembrane region (Hübscher et al., 2008) of LCP enzymes recruit undecaprenyl-linked substrates from the phospholipid bilayer. Indeed, a similar mechanism exists for known polyisoprenyl-glycosyltransferases that translocate membrane-embedded substrates to their active site via transmembrane and amphipathic helices (Dufrisne et al., 2016).

We discovered that LCP-mediated catalysis requires both magnesium and the polyisoprenoid moiety of donor glycopolymers. This is perhaps not surprising, given crystal structures of *Streptococcus pneumoniae* LCP protein Cps2A reveal bound divalent cations and polyisoprenoid phosphate lipids (Kawai et al., 2011). Furthermore, *S. aureus* LCP proteins were shown recently to transfer

hexaprenyl-linked WTA analogs (Table S1; LIIA^{WTA}) to short non-crosslinked peptidoglycan oligomers (Schaefer et al., 2017). The geometric configuration and number of isoprene units of the WTA substrate used by Schaefer and coworkers differ from that reported here, however, these substrates are identical if one focuses on the first three isoprene units (Table S1; Khidirova and Shakhidoyatov, 2002). Therefore, we suggest that key interactions between LCP enzymes and donor glycopolymers occur in the region of the polyisoprenoid lipid that is proximal to the pyrophosphate moiety. The role of magnesium in catalysis is still unknown. Given its coordination by generally conserved aspartic acid residues, its speculated to participate in general acid/base catalysis (Hübscher et al., 2008; Kawai et al., 2011). Assessing transferase activity using active-site mutants will help elucidate the mechanism of LCP-mediated catalysis and further define the role of these important features.

Here, we showed that all LCP enzymes from *B. subtilis* can transfer Lipid β to mature peptidoglycan *in vitro*. This finding corroborates genetic work showing functional redundancy for these enzymes *in vivo* (Kawai et al., 2011). Some studies suggest that the functional redundancy of LCP enzymes may only be partial and that each enzyme could have distinct cellular functions (Over et al., 2011). We saw significant differences in WTA transferase activity between the *B. subtilis* truncated LCP proteins (although, we note that removal of the transmembrane domain and/or buffer conditions may have influenced transferase activity). It remains possible that each LCP member transfers a unique glycopolymer in the cell. Furthermore, studies of *S. aureus* LCP members have suggested functional roles for LcpA as the primary WTA transferase (Schaefer et al., 2017) and LcpC as the capsule polysaccharide transferase (Chan et al., 2014). Comparing the activity of LCP enzymes using a variety of glycopolymer substrates in our assay system may ultimately help to elucidate this paradox.

We were unable to demonstrate WTA transfer to the peptidoglycan biosynthetic intermediate Lipid II (Table S1). Other groups have reported similar struggles (Grzegorzewicz et al., 2016; Harrison et al., 2016; Schaefer et al., 2017); thus, we suggest that only higher order structures like nascent (non-crosslinked) and mature (cross-linked) peptidoglycan can serve as acceptor substrates *in vitro*. Whether both of these structures are tethered *in vivo* is still unclear. LCP proteins from *B. subtilis* and other organisms localize to the septum where peptidoglycan biosynthesis is the highest and where nascent glycan strands are incorporated into an aging meshwork (Baumgart et al., 2016; Eberhardt et al., 2012; Maréchal et al., 2016). Since LCP enzymes are anchored to the membrane and contain only a short extension to their catalytic domain, they may sample only nascent glycan strands and/or the first few layers of the mature peptidoglycan sacculus. Having a strict requirement for these substrates could be a safety mechanism to ensure precious resources are allocated only when peptidoglycan synthesis is near completion. Furthermore, this specificity would prevent LCP enzymes from transferring glycopolymers to peptidoglycan debris derived from cell wall recycling (Johnson et al., 2013), sporulation induction (Lee et al., 2010) and/or host immune evasion (Humann and Lenz, 2008). More work needs to be conducted to see how the oligomeric repeats of peptidoglycan are specifically recognized. Of particular interest would be to see how precursor Lipid II is excluded from meaningful catalysis, despite the similar features it bears to the undecaprenyl-linked WTA donor molecules.

Our data indicate that truncated *B. subtilis* TagU prefers its cognate peptidoglycan over sacculi from Gram-positive bacteria *Streptomyces sp.* These peptidoglycan sources differ greatly in composition, organization, and architecture (Turner et al., 2014). However, we note that these features are ill-

defined in our assays, as the murein sacculi were prepared by commercial vendors using propriety methods. These limitations hinder our ability to quantify the number of free C(6) MurNAc hydroxyl groups available for glycopolymer attachment and thus, we are unable to normalize activity across the peptidoglycan substrates. Preparations of chemically-defined peptidoglycan will undoubtedly shed light on acceptor substrate preferences for LCP members and help confirm the hypothesis that cognate peptidoglycan acceptors are optimal for LCP-mediated glycopolymer transfer. Nevertheless, it appears that LCP enzymes have some degree of relaxed specificity for the acceptor peptidoglycan substrate.

We demonstrate that more elaborate WTA intermediates containing poly(glycerol phosphate) moieties are capable substrates for LCP-mediated transfer, including the physiological donor glycopolymer Lipid γ (Figure 2B, Table 1). Using these WTA polymers in transferase assays allowed us to confirm LCP-mediated WTA-peptidoglycan tethering through hydrolysis and HPLC methods. These techniques define the carbohydrate composition and the polymeric nature of phosphodiester-linked molecules to peptidoglycan. Therefore, we propose that similar strategies can be used to characterize products from the LCP-mediated transfer of other glycopolymers - provided trackable substrate glycopolymers can be prepared.

We highlight a reaction window where LCP-mediated transfer activity is proportional to time and enzyme concentration. While the turnover observed was modest, we believe these reaction conditions can be used to validate potential therapeutic agents and guide drug discovery and development programs targeting the LCP protein family. Drugs inhibiting glycopolymer transfer promise to disarm pathogens of essential polymers required for survival and virulence. In

addition, these agents have incredible potential in combination therapies focused on restoring the clinical efficacy of cell-wall targeting drugs. Indeed, early work has shown that *lcp* gene deletion mutants in *M. tuberculosis* and *S. aureus* are highly susceptible to β -lactams (Grzegorzewicz et al., 2016; Schaefer et al., 2017).

Significance

Bacteria tether numerous glycopolymers to their peptidoglycan layer. This action provides the cell with a suite of essential functions required for optimal growth, division, and virulence. The LytR-CpsA-LytR (LCP) family of enzymes are thought to perform the glycopolymer transfer function and, as such, represent exciting new drug targets. Despite a growing body of genetic and phenotypic studies conducted on LCP members, a lack of tools and functional assays has hindered their full biochemical characterization. While some research groups have recently reconstituted glycopolymer transfer *in vitro*, fundamental features of the reaction remained enigmatic. In particular, little was known about the requirements for catalysis, even the exact substrates involved. Here, we synthesized phosphate-rich glycopolymers called wall teichoic acids (WTAs) and built an assay system capable of evaluating the transferase activity of LCP enzymes. This work provides the first detailed characterization of LCP enzymes from *B. subtilis* using authentic WTA glycopolymers. We've identified several key features of catalysis and assessed substrate preferences for these LCP enzymes. We have also elaborated assay conditions to facilitate testing the activity of LCP enzymes in the presence of novel inhibitory compounds. This work marks an important first step towards better understanding of glycopolymer-peptidoglycan tethering in Gram-positive bacteria and aims to aid drug discovery and development programs focused on this important cell wall biosynthetic machinery.

Author contributions

Conceptualization, R.T.G., and E.D.B.; Methodology, R.T.G.; Formal Analysis, R.T.G.; Investigation, R.T.G.; Resources, F.K.K.L and T.S.; Writing- Original draft: R.T.G. and E.D.B.; Writing – Review & Editing: R.T.G., F.K.K.L., N.C.J.S., and E.D.B.; Supervision, E.D.B.; Funding Acquisition, E.D.B.

Acknowledgements

We thank Dr. Cullen Myers and Dr. Garima Kumar for insightful discussions in the preparation of this manuscript. RTG acknowledges support from a Canadian Institute of Health Research graduate scholarship. This work was supported by operating funds from the Canadian Institute of Health Research (FDN-143215) and salary support from the Canada Research Chairs program to E.D.B.

References

- Allison, S.E., D'Elia, M.A., Arar, S., Monteiro, M.A., and Brown, E.D. (2011). Studies of the genetics, function, and kinetic mechanism of TagE, the wall teichoic acid glycosyltransferase in *Bacillus subtilis* 168. *J. Biol. Chem.* **286**, 23708–23716.
- Armstrong, J.J., Baddiley, J., and Buchanan, J.G. (1960). Structure of the ribitol teichoic acid from the walls of *Bacillus subtilis*. *Biochem. J.* **76**, 610-621.
- Badurina, D.S., Zolli-Juran, M., and Brown, E.D. (2003). CTP: glycerol 3-phosphate cytidyltransferase (TarD) from *Staphylococcus aureus* catalyzes the cytidyl transfer via an ordered Bi–Bi reaction mechanism with micromolar K_m values. *Biochim. Biophys. Acta, Proteins Proteomics* **1646**, 196–206.
- Baumgart, M., Schubert, K., Bramkamp, M., and Frunzke, J. (2016). Impact of LytR-CpsA-Psr proteins on cell wall biosynthesis in *Corynebacterium glutamicum*. *J. Bacteriol.* **198**, 3045–3059.
- Bhavsar, A.P., Truant, R., and Brown, E.D. (2005). The TagB protein in *Bacillus subtilis* 168 is an intracellular peripheral membrane protein that can incorporate glycerol phosphate onto a membrane-bound acceptor in vitro. *J. Biol. Chem.* **280**,

36691–36700.

Brown, E.D., and Wright, G.D. (2016). Antibacterial drug discovery in the resistance era. *Nature*. *529*, 336–343.

Brown, S., Santa Maria, J.P. Jr., and Walker, S. (2013). Wall teichoic acids of Gram-positive bacteria. *Annu. Rev. Microbiol.* *67*, 313–336.

Bugg, T.D.H., and Walsh, C.T. (1992). Intracellular steps of bacterial cell wall peptidoglycan biosynthesis: enzymology, antibiotics, and antibiotic resistance. *Nat. Prod. Rep.* *9*, 199–215.

Chan, Y.G.Y., Kim, H.K., Schneewind, O., and Missiakas, D. (2014). The capsular polysaccharide of *Staphylococcus aureus* is attached to peptidoglycan by the LytR-CpsA-Psr (LCP) family of enzymes. *J. Biol. Chem.* *289*, 15680–15690.

Chan, Y.G.Y., Frankel, M.B., Dengler, V., Schneewind, O., and Missiakas, D. (2013). *Staphylococcus aureus* mutants lacking the LytR-CpsA-Psr family of enzymes release cell wall teichoic acids into the extracellular medium. *J. Bacteriol.* *195*, 4650–4659.

Desmarais, S.M., de Pedro, M.A., Cava, F., and Huang, K.C. (2013). Peptidoglycan at its peaks: how chromatographic analyses can reveal bacterial cell wall structure and assembly. *Mol. Microbiol.* *89*, 1–13.

Dufrisne, M.B., Petrou, V.I., Clarke, O.B., and Mancina, F. (2016). Structural basis for catalysis at the membrane-water interface. *Biochim. Biophys. Acta.* *1862*, 1368-1385.

Eberhardt, A., Hoyland, C.N., Vollmer, D., Bisle, S., Cleverley, R.M., Johnsborg, O., Håvarstein, L.S., Lewis, R.J., and Vollmer, W. (2012). Attachment of capsular polysaccharide to the cell wall in *Streptococcus pneumoniae*. *Microb. Drug Resist.* *18*, 240–255.

Egan, A.J.F., and Vollmer, W. (2012). The physiology of bacterial cell division. *Ann. N.Y. Acad. Sci.* *1277*, 8–28.

Farha, M.A., Leung, A., Sewell, E.W., D’Elia, M.A., Allison, S.E., Ejim, L., Pereira, P.M., Pinho, M.G., Wright, G.D., and Brown, E.D. (2013). Inhibition of WTA Synthesis Blocks the Cooperative Action of PBPs and Sensitizes MRSA to β -Lactams. *ACS Chem. Biol.* *8*, 226–233.

Gale, R.T., and Brown, E.D. (2015). New chemical tools to probe cell wall biosynthesis in bacteria. *Curr. Opin. Microbiol.* 27, 69–77.

Gale, R.T., Sewell, E.W., Garrett, T.A., and Brown, E.D. (2014). Reconstituting poly(glycerol phosphate) wall teichoic acid biosynthesis *in vitro* using authentic substrates. *Chem. Sci.* 5, 3823–3830.

Glauner, B., Höltje, J.V., and Schwarz, U. (1988). The composition of the murein of *Escherichia coli*. *J. Biol. Chem.* 263, 10088–10095.

Grzegorzewicz, A.E., De Sousa-d'Auria, C., McNeil, M.R., Huc-Claustre, E., Jones, V., Petit, C., Angala, S.K., Zemanová, J., Wang, Q., Belardinelli, J.M., Gao, Q., Ishizaki, Y., Mikusova, K., Brennan, P.J., Ronning, D.R., Chami, M., Houssin, C., and Jackson, J.M. (2016). Assembling of the *Mycobacterium tuberculosis* cell wall core. *J. Biol. Chem.* 291, 18867–18879.

Hanson, B.R., Lowe, B.A., and Neely, M.N. (2010). Membrane topology and DNA-binding ability of the Streptococcal CpsA protein. *J. Bacteriol.* 193, 411–420.

Hanson, B.R., Runft, D.L., Streeter, C., Kumar, A., Carion, T.W., and Neely, M.N. (2012). Functional analysis of the CpsA protein of *Streptococcus agalactiae*. *J. Bacteriol.* 194, 1668–1678.

Harrison, J., Lloyd, G., Joe, M., Lowary, T.L., Reynolds, E., Walters-Morgan, H., Bhatt, A., Lovering, A., Besra, G.S., and Alderwick, L.J. (2016). Lcp1 is a phosphotransferase responsible for ligating arabinogalactan to peptidoglycan in *Mycobacterium tuberculosis*. *MBio* 7, e00972–16.

Höltje, J.V. (1998). Growth of the stress-bearing and shape-maintaining murein sacculus of *Escherichia coli*. *Microbiol. Mol. Biol. Rev.* 62, 181–203.

Humann, J., and Lenz, L.L. (2008). Bacterial peptidoglycan-degrading enzymes and their impact on host muropeptide detection. *J. Innate Immun.* 1, 88–97.

Hübscher, J., Lüthy, L., Berger-Bächi, B., and Stutzmann Meier, P. (2008). Phylogenetic distribution and membrane topology of the LytR-CpsA-Psr protein family. *BMC Genomics.* 9, 617–16.

Hübscher, J., McCallum, N., Sifri, C.D., Majcherczyk, P.A., Entenza, J.M., Heusser, R., Berger-Bächi, B., and Stutzmann Meier, P. (2009). MsrR contributes to cell surface characteristics and virulence in *Staphylococcus aureus*. *FEMS*

Microbiol. Lett. 295, 251–260.

Johnson, J.W., Fisher, J.F., and Mobashery, S. (2013). Bacterial cell-wall recycling. Ann. N.Y. Acad. Sci. 1277, 54–75.

Kawai, Y., Marles-Wright, J., Cleverley, R.M., Emmins, R., Ishikawa, S., Kuwano, M., Heinz, N., Bui, N.K., Hoyland, C.N., Ogasawara, N., et al. (2011). A widespread family of bacterial cell wall assembly proteins. EMBO J. 30, 4931–4941.

Kojima, N., Araki, Y., and Ito, E. (1985). Structure of the linkage units between ribitol teichoic acids and peptidoglycan. J. Bacteriol. 161, 299–306.

Leclercq, S., Derouaux, A., Olatunji, S., Fraipont, C., Egan, A.J.F., Vollmer, W., Breukink, E., and Terrak, M. (2017). Interplay between Penicillin-binding proteins and SEDS proteins promotes bacterial cell wall synthesis. Sci. Rep. 7, 43306.

Lee, M., Hesek, D., Shah, I.M., Oliver, A.G., Dworkin, J., and Mobashery, S. (2010). Synthetic peptidoglycan motifs for germination of bacterial spores. ChemBioChem. 11, 2525–2529.

Lee, S.H., Wang, H., Labroli, M., Koseoglu, S., Zuck, P., Mayhood, T., Gill, C., Mann, P., Sher, X., Ha, S., et al. (2016). TarO-specific inhibitors of wall teichoic acid biosynthesis restore β -lactam efficacy against methicillin-resistant staphylococci. Sci. Transl. Med. 8, 329ra32

Liechti, G., Kuru, E., Packiam, M., Hsu, Y.-P., Tekkam, S., Hall, E., Rittichier, J.T., VanNieuwenhze, M., Brun, Y.V., and Maurelli, A.T. (2016). Pathogenic chlamydia lack a classical sacculus but synthesize a narrow, mid-cell peptidoglycan ring, regulated by MreB, for cell division. PLoS Pathog. 12, e1005590.

Liechti, G.W., Kuru, E., Hall, E., Kalinda, A., Brun, Y.V., VanNieuwenhze, M., and Maurelli, A.T. (2015). A new metabolic cell-wall labelling method reveals peptidoglycan in *Chlamydia trachomatis*. Nature. 506, 507–510.

Ligozzi, M., Pittaluga, F., and Fontana, R. (1993). Identification of a genetic element (psr) which negatively controls expression of *Enterococcus hirae* penicillin-binding protein 5. J. Bacteriol. 175, 2046–2051.

Liszewski Zilla, M., Chan, Y.G.Y., Lunderberg, J.M., Schneewind, O., and Missiakas, D. (2014). LytR-CpsA-Psr Enzymes as Determinants of *Bacillus*

anthracis Secondary Cell Wall Polysaccharide Assembly. *J. Bacteriol.* **197**, 343–353.

Liszewski Zilla, M., Lunderberg, J.M., Schneewind, O., and Missiakas, D. (2015). *Bacillus anthracis* *lcp* genes support vegetative growth, envelope assembly, and spore formation. *J. Bacteriol.* **197**, 3731–3741.

Maréchal, M., Amoroso, A., Morlot, C., Vernet, T., Coyette, J., and Joris, B. (2016). *Enterococcus hirae* LcpA (Psr), a new peptidoglycan-binding protein localized at the division site. *BMC Microbiol.* **16**, 239.

Marrakchi, H., Lanéelle, M.-A., and Daffé, M. (2014). Mycolic acids: structures, biosynthesis, and beyond. *Chem. Biol.* **21**, 67–85.

Meeske, A.J., Riley, E.P., Robins, W.P., Uehara, T., Mekalanos, J.J., Kahne, D., Walker, S., Kruse, A.C., Bernhardt, T.G., and Rudner, D.Z. (2016). SEDS proteins are a widespread family of bacterial cell wall polymerases. *Nature.* **537**, 634–638.

Meeske, A.J., Sham, L.-T., Kimsey, H., Koo, B.-M., Gross, C.A., Bernhardt, T.G., and Rudner, D.Z. (2015). MurJ and a novel lipid II flippase are required for cell wall biogenesis in *Bacillus subtilis*. *Proc. Nat. Acad. Sci. U.S.A.* **112**, 6437–6442.

Myers, C.L., Ireland, R.G., Garrett, T.A., and Brown, E.D. (2015). Characterization of wall teichoic acid degradation by the bacteriophage $\phi 29$ appendage protein GP12 using synthetic substrate analogs. *J. Biol. Chem.* **290**, 19133–19145.

Myers, C.L., Li, F.K.K., Koo, B.-M., El-Halfawy, O.M., French, S., Gross, C.A., Strynadka, N.C.J., and Brown, E.D. (2016). Identification of two phosphate starvation-induced wall teichoic acid hydrolases provides first insights into the degradative pathway of a key bacterial cell wall component. *J. Biol. Chem.* **291**, 26066–26082.

Nallamsetty, S., Austin, B.P., Penrose, K.J., and Waugh, D.S. (2005). Gateway vectors for the production of combinatorially-tagged His6-MBP fusion proteins in the cytoplasm and periplasm of *Escherichia coli*. *Protein Sci.* **14**, 2964–2971.

Neuhaus, F.C., and Baddiley, J. (2003). A continuum of anionic charge: structures and functions of D-alanyl-teichoic acids in Gram-positive bacteria. *Microbiol. Mol. Biol. Rev.* **67**, 686–723.

O'Riordan, K., and Lee, J.C. (2004). *Staphylococcus aureus* capsular polysaccharides. Clin. Microbiol. Rev. 17, 218–234.

Oh, S.-Y., Lunderberg, J.M., Chateau, A., Schneewind, O., and Missiakas, D. (2016). Genes required for *Bacillus anthracis* secondary cell wall polysaccharide synthesis. J. Bacteriol. 199, p.e000613-16

Over, B., Heusser, R., McCallum, N., Schulthess, B., Kupferschmied, P., Gaiani, J.M., Sifri, C.D., Berger-Bächi, B., and Stutzmann Meier, P. (2011). LytR-CpsA-Psr proteins in *Staphylococcus aureus* display partial functional redundancy and the deletion of all three severely impairs septum placement and cell separation. FEMS Microbiol. Lett. 320, 142–151.

Pereira, M.P., Schertzer, J.W., D'Elia, M.A., Koteva, K.P., Hughes, D.W., Wright, G.D., and Brown, E.D. (2008). The wall teichoic acid polymerase TagF efficiently synthesizes poly(glycerol phosphate) on the TagB product lipid III. ChemBioChem. 9, 1385–1390.

Rossi, J., Bischoff, M., Wada, A., and Berger-Bächi, B. (2003). MsrR, a putative cell envelope-associated element involved in *Staphylococcus aureus* sarA attenuation. Antimicrob. Agents Chemother. 47, 2558–2564.

Schaefer, K., Matano, L.M., Qiao, Y., Kahne, D., and Walker, S. (2017). *In vitro* reconstitution demonstrates the cell wall ligase activity of LCP proteins. Nat. Chem. Biol. 13, 396-401.

Schäffer, C., and Messner, P. (2005). The structure of secondary cell wall polymers: how Gram-positive bacteria stick their cell walls together. Microbiology. 151, 643–651.

Schäffer, C., Wugeditsch, T., Messner, P., and Whitfield, C. (2002). Functional expression of enterobacterial O-polysaccharide biosynthesis enzymes in *Bacillus subtilis*. Appl. Environ. Microbiol. 68, 4722–4730.

Schertzer, J.W., and Brown, E.D. (2003). Purified, recombinant TagF protein from *Bacillus subtilis* 168 catalyzes the polymerization of glycerol phosphate onto a membrane acceptor *in vitro*. J. Biol. Chem. 278, 18002–18007.

Sewell, E.W. and Brown, E.D. (2014). Taking aim at wall teichoic acid synthesis: new biology and new leads for antibiotics. J. Antibiot. 67, 43–51.

Sewell, E.W.C., Pereira, M.P., and Brown, E.D. (2009). The wall teichoic acid

polymerase TagF is non-processive *in vitro* and amenable to study using steady state kinetic analysis. *J. Biol. Chem.* *284*, 21132–21138.

Sigle, S., Steblau, N., Wohlleben, W., and Muth, G. (2016). Polydiglycosylphosphate transferase PdtA (SCO2578) of *Streptomyces coelicolor* A3(2) is crucial for proper sporulation and apical tip extension under stress conditions. *Appl. Environ. Microbiol.* *82*, 5661–5672.

Turner, R.D., Vollmer, W., and Foster, S.J. (2014). Different walls for rods and balls: the diversity of peptidoglycan. *Mol. Microbiol.* *91*, 862–874.

Vollmer, W. (2008). Structural variation in the glycan strands of bacterial peptidoglycan. *FEMS Microbiol. Rev.* *32*, 287–306.

Weidenmaier, C., and Peschel, A. (2008). Teichoic acids and related cell-wall glycopolymers in Gram-positive physiology and host interactions. *Nat. Rev. Micro.* *6*, 276–287.

Wen, Z.T., Baker, H.V., and Burne, R.A. (2006). Influence of BrpA on critical virulence attributes of *Streptococcus mutans*. *J. Bacteriol.* *188*, 2983–2992.

STAR * METHODS

KEY RESOURCE TABLE

| REAGENT or RESOURCE | SOURCE | IDENTIFIER |
|---|---|--------------|
| Bacterial and Virus Strains | | |
| <i>Escherichia coli</i> NovaBlue | MilliporeSigma | Cat#70181 |
| <i>Escherichia coli</i> BL21 (DE3) pLysS | MilliporeSigma | Cat#69451 |
| Chemicals, Peptides, and Recombinant Proteins | | |
| <i>Bacillus subtilis</i> peptidoglycan | Sigma-Aldrich | Cat#69554 |
| <i>Streptomyces</i> sp. peptidoglycan | Sigma-Aldrich | Cat#79682 |
| UDP-GlcNAc | Sigma-Aldrich | Cat#U4375 |
| UDP-ManNAc | Pereira et al., 2008 | N/A |
| CDP-glycerol | Badurina et al., 2003 | N/A |
| UDP-[¹⁴ C]GlcNAc | American Radiolabeled Chemicals | ARC 0152 |
| Sn-[U- ¹⁴ C]glycerol-3-phosphate | PerkinElmer | NEC608V050UC |
| UDP-[¹⁴ C]glucose | PerkinElmer | NEC403010UC |
| CDP-[U- ¹⁴ C]glycerol | Badurina et al., 2003 | N/A |
| [¹⁴ C]glycerol | This paper | N/A |
| [¹⁴ C]glucose | This paper | N/A |
| [¹⁴ C]GlcNAc | This paper | N/A |
| Alkaline phosphatase | Sigma-Aldrich | Cat#P5521 |
| <i>S. aureus</i> TarD | Badurina et al., 2003 | N/A |
| <i>B. subtilis</i> MnaA | Pereira et al., 2008 | N/A |
| <i>S. aureus</i> TagA | Pereira et al., 2008 | N/A |
| <i>B. subtilis</i> TagB | Bhavsar et al., 2005 | N/A |
| <i>B. subtilis</i> TagF | Schertzert and Brown, 2003 | N/A |
| <i>B. subtilis</i> TagE | Allison et al., 2011 | N/A |
| <i>B. subtilis</i> ΔTMTagT | This paper | N/A |
| <i>B. subtilis</i> ΔTMTagU | This paper | N/A |
| <i>B. subtilis</i> ΔTMTagV | This paper | N/A |
| Gateway® Technology LR Clonase® II Enzyme Mix | Invitrogen, Thermo Fisher Scientific | Cat#11791020 |
| Gateway® Technology BP Clonase® II Enzyme Mix | Invitrogen, Thermo Fisher Scientific | Cat#11789020 |
| Pierce™ Protease Inhibitor Tablets | Thermo Fisher Scientific | Cat#A32953 |
| HIS-Select® Nickel Affinity Gel | Sigma-Aldrich | Cat#P6611 |
| Aminex HPX-87H column | Bio-Rad | Cat#1250140 |
| DNAPac™ PA200 column | Thermo Fisher Scientific | Cat#063000 |
| C ₅₅ -Lipid α | Gale et al., 2014 | N/A |
| C ₅₅ -[¹⁴ C]Lipid β | This paper, adapted from Gale et al. (2014) | N/A |
| C ₅₅ -[¹⁴ C]Lipid φ.1 | This paper, adapted from Gale et al. (2014) | N/A |
| C ₅₅ -[¹⁴ C]Lipid φ.η | This paper, adapted from Gale et al. (2014) | N/A |
| C ₅₅ -[¹⁴ C]Lipid γ | This paper, adapted from Gale et al. (2014) | N/A |
| C ₁₃ -Lipid α | Pereira et al., 2008 | N/A |
| C ₁₃ -[¹⁴ C]Lipid β | Pereira et al., 2008 | N/A |

Continued

| REAGENT or RESOURCE | SOURCE | IDENTIFIER |
|---|-------------------------------------|---|
| C ₁₃ -[¹⁴ C]Lipid φ.10 | Sewell et al., 2009 | N/A |
| C ₁₃ -[¹⁴ C]Lipid φ.50 | Sewell et al., 2009 | N/A |
| Experimental Models: Organisms/Strains | | |
| Expression clone <i>E. coli</i> BL21 (DE3) pLysS with truncated <i>tagT</i> (<i>ywtF</i>) | This paper | N/A |
| Expression clone <i>E. coli</i> BL21 (DE3) pLysS with truncated <i>tagU</i> (<i>lytR</i>) | This paper | N/A |
| Expression clone <i>E. coli</i> BL21 (DE3) pLysS with truncated <i>tagV</i> (<i>yvhJ</i>) | This paper | N/A |
| Recombinant DNA | | |
| Plasmid pDONR TM 221 with truncated <i>tagT</i> | Invitrogen GeneArt | N/A |
| Plasmid pDONR TM 221 with truncated <i>tagU</i> | Invitrogen GeneArt | N/A |
| Plasmid pDONR TM 221 with truncated <i>tagV</i> | Invitrogen GeneArt | N/A |
| Plasmid pDEST TM 17 with truncated <i>tagT</i> | This paper | N/A |
| Plasmid pDEST TM 17 with truncated <i>tagU</i> | This paper | N/A |
| Plasmid pDEST TM 17 with truncated <i>tagV</i> | This paper | N/A |
| Software and Algorithms | | |
| Empower 3 build 3471 | Waters | http://www.waters.com/waters/en_US/Empower-3-Chromatography-Data-Software/nav.htm?locale=en_US&cid=10190669 |
| R 3.2.3 | The R Project | https://www.r-project.org/ ; RRID:SCR_001905 |
| IGOR Pro 6.36 | WaveMetrics | https://www.wavemetrics.com/ ; RRID:SCR_000325 |

EXPERIMENTAL MODEL AND SUBJECT DETAILS**Bacterial Cultures**

All bacterial strains used in this study are listed in the Key Resource Table (KRT). *E. coli* strains NovaBlue and BL21 DE3 (pLysS) were used for cloning and protein expression respectively. These strains were cultivated in 2x YT medium containing either ampicillin (50 µg/mL), tetracycline (15 µg/mL) or chloramphenicol (20 µg/mL) when required.

METHOD DETAILS**Chemicals and resources**

Please refer to KRT. CDP-[U-¹⁴C]glycerol was prepared enzymatically from *sn*-[U-¹⁴C]glycerol-3-phosphate (0.05 mCi/mL) and CTP by *S. aureus* TarD as described (Badurina et al., 2003).

HPLC Standards for [¹⁴C]glycerol, [¹⁴C]glucose, and [¹⁴C]GlcNAc were prepared via acid hydrolysis (1 N HCl, 100°C, 35 min) of molecules *sn*-[U-¹⁴C]glycerol-3-

phosphate (0.05 mCi/mL), UDP-[¹⁴C]glucose (0.02 mCi/mL), and UDP-[¹⁴C]GlcNAc (0.1 mCi/mL) respectively. Hydrolysates were neutralized to pH ~8 using NaOH prior to HPLC analysis.

Recombinant WTA biosynthetic enzymes TarD, MnaA, TagA, TagB, TagF, and TagE were prepared following described methods (Allison et al., 2011; Badurina et al., 2003; Bhavsar et al., 2005; Pereira et al., 2008; Schertzer and Brown, 2003).

Cloning, expression, and purification of LCP enzymes

Truncated open reading frames (ORFs) encoding *B. subtilis* TagT (YwtF; residues 46-322), TagU (LytR; residues 37-306), and TagV (YvhJ; residues 41-391) were optimized for expression in *E. coli* and inserted into pDONR221 by Invitrogen™ GeneArt Gene Synthesis. Invitrogen™ Gateway™ recombination cloning technology was used to transfer optimized sequences into pDEST17. These plasmid constructs were transformed into *E. coli* BL21 (DE3) pLysS for protein expression. Cells were grown in 2X YT medium containing ampicillin (50 µg/mL) at 37°C until OD_{600nm} of 0.6 - 0.8. Protein expression was induced using 1 mM of isopropyl β-D-1-thiogalactopyranoside and continued overnight at 18°C. Cultures were pelleted and washed with 0.85% (w/v) NaCl. Cells were resuspended in lysis buffer (50 mM Tris-HCl [pH = 7.5], 500 mM NaCl, 10 mM imidazole, 10% glycerol, 0.1 mg/mL DNase I, 0.1 mg/mL RNase A and a solubilized Pierce™ Protease Inhibitor Tablet) and lysed by disruption at 30,000 psi. The lysate was then clarified by centrifugation at 48,000 x g for 60 min. The resulting supernatant was loaded onto a short bed (~5 mL) of HIS-Select® Nickel Affinity Gel and eluted using sequential buffers containing 10, 35 and 300 mM imidazole in 50 mM Tris-HCl (pH = 7.5), 500 mM NaCl and 10% glycerol. Fractions containing pure protein (as determined by SDS-PAGE) were pooled,

concentrated and dialyzed against elution buffer without imidazole. Proteins were flash-frozen using liquid N₂ and stored at -80°C until use.

Synthesis of WTA donor substrates

Lipid α and Lipid β

Authentic undecaprenyl-linked Lipid α was prepared from a semi-synthetic strategy as described (Gale et al., 2014). Lipid α was elaborated to [¹⁴C]-labeled WTA intermediates Lipid β , Lipid ϕ .1 Lipid ϕ .*n*, and Lipid γ following established protocols (Gale et al., 2014) with the slight modification that Triton X-100 was omitted from syntheses. See also Figure S2. Briefly, authentic [¹⁴C]Lipid β was synthesized from a one-pot reaction utilizing dried semi-synthetic Lipid α (30 μ M), UDP-[¹⁴C]GlcNAc (2.5 μ M, 0.04 μ Ci), TagA (3 μ M), and MnaA (3 μ M) in buffer containing 50 mM Tris-HCl (pH 7.5) and 40 mM MgCl₂. The reaction mixture was incubated at 30°C for 30 min, after which alkaline phosphatase (2 U) was added. The reaction was incubated for an additional 2.5 hours at 30°C and subsequently used directly in transferase assays.

To determine the concentration of product [¹⁴C]Lipid β parallel reactions were performed where lipid-linked materials were extracted from soluble reaction components using described methods (Farha et al., 2013; Gale et al., 2014; Schaffer et al., 2002). Briefly, reactions were quenched using 1250 μ L of CHCl₃/MeOH (3:2). These samples were vortexed vigorously for 3 minutes, after which, insoluble material was removed via centrifugation (13,000 x g, 5 min). Samples were then washed with 150 μ L of 40 mM MgCl₂ and vortexed vigorously for 5 min. The upper aqueous layer was removed following centrifugation (13,000 x g, 5 min). The lipid-containing bottom organic layer was subsequently washed three times with 400 μ L of pure solvent upper phase (CHCl₃/MeOH/H₂O/1 M MgCl₂; 18:294:282:1); the upper aqueous layer was removed from each wash following centrifugation (13,000 x g, 5 min). The

resulting lipid solution was then dried using a stream of N₂ and the concentration of radioactive Lipid β was determined by scintillation counting of all fractions.

Lipid ϕ .1, Lipid ϕ .n, and Lipid γ

See also Figure S2. [¹⁴C]Lipid ϕ .1 was prepared in a similar manner to [¹⁴C]Lipid β except: i) reactions contained UDP-GlcNAc (30 μ M) to generate non-radiolabeled Lipid β ; and ii) TagB (3 μ M) and CDP-[¹⁴C]Gro (10.2 μ M, 0.04 μ Ci) were added 30 min after alkaline phosphatase (2 U) addition. This mixture was incubated at 30°C for an additional 2 hours before being quenched by heat-inactivation (80°C for 10 min). The concentration of product [¹⁴C]Lipid ϕ .1 was determined as per the methods utilized for [¹⁴C]Lipid β (see above).

To generate [¹⁴C]Lipid ϕ .n, first, non-radiolabeled Lipid ϕ .1 (1.5 μ M) was prepared using only CDP-Gro (10.2 μ M) in standard synthesis conditions outlined above. Following heat-inactivation, TagF (3 μ M) and CDP-[¹⁴C]Gro (10.2 μ M, 0.04 μ Ci) were added to the reaction mixture and incubated at 30°C for 1 hour. Non-radiolabeled Lipid ϕ .n was prepared in a similar manner, with the exception that only CDP-Gro (10.2 μ M) was added along with the TagF protein. This reaction mixture was then incubated with TagE (3 μ M) and UDP-[¹⁴C]Glu (3 μ M; 0.04 μ Ci) for 1 hour at 30°C to elaborate Lipid ϕ .n to [¹⁴C]Lipid γ .

A more radioactive sample of Lipid ϕ .n was prepared for HPLC characterization of transferase product material. This sample was synthesized instead using Lipid α (50 μ M) and UDP-GlcNAc (50 μ M) during Lipid β synthesis, and CDP-[¹⁴C]Gro (45 μ M; 0.9 μ Ci) in the TagF-mediated reaction.

All late-stage radiolabeled WTA intermediate synthesis reactions were used directly in transferase assays.

WTA intermediate analogs

Tridecyl-linked [^{14}C]Lipid β , [^{14}C]Lipid ϕ .10 and [^{14}C]Lipid ϕ .50 analogs were prepared from described methods (Gale et al., 2014; Pereira et al., 2008; Sewell et al., 2009).

In vitro LCP transferase assays

Standard assay procedure

Typical transferase reactions involved the addition of insoluble *B. subtilis* peptidoglycan (0.25 mg) and LCP enzymes (0.5–4.0 μM) to synthesis reactions containing ^{14}C -radiolabeled WTA donor substrates (0.6 μM – 1.5 μM). These mixtures were incubated at 30°C for 40 min, before being quenched with boiling 5% (w/v) SDS. Insoluble product peptidoglycan was pelleted from soluble lipids, proteins, and radiolabeled precursors by centrifugation at 13,000 x g for 10 min. The resulting peptidoglycan pellet was washed three times against boiling 5% (w/v) SDS until no radioactivity could be detected in the soluble fractions. Product peptidoglycan was resuspended in 100 μL ddH₂O and all fractions were subject to scintillation counting to determine the amount of WTA incorporation into the insoluble peptidoglycan sacculus. All transferase reactions and workups were conducted in this manner unless otherwise stated. More specific experimental details and deviations are provided below.

B. subtilis LCP protein mix

To test for cell-free and membrane-free transferase activity, [^{14}C]Lipid β (0.6 μM) was incubated with insoluble *B. subtilis* peptidoglycan (0.25 mg) and all of the *B. subtilis* truncated LCP enzymes ΔTMTagT , ΔTMTagU , and ΔTMTagV (2 μM

each). Negative controls of the reaction used either heat-inactivated LCP proteins (65°C, 30 min) or lacked a source of [^{14}C]Lipid β ; the latter control was created by omitting semi-synthetic Lipid α in [^{14}C]Lipid β synthesis reactions. To investigate if efficient transferase activity required Mg^{2+} , the chelating agent EDTA (100 mM) was added to [^{14}C]Lipid β synthesis reactions prior to the addition of peptidoglycan and LCP enzymes. To investigate if efficient transferase activity required the polyisoprenoid moiety of donor substrates, the tridecyl-linked (C_{13}) [^{14}C]Lipid β analog (30 μM , 0.04 μCi) was used in place of the authentic undecaprenyl-linked (C_{55}) [^{14}C]Lipid β substrate in transferase reactions.

Individual B. subtilis LCP enzymes

To test which *B. subtilis* LCP enzymes specifically had transferase activity, reactions contained only one truncated *B. subtilis* LCP enzyme (4 μM ; either of ΔTMTagT , ΔTMTagU , or ΔTMTagV) and followed standard reaction procedures using [^{14}C]Lipid β (0.6 μM) and *B. subtilis* peptidoglycan (0.25 mg). Negative controls of the reaction used heat-inactivated LCP proteins (100°C, 30 min).

Alternative acceptor and donor substrates

To test the influence of alternative peptidoglycan acceptor molecules on TagU-mediated glycopolymer transfer activity, ΔTMTagU (4 μM) was incubated with [^{14}C]Lipid β (0.6 μM) and mature peptidoglycan (0.25 mg) sourced from either *B. subtilis* or *Streptomyces sp.* Late-step WTA intermediates Lipid $\phi.1$, Lipid $\phi.n$, and Lipid γ (1.5 μM) were independently evaluated as suitable glycopolymer donor substrates by incubating [^{14}C]-radiolabeled synthesis reaction mixtures for each intermediate with ΔTMTagU (4 μM) and *B. subtilis* peptidoglycan (0.25 mg). All reactions followed standard procedures outlined above. Negative controls of the reaction used heat-inactivated LCP proteins (100°C, 30 min).

Linearity with time and enzyme concentration

Various concentrations of Δ TMTagU (0.5-4 μ M) were incubated with [14 C]Lipid β (0.6 μ M) and *B. subtilis* peptidoglycan (0.25 mg) substrates between 5-40 minutes following standard assay procedures.

WTA-peptidoglycan hydrolysis and HPLC analysis

To generate a WTA-peptidoglycan product for characterization, transferase reactions were conducted using a more radioactive [14 C]Lipid $\phi.n$ (0.9 μ Ci) substrate, Δ TMTagU (4 μ M), and *B. subtilis* peptidoglycan (2 mg). Reactions were incubated for 16 hours at ambient temperature. To test specifically for glycerol incorporation into the peptidoglycan layer, the insoluble product material was first incubated in mild alkali solution (0.5 M NaOH, 37°C, 30 min). The hydrolysate was then recovered from the insoluble peptidoglycan material via centrifugation at 13,000 x g for 10 min and the peptidoglycan layer was subsequently washed with ddH₂O. The efficiency of hydrolysis was measured by scintillation counting of all fractions. The hydrolysate material from alkali treatment was neutralized to pH ~7.0 using HCl and further subjected to acidic conditions (1 N HCl, 100°C, 30 min). The resulting sample was neutralized to pH ~8.0 and compositional analysis was determined by HPLC using a carbohydrate column (see more details below).

To test specifically for full WTA polymer incorporation into peptidoglycan, insoluble material recovered under the same initial transferase reaction conditions was instead incubated in 10% (w/v) TCA at 4°C for 16 hours. The hydrolysate was recovered as before and subsequently neutralized to pH ~8.0 using NaOH. This fraction was then analyzed for the presence of WTAs by anion-exchange HPLC analysis (see more details below). See also Figure 3.

HPLC analysis was conducted on a Waters ACQUITY UPLC H-Class system using Empower 3 (build 3471) software. Alditols, hexoses, and hexosamines were separated using a Bio-Rad Aminex HPX-87H (7.8 x 300 mm) carbohydrate column under ambient temperatures. Compound elution was achieved with isocratic 5 mM H₂SO₄ at a flow rate of 1 mL/min.

WTA polymers were separated using a ThermoScientific DNAPac PA200 (4 x 250 mm) anion-exchange column under ambient temperatures as described (Gale et al., 2014; Myers et al., 2016; 2015). Briefly, compounds were eluted using a two-step gradient starting from 0 -> 5% 1 M NaCl in 20 mM NH₄HCO₃ (pH = 8) and 10% (v/v) MeCN over 10 minutes, then from 5% -> 60% 1 M NaCl in the same solvent system over 5 minutes.

Radioactive molecules from both HPLC separations were visualized with in-line scintillation counting using a PerkinElmer Radiomatic 150TR paired with a Waters e-SAT/IN module.

QUANTIFICATION AND STATISTICAL ANALYSIS

To test the influence of different assay components on transferase activity, we used a one-way analysis of variance (ANOVA). Post hoc comparisons were performed using Tukey's HSD tests. All the data are presented as the mean \pm standard deviation from two independent replicates. Data fitting and graphing was performed using Igor Pro (version 6.36) and all statistical analyses were performed in the R statistical software (version 3.2.3). Statistical significance for each dataset is reported in the Figure legends.

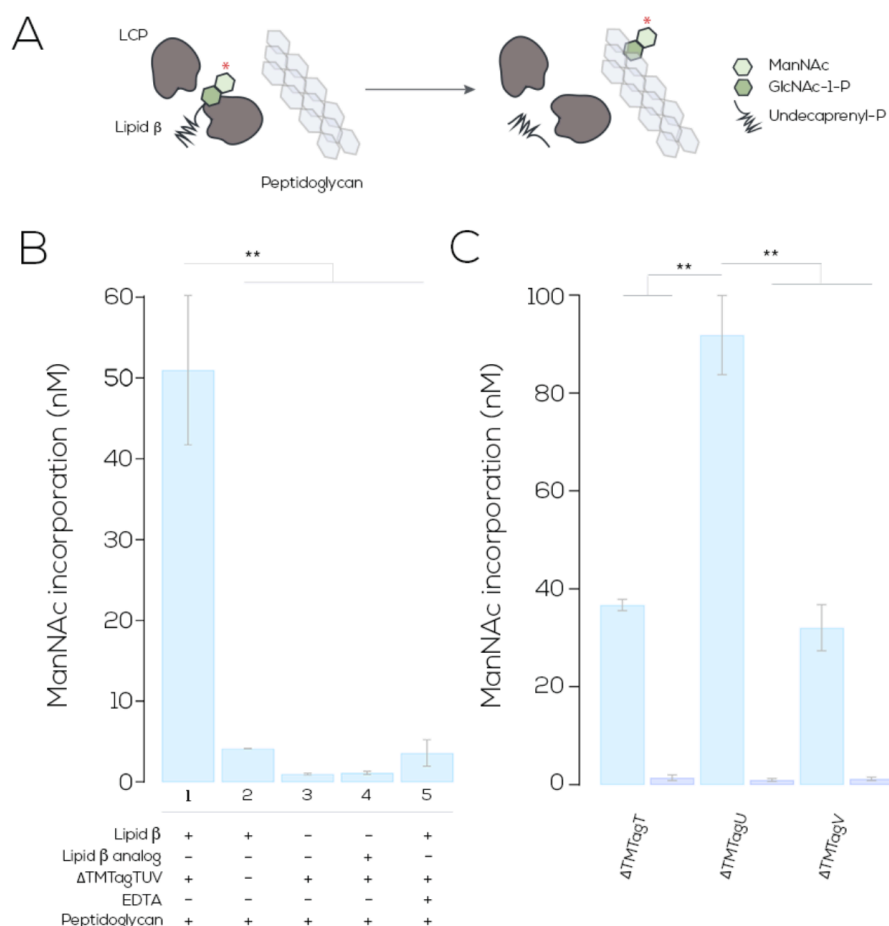


Figure 1. *B. subtilis* LCP enzymes transfer WTA intermediates to peptidoglycan *in vitro*. (A) Standard *in vitro* transferase assay schematic. Authentic [14 C]Lipid β WTA intermediate (0.6 μ M) is incubated with insoluble *B. subtilis* peptidoglycan (0.25 mg) and LCP enzymes (2-4 μ M). Reactions were performed at 30°C for 40 min and subsequently quenched and washed with boiling 5% (w/v) SDS to remove protein and lipid contaminants. Product peptidoglycan is purified and WTA intermediate incorporation is measured by liquid scintillation counting. Red asterisks denote 14 C-labelled molecules. See also Figure S2. (B) *In vitro* system analysis employing *B. subtilis* Δ TMTAGT, Δ TMTAGU and Δ TMTAGV LCP enzymes (2 μ M each). Reactions contained authentic [14 C]Lipid β (0.6 μ M; lane 1,2 and 5), analogs thereof (30 μ M, 0.04 μ Ci; lane 4) and EDTA (100 μ M; lane 5). Components are indicated (+/-) for each lane. Heat-inactivated (65°C, 30 min) LCP proteins were used as a negative control for the reaction (lane 2). (C) Analysis of individual truncated LCP enzymes from *B. subtilis* (Δ TMTAGT, Δ TMTAGU, or Δ TMTAGV; blue). See also Figure S1. Reactions contained the indicated LCP enzyme (4 μ M), [14 C]Lipid β (0.6 μ M) and *B. subtilis* peptidoglycan (0.25 mg). Heat-inactivated enzymes were used as negative controls (100°C, 30 min; purple). Reactions in (B) and (C) were performed following standard assay procedures described in (A). Differences between groups were assessed for significance by one-way analysis of variance (ANOVA). Tukey's HSD post hoc results are indicated: **, $p < 0.01$; $n = 2$; Data are represented as mean \pm SD. Wild-type enzyme reactions (blue) in (C) were found to be statistically significant over heat-inactivated (purple) controls ($p < 0.01$).

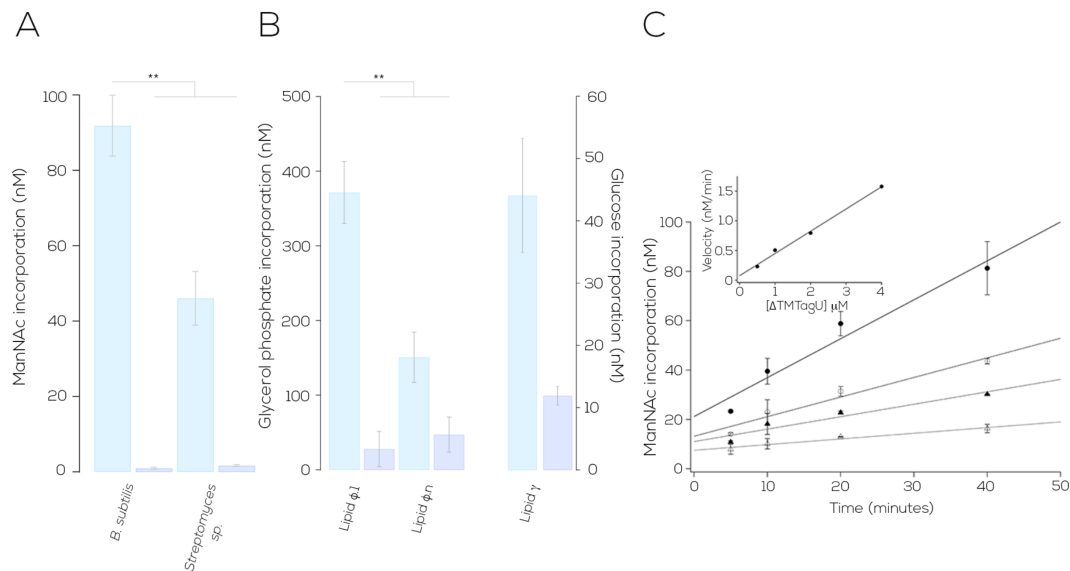


Figure 2. TagU-mediated activity varies with alternative acceptor/donor substrates and is linear with time and enzyme concentration.

In vitro transferase reactions were conducted as in Figure 1C, but instead used alternative peptidoglycan acceptor and WTA donor substrates.

(A) Peptidoglycan acceptor substrate preferences for *B. subtilis* LCP enzyme TagU. Δ TMTAGU (4 μ M; blue) was independently assessed for transferase activity using insoluble peptidoglycan (0.25 mg) from either *B. subtilis* or *Streptomyces sp.* [14 C]Lipid β (0.6 μ M) was used as the donor WTA glycopolymer. Heat-inactivated enzymes were used as negative controls (100°C, 30 min; purple).

(B) *B. subtilis* TagU transfers late-stage WTA intermediates to peptidoglycan *in vitro*. [14 C]-labeled WTA substrates (1.5 μ M) Lipid $\phi.1$, Lipid $\phi.n$, and Lipid γ were independently incubated with Δ TMTAGU (4 μ M; blue) and *B. subtilis* peptidoglycan (0.25 mg) *in vitro*. Composition and structures of these WTA intermediates are shown in Table 1. Radioactivity was incorporated into the glycerol phosphate moieties of these donor molecules – see also Figure S2 for synthesis details. Heat-inactivated enzymes were used as negative controls (100°C, 30 min; purple).

(C) Dependence of transferase activity on time and enzyme concentration. *B. subtilis* Δ TMTAGU LCP protein (0.5 μ M, Δ ; 1.0 μ M, \blacktriangle ; 2.0 μ M, \circ ; 4.0 μ M, \bullet) was assayed with *B. subtilis* peptidoglycan (0.25 mg) and [14 C]Lipid β (0.6 μ M).

Reactions were quenched at 5, 10, 20 and 40 min. Reactions in (A), (B), and (C) were all performed following standard assay procedures. Differences between groups were assessed for significance by one-way analysis of variance (ANOVA). Tukey's HSD post hoc results are indicated. **, $p < 0.01$; $n = 2$; Data are represented as mean \pm SD. Wild-type enzyme reactions (blue) in (A) and (B) were found to be statistically significant over heat-inactivated (purple) controls [(A) $p < 0.01$; (B) Lipid $\phi.1$: $p < 0.01$; Lipid $\phi.n$ & Lipid γ : $p < 0.05$].

Reactions in (B) and (C) were performed following standard assay procedures described in (A). Differences between groups were assessed for significance by one-way analysis of variance (ANOVA). Tukey's HSD post hoc results are indicated: **, $p < 0.01$; $n = 2$; Data are represented as mean \pm SD. Wild-type enzyme reactions (blue) in (C) were found to be statistically significant over heat-inactivated (purple) controls ($p < 0.01$).

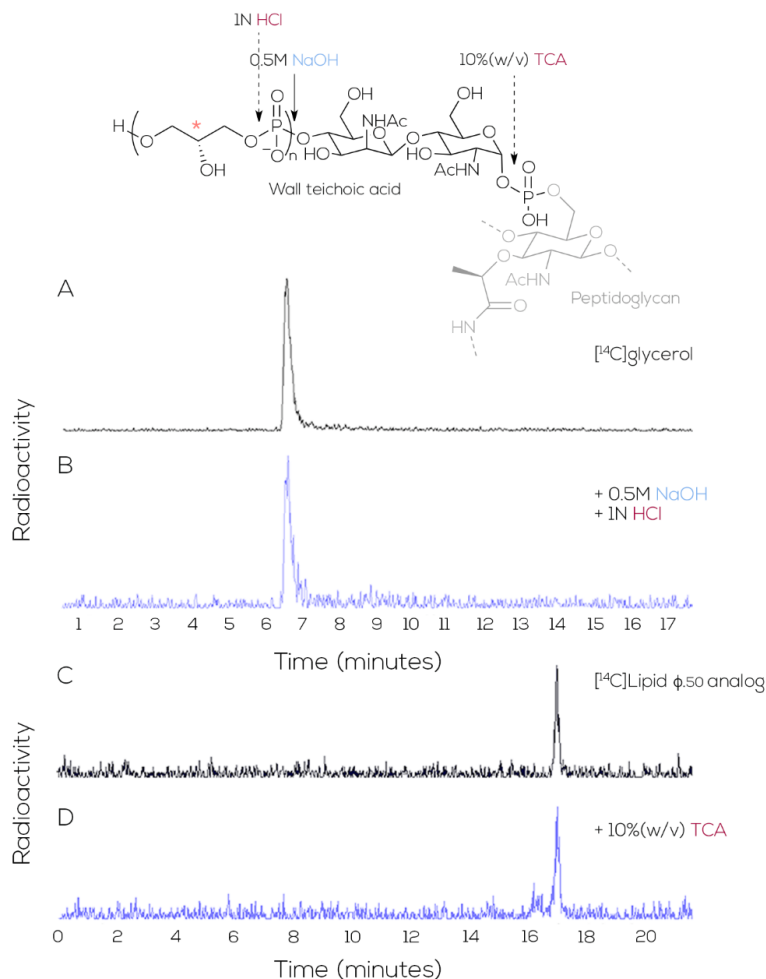
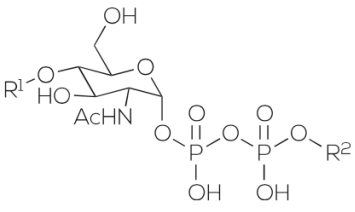
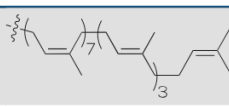
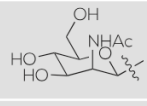
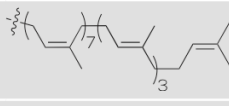
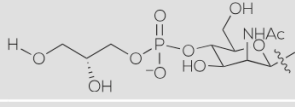
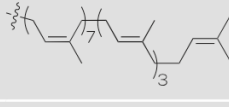
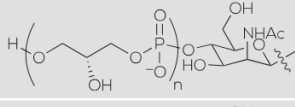
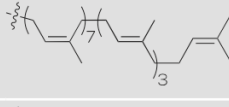
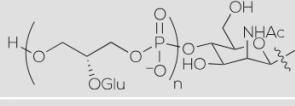
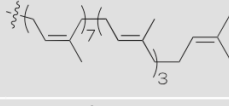

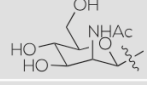
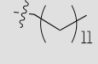
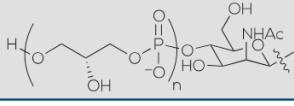
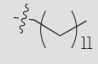


Figure 3. Hydrolysis and HPLC analysis confirm the transfer of WTAs to peptidoglycan by *B. subtilis* TagU.

Top: Predicted structure of the WTA-peptidoglycan tethered product after transfer of [^{14}C]Lipid $\phi.n$ WTA intermediates to peptidoglycan by *B. subtilis* $\Delta\text{TMTTagU}$. $\Delta\text{TMTTagU}$ (4 μM) was incubated with [^{14}C]Lipid $\phi.n$ and *B. subtilis* peptidoglycan (0.25 mg) at 30°C for 16 hours. WTAs were hydrolyzed from purified peptidoglycan by treatment with mild acid (red) and/or alkali (blue) solutions. Relevant linkages labile under these conditions are shown with arrows.

Bottom: HPLC analysis of hydrolysates using carbohydrate (A, B; Bio-Rad Aminex HPX-87H) and anion-exchange (C, D; ThermoScientific DNAPac PA200) chromatography columns. [^{14}C]-labelled molecules were visualized with in-line scintillation counting. Elution profiles for the following are shown: (A) [^{14}C]glycerol standard; (B) hydrolysate from WTA-peptidoglycan product treated sequentially with NaOH (0.5 M NaOH, 37°C, 30 min) and HCl (1 N, 100°C, 30 min); (C) [^{14}C] Lipid $\phi.50$ analog standard (Sewell et al., 2009); and (D) hydrolysate from WTA-peptidoglycan product treated with TCA (10% w/v, 4°C, 16 hr). TCA, trichloroacetic acid. See also Figure S3.

Table 1. WTA intermediates and analogs^a

| | |  | |
|-----------------------|--|--|---|
| Compound | Chemical Composition | R ¹ | R ² |
| Lipid α | GlcNAc-1-P-P-Und | H |  |
| Lipid β | ManNAc- β -(1-4)-GlcNAc-1-P-P-Und |  |  |
| Lipid ϕ_1 | GroP-ManNAc- β -(1-4)-GlcNAc-1-P-P-Und |  |  |
| Lipid ϕ_n | (GroP) _n -ManNAc- β -(1-4)-GlcNAc-1-P-P-Und |  |  |
| Lipid γ | (α -D-Glu(1- \rightarrow 2)GroP) _n -ManNAc- β -(1-4)-GlcNAc-1-P-P-Und |  |  |
| Lipid α analog | GlcNAc-1-P-P-tridecane | H |  |
| Lipid β analog | ManNAc- β -(1-4)-GlcNAc-1-P-P-tridecane |  |  |
| Lipid ϕ_n analog | (GroP) _n -ManNAc- β -(1-4)-GlcNAc-1-P-P-tridecane |  |  |

^aWTA intermediates are named according to the enzyme utilizing them as substrates. GlcNAc, *N*-acetylglucosamine; ManNAc, *N*-acetylmannosamine; Und, undecaprenol; GroP, *sn*-glycerol-3-phosphate. See also Table S2.

Supplemental figures

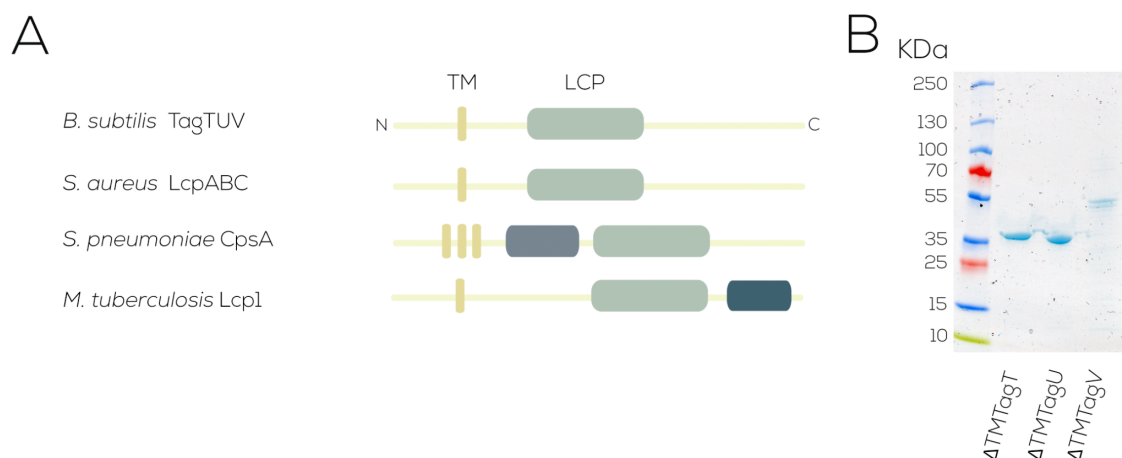


Figure S1. Purification of truncated *B. subtilis* LCP enzymes. Related to Figure 1

(A) Domain organization of LCP proteins. The majority of LCP enzymes contain a short N-terminal cytoplasmic domain, a transmembrane segment (one or three helices) and an extracellular catalytic LCP domain (Hübscher et al., 2008). *Streptococcus pneumoniae* CpsA protein contains an N-terminal DNA processivity factor domain (Hanson et al., 2010). Several LCP proteins from *Mycobacteria tuberculosis* and other Actinobacteria possess an uncharacterized C-terminal LytR_C domain (Harrison et al., 2016; Sigle et al., 2016). TM, transmembrane domain; LCP, catalytic domain.

(B) SDS-PAGE analysis of purified recombinant *B. subtilis* LCP proteins used in this study. Truncated LCP proteins lack transmembrane domains (Δ TM).

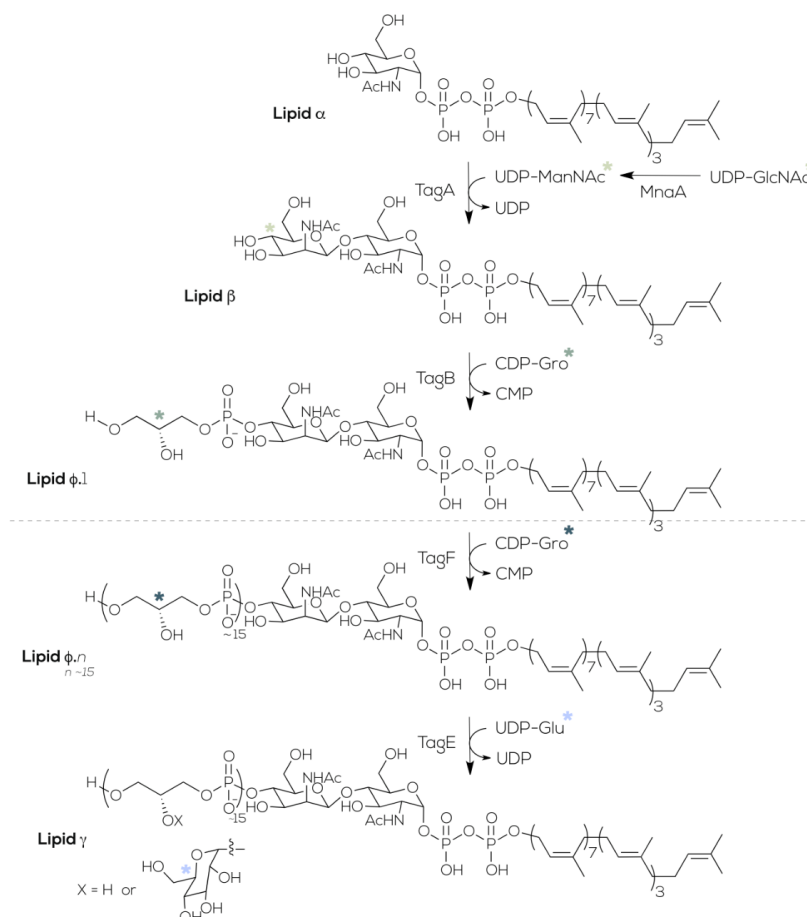


Figure S2. Synthesis of WTA intermediates for LCP transferase assays. Related to STAR Methods and Figures 1&2

^{14}C -labeled WTA intermediates were prepared from synthetic Lipid α *in vitro* using recombinant WTA biosynthetic enzymes and radioactive nucleotide-activated donors as described (Gale et al., 2014). Radioactivity was only incorporated into each WTA intermediate in the final enzymatic step of its synthesis (light green → blue). A heat-inactivation step (80°C, 10 min) was incorporated after preparation of Lipid φ.1 (represented by a dashed line in the above scheme) to ensure that no additional Lipid φ.1 was synthesized from TagB during ^{14}C Lipid φ.n and ^{14}C Lipid γ syntheses.

The concentrations of ^{14}C Lipid β and ^{14}C Lipid φ.1 were determined post synthesis using a previously described lipid extraction method (Farha et al., 2013; Gale et al., 2014; Schaffer et al., 2002). The degree of polymerization of the ^{14}C Lipid φ.n intermediate was estimated based on the ratio of CDP-Gro consumption to the initial concentration of the Lipid φ.1 intermediate, as per established methods (Pereira et al., 2008; Sewell et al., 2009). TagE has not been fully characterized biochemically, and thus, it is not known how many glycerol phosphate residues are glycosylated within a WTA polymer.

Radiolabeled WTA intermediate synthesis reactions were used directly in transferase assays. The asterisk (*) denotes ^{14}C -radiolabeled molecules: UDP- ^{14}C GlcNAc, UDP- ^{14}C ManNAc, CDP- ^{14}C Gro and UDP- ^{14}C Glu. Abbreviations: GlcNAc, *N*-acetylglucosamine; ManNAc, *N*-acetylmannosamine; Gro, glycerol; Glu, glucose.

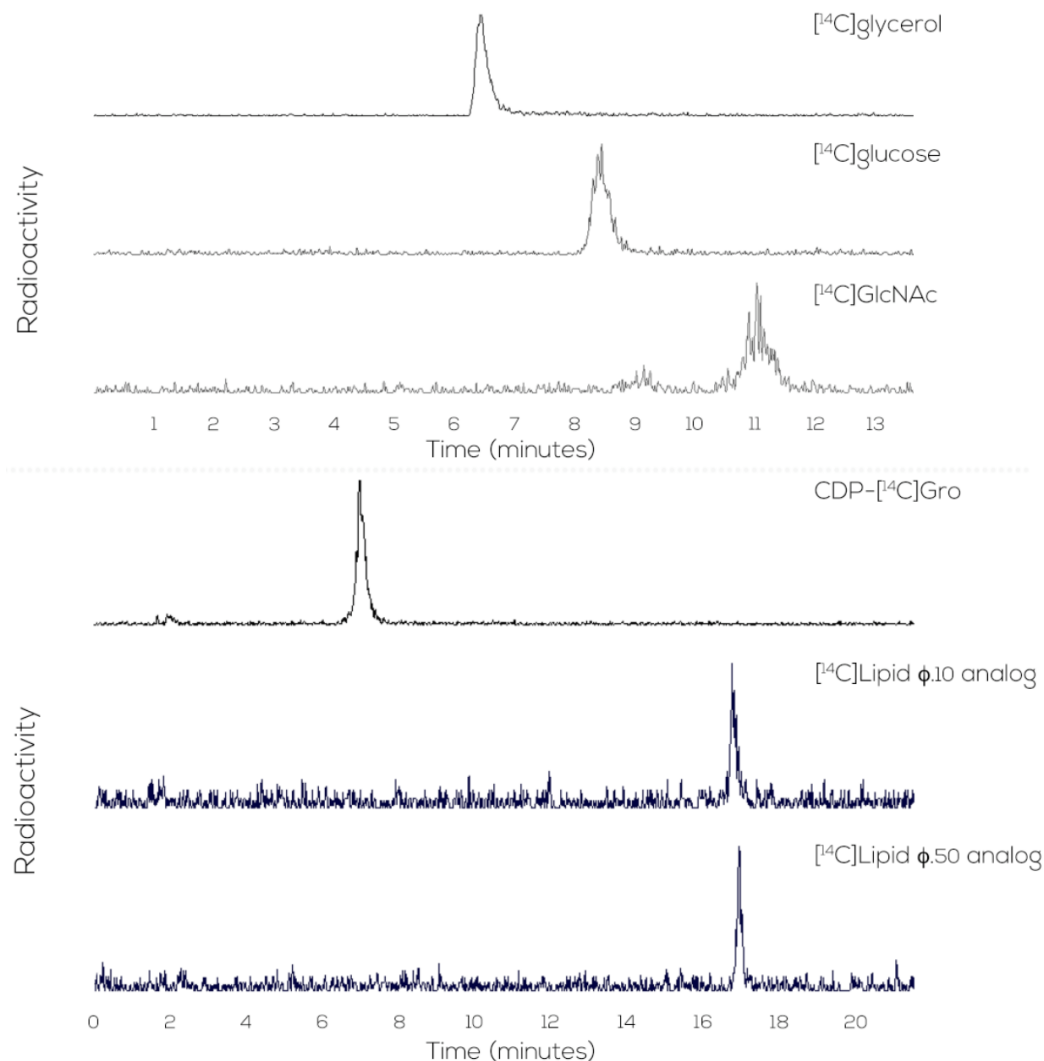


Figure S3. HPLC analysis of radiolabeled standards. Related to Figure 3

Standards subject to HPLC analysis are indicated to the right of the frame. [^{14}C]-labeled molecules were visualized with in-line scintillation counting. Elution profiles of standards using a:

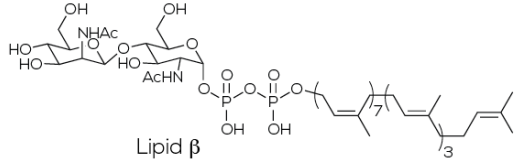
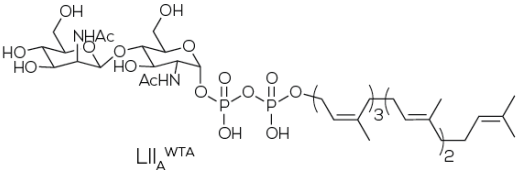
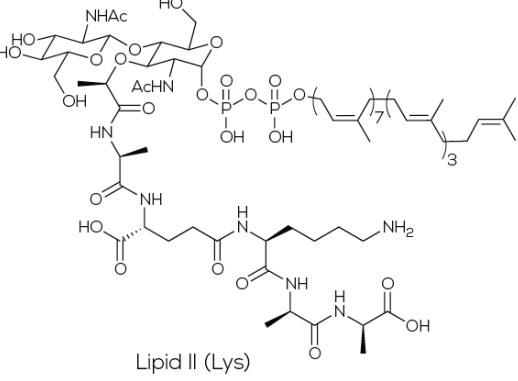
(Top) Bio-Rad Aminex HPX-87H carbohydrate analysis column. Samples were prepared by acid hydrolysis (1 N HCl, 100 °C, 35 min) of *sn*-[^{14}C]glycerol-3-phosphate, UDP-[^{14}C]glucose, and UDP-[^{14}C]GlcNAc.

(Bottom) ThermoScientific DNAPac PA 200 anion-exchange column. CDP-[^{14}C]Gro, [^{14}C]Lipid ϕ .10, and [^{14}C]Lipid ϕ .50 analogs were synthesized as described elsewhere (Badurina et al., 2003; Gale et al., 2014; Sewell et al., 2009).

Abbreviations: GlcNAc, *N*-acetylglucosamine; Gro, glycerol.

Supplemental table

Table S1. Polyisoprenoid-linked WTA and peptidoglycan intermediates. Related to Table 1

| References | Compound name/structure |
|---|--|
| Gale <i>et al.</i> , 2014 & <i>this study</i> |  <p>Lipid β</p> |
| Schaefer <i>et al.</i> , 2017 |  <p>Lipid A WTA</p> |
| Breukink <i>et al.</i> , 2003 |  <p>Lipid II (Lys)</p> |

CHAPTER IV - Conclusion

Summary

The most successful antibiotics used in the clinic inhibit cell wall assembly. WTAs are a major component of Gram-positive bacterial cell walls and their synthesis pathway offers several unexploited targets for antibacterial drug discovery and development. Rational whole-cell screens are frequently conducted against WTA assembly. However, as industry pundits suggest (Sutterlin et al., 2017), the success of these screens relies on understanding the complex biology of WTAs. We endeavored herein to prepare authentic WTA substrates that would help resolve enigmatic features of WTA assembly.

In Chapter 2 we applied a novel chemoenzymatic strategy to obtain authentic WTA substrates. We show that these materials can be used to study WTA glycosyltransferases *in vitro*. In Chapter 3 we used authentic substrates to characterize, for the first time, LCP enzyme-mediated WTA-peptidoglycan ligation in *B. subtilis*.

Practical applications for authentic WTA substrates

Undecaprenyl pyrophosphate-linked sugars are common intermediates in bacterial glycopolymer assembly. Bacteria use these molecules to assemble WTAs, peptidoglycan, and *O*-antigens. Protein *N*-/*O*-glycosylation also employs lipid-linked sugars. These intermediates are not available from commercial sources to study these processes. Further, authentic undecaprenyl pyrophosphate-linked sugars are difficult to isolate in quantity from bacteria. Many labs have leveraged chemoenzymatic methods to prepare them from expensive undecaprenyl-phosphate precursors (reviewed in Li et al., 2016). We took inspiration from these studies when designing our synthetic route to the WTA intermediate Lipid α . However, our semisynthetic preparation of Lipid α is unique in that it utilizes *L. nobilis* leaves as a source of undecaprenol precursor.

With Lipid α in mixed-micelles, we reconstituted the intracellular steps of *B. subtilis* poly(glycerol phosphate) biosynthesis *in vitro*. Consequently, we gained access to authentic substrates for all WTA enzymes of this pathway. Before, enzymatic synthesis was the only route to crude preparations of Lipid α and Lipid β (Muller 2012). For more than a decade, our lab and others didn't have a supply of defined authentic substrates to study WTA glycosyltransferases. Soluble analogs or crude membrane preparations were sources of substrates in assays instead.

Reconstituting our authentic WTA substrates in mixed-micelles provides an interface for enzyme catalysis. This system better represents the physiological environment that WTA glycosyltransferases work in. We wanted to learn more about WTA glycosyltransferase-mediated reactions and characterize enigmatic steps in WTA biosynthesis using this system. Unfortunately, experiments to address the latter consumed the lions-share of our time. We never investigated exactly how authentic substrates in an interfacial system influence WTA glycosyltransferase activity. But, the kinetics and mechanism of WTA glycosyltransferases can be investigated using the system described in Chapter 2. Comparing such data to that obtained using soluble substrate analogs in assays may unveil useful information to drug discovery efforts against these targets.

An obvious limitation of our work in Chapter 2 is that we did not collect reaction rates or turnover numbers for any enzyme-mediated reactions. Neither did we experiment with different interfaces like unilamellar vesicles. Thus, we have little information on how ideal the mixed-micelle system is to study WTA glycosyltransferases on authentic substrates. I recommend identifying the most

optimal interfacial system before conducting more assays with authentic substrates.

Late-steps in WTA assembly are conditionally essential and vital for pathogenesis. Thus, these processes may be an Achilles' heel in Gram-positive bacteria that can be targeted with novel chemical matter. When I started graduate school (2011), studying these late-steps in *B. subtilis* was a major focus of the lab. Our group has described the mechanism and mode of TagF-mediated WTA polymerization in *B. subtilis* (Pereira et al., 2008; Schertzer and Brown, 2003; 2008; Schertzer et al., 2005; Sewell et al., 2009). Our collaborators at UBC solved the structure for the TagF orthologue protein in *S. epidermidis* (Lovering et al., 2010) – the first crystal structure of a WTA glycosyltransferase. Despite these advances, the length sensing function of *B. subtilis* TagF is not well understood. In assays using soluble tridecyl-linked substrates, TagF elongates poly(glycerol phosphate) polymers exceeding physiological lengths (100+ units) and displays kinetic parameters that do not discriminate for polymer length (Pereira et al., 2008; Schertzer and Brown, 2008; Sewell et al., 2009). Yet, in assays employing crude membranes, TagF regulates polymers to near physiological lengths (~30 residues) (Schertzer and Brown, 2003). Clearly, membrane interaction influences the length sensing capacity of the TagF polymerase. But, the undefined nature of crude-membrane systems makes it challenging to probe the molecular features of this process. Using our authentic substrates in defined interfacial systems could shed light on mechanisms of TagF polymer length sensing.

The number of reported structural studies on WTA glycosyltransferases is rising (Lovering et al., 2010; Mann et al., 2016; Sobhanifar et al., 2016; 2015; Xia et al., 2010). Authentic WTA substrates could soak in with protein crystals to showcase

the molecular interactions between WTA glycosyltransferases and their lipid-linked substrates. This information is currently lacking and would be useful to structure-based drug design efforts. Moreover, as exemplified by the Schneider group and others, these molecules can elucidate the mechanism of action of cell wall biosynthetic inhibitors (Ling et al., 2015; Munch et al., 2014; Müller et al., 2012). Indeed, our laboratory employed authentic substrates sourced from crude bacterial membranes to confirm that the antiplatelet drug ticlopidine, and its analogs, inhibit the action of TagO *in vitro* (Farha et al., 2014; 2013). Authentic substrates could also have important immunological applications. An effective WTA antibody-antibiotic conjugate recently emerged that eliminates chronic *S. aureus* infections (Lehar et al., 2015). Furthermore, several novel vaccine formulations use teichoic acid fragments (van der Es et al., 2017; Zhou et al., 2017).

But which studies have priority? The procedure to prepare authentic substrates is tedious and requires an experienced hand in chemistry to produce useful quantities (milligrams) of pure glycolipids. So, these materials are rather precious. I believe these resources should continue to be used to better understand LCP-mediated catalysis and to aid any drug discovery efforts against these targets. We still know little about LCP-mediated glycopolymer transfer. Furthermore, if whole-cell screens are developed to target LCP enzymes, authentic substrates could be useful in validating small molecule inhibitors. The rest of the discussion focuses on these objectives.

Probing the glycopolymer transfer reaction

Authentic WTA substrates finally allowed us to reconstitute WTA-peptidoglycan ligation *in vitro*. We prepared recombinant *B. subtilis* LCP proteins in early 2015. Yet, we consistently failed to reconstitute their transferase activity. It was

challenging to identify the right combination of WTA donor and peptidoglycan acceptor substrates for activity. We hoped that soluble WTA intermediate analogs would be suitable substrates. These materials simplify assay design and product characterization. However, as Chapter 3 details, only authentic WTA glycopolymers are suitable substrates for LCP-mediated catalysis. The glycopolymer transfer reaction likely eluded biochemical characterization for so long because authentic substrates were not available.

Several reports suggested that *M. tuberculosis* arabinogalactan components are tethered to cross-linked peptidoglycan (Hancock et al., 2002; Harrison et al., 2016b). Thus, we purchased cross-linked peptidoglycan from commercial vendors for use in transferase assays. While this material worked as an acceptor substrate in our assay, it is undefined. The exact features of the peptidoglycan acceptor necessary for transferase activity are still unknown. Understanding these features may aid drug discovery efforts against the LCP machinery. They could contribute fresh ideas for target-based screens and/or guide inhibitor design and lead compound optimization. Moreover, this information will inform on the spatial and temporal requirements of glycopolymer transfer to peptidoglycan. Various genetic and chemical methods can produce defined peptidoglycan materials (Chan et al., 2014; Larson and Yother, 2017). But, characterizing this material before and after ligation will be challenging. Peptidoglycan has a non-crystalline arrangement, an enormous size (multi-gigadaltons), and a high degree of variability.

We still know very little about cell wall assembly in Gram-positive bacteria. Recently, investigators unearthed a new set of peptidoglycan synthesis enzymes. These SEDS proteins co-ordinate with canonical class B PBPs to build the peptidoglycan wall (Emami et al., 2017; Leclercq et al., 2017; Meeske et al.,

2016). LCP enzymes might also interact with components of the cell wall synthesis ensemble. Likely interactions are with peptidoglycan- and/or other WTA- assembly proteins. It is possible that the ABC transporters that export WTAs help lipid substrate loading and/or product exit at the LCP active site. This interaction might provide the rate enhancement required for cellular glycopolymer transfer. Conducting *in vitro* transferase assays with cell wall biosynthetic components added is one strategy to test these hypotheses.

The mechanism of LCP-mediated catalysis is still unknown. LCP enzymes have several conserved residues including aspartic acid, arginine, and lysine (Hübscher et al., 2008). It seems likely that some of these charged residues participate in catalysis. Crystal structures of LCP enzymes from *B. subtilis* and *S. pneumoniae* show conserved arginine residues interacting with phosphate oxygens of bound polyisoprenoid pyrophosphate molecules (Eberhardt et al., 2012; Kawai et al., 2011). These arginines may create a positively charged pocket to harbour the pyrophosphate moiety of donor molecules. They also are in close contact with conserved aspartic acid residues. Figure 1 shows these important interactions. A few groups have proposed that the phosphotransfer reaction proceeds through a general acid/base catalytic mechanism (Kawai et al., 2011; Harrison, 2016a). This mechanism is only putative however and detailed biochemical studies will be necessary to confirm these claims. I suggest that mutant LCP constructs be made with amino acid substitutions at conserved residues to elucidate the mechanism of glycopolymer transfer to peptidoglycan. I would start with the charged arginines and aspartic acids. Furthermore, analyzing the transferase reaction in conditions of varying pH may also confirm the need for acidic and basic amino acid side chains in catalysis.

In Chapter 3, we saw that glycopolymer transfer requires Mg^{2+} . Exactly how this cofactor participates in catalysis is unknown. In published structures of LCP enzymes, Mg^{2+} coordinates with phosphate oxygens of the donor lipid molecule and with conserved aspartic acids (Figure 1) (Kawai et al., 2011). Mg^{2+} might stabilize the transition state or intermediate molecules by neutralizing negative charges. Mg^{2+} may also take part in generating a nucleophile on the incoming peptidoglycan MurNAc moiety and/or function to orient the phosphoanhydride moiety of the WTA donor molecule. More detailed biochemical and structural studies of LCP enzymes are required to examine these possibilities.

Are LCP proteins druggable antibiotic targets?

Earlier genetic and phenotypic work suggested that LCP enzymes were glycopolymer transferases. I believe LCP enzymes are attractive antibiotic targets now that biochemical studies have confirmed their activity. LCP enzymes localize to the same extramembrane compartment as some of the most successful antibiotic protein and structural targets (PBPs and Lipid II). Thus, LCP enzyme inhibitors don't need to traverse the problematic cytoplasmic membrane or avoid efflux. LCP proteins will likely represent a range of possible target types. In some organisms, inactivation of a single (*S. coliecolour*, *M. tuberculosis*, and *M. smegmatis*) or all (*B. subtilis*) *lcp* genes results in a lethal phenotype. Small molecule inhibitors of these gene products would resemble conventional antibiotics that target essential processes (Harrison et al., 2016b; Kawai et al., 2011; Sigle et al., 2016). In some pathogens like *S. aureus*, *lcp*-null mutants are viable (Over et al., 2011). But, inhibition of LCP catalysis would disarm the bug of glycopolymers like WTAs and capsule polysaccharides that are essential for pathogenesis and virulence. These molecules could be anti-virulence agents. Lastly, inactivation of the *lcpA* (*msrR*) gene in methicillin-resistant strains of *S.*

aureus restores β -lactam sensitivity (Schaefer et al., 2017). Thus, LCP enzymes may also be β -lactam potentiator targets in some bacteria.

Glycopolymer ligation to peptidoglycan is an important process in bacteria. It is not surprising then that bacteria encode many LCP enzymes for this function. This redundancy may present a significant obstacle for their exploitation as drug targets. In some organisms, multiple LCP enzymes may have to be inhibited to produce desired effects. Fortunately, despite the LCP family displaying a high degree of sequence divergence (17-37% amino acid identity; Hübscher et al., 2008), LCP proteins have structural similarities in catalytic domains (Eberhardt et al., 2012; Kawai et al., 2011). So, it may be possible for an active site-inhibitor of one enzyme to prevent the catalysis of other homologous.

Combating multidrug- and extensively drug-resistant Gram-negative pathogens are the focus of modern antibiotic R&D (World Health Organization, 2017a,b). But, novel antimicrobial agents are still urgently needed to deal with several troublesome multidrug-resistant Gram-positive pathogens. These bacteria would be the obvious primary targets for LCP catalysis inhibitors. Such agents may also be useful in the fight against tuberculosis (TB). *M. tuberculosis* is the causative agent of TB and harbours three *lcp* genes in its genome. Mycobacterial bacilli do not synthesize WTA polymers. In this organism, LCP enzymes link the arabinogalactan-mycolic acid layer to the peptidoglycan cell wall (Harrison et al., 2016b). One LCP enzyme, CpsA, was recently highlighted to have crucial roles in *M. tuberculosis* innate immune evasion (Köster et al., 2017). Moreover, inactivation of *cpsA* impairs mutants during *in vivo* infection and makes them susceptible to several cell wall-targeting antibiotics including CPZEN-45 (Ishizaki et al., 2013), vancomycin, and β -lactams (Grzegorzewicz et al., 2016).

A question to consider: why haven't we found LCP inhibitors using empirical or target-based drug discovery platforms? No natural products or small molecule synthetics are known to inhibit glycopolymer transfer to peptidoglycan. It could be that the redundancy discussed above is too challenging to overcome for phenotypes to arise. Or, mutations in other genes alleviate lethal or growth-defective phenotypes. This phenomenon is common when inhibiting late-step WTA glycosyltransferases whose genes are conditionally essential. For example, resistance to targocil – which inhibits the activity of *S. aureus* TarG - occurs at a high frequency partly due to pre-existing loss-of-function mutations in the early-step genes *tarO* or *tarA* (Lee et al., 2010). Still, it is not known if LCP enzymes are truly druggable. Identifying inhibitors of glycopolymer transfer likely requires unique target-based screens.

Screening for small molecule inhibitors of LCP enzymes

We found no reports in the literature detailing screening campaigns against LCP enzymes. Demuris Ltd lists LCP inhibitors in its online portfolio (<http://www.demuris.co.uk/portfolio.htm>). This company holds a natural product collection sourced from over 10,000 actinomycete strains. Thus, it is likely these putative inhibitors are natural products. But, how these investigators identified and validated these agents is unknown. Virtual docking studies have also been conducted against LCP enzymes. These efforts identified the plant-derived compounds ellagic acid and fisetin as binders of *Streptococcus dysgalactiae* LytR. Unfortunately, these compounds did not bind recombinant LytR *in vitro* (Ramos, 2017).

Both the Walker lab and Merck & Co. have used whole-cell screens to find inhibitors of *S. aureus* late-stage WTA assembly proteins (Lee et al., 2010; Swoboda et al., 2009; Wang et al., 2013). These groups designed screens that

phenocopy the conditional essentiality of late-stage lesions in WTA assembly. These screens involve first mining for compounds that prevent the growth of wild-type *S. aureus*. Actives in this assay are counter-screened in $\Delta tarO$ mutants that do not initiate WTA synthesis. Any agents losing bioactivity in the latter screen are putative late-stage WTA assembly inhibitors. These investigators found many inhibitors of the TarG using this screening method. As described before, *S. aureus lcp*-null ($\Delta lcpABC$) mutants display only a modest growth defect. Thus, *S. aureus lcp* genes are not conditionally essential like other late-stage WTA synthesis genes. So, potential inhibitors of LCP enzymes would have been missed in these screening campaigns.

I believe whole-cell screens can discover small molecule inhibitors of LCP catalysis. *S. aureus* would only have a subtle growth defect upon challenge with LCP inhibitors. I propose using *B. subtilis* instead for initial screens. An *lcp*-null mutant in *B. subtilis* ($\Delta tagTUV$) is non-viable. Thus, a simple live/dead primary screen could identify putative LCP inhibitors from chemical libraries. Additionally, double *lcp* deletion *B. subtilis* mutants display no growth defects (Kawai et al., 2011). Molecules only need to target one LCP enzyme in these mutants to cause lethality. Therefore, screening with these mutants would likely enrich for LCP inhibitors. Unlike *S. aureus*, *B. subtilis lcp* genes are conditionally essential. Thus, actives against either wild-type *B. subtilis* or double *lcp* deletion mutants could be counter-screened against a $\Delta tagO$ mutant. Compounds with attenuated activity in these screens would be putative inhibitors of LCP catalysis. We could process such agents through our *in vitro* LCP assay for target validation and mechanistic studies. These molecules could then act as leads for optimization/derivatization.

Concluding remarks

Antibiotic resistance is rife and the drug pipeline is lean - too lean to handle the threat. The post-antibiotic era looms ahead. But it isn't all doom-and-gloom. The rates of approved antibiotics over the years has increased. Several first-in-class antibiotics are in the pipeline. Biological agents are being developed as alternatives to antibiotics. Many private-public and other initiatives are underway to bring new innovations to the pipeline. And the antibiotic resistance problem has garnered the attention of policymakers and the public (Butler et al., 2016; World Health Organization, 2017a,b; Silver, 2017).

Target-based screening is still a reasonable strategy to deliver new antibacterial matter. However, we must learn from the past failures of this strategy. Understanding the complex biology of a target is pivotal to the success of this modern screening approach.

Disruption of WTA assembly has serious consequences to the physiology and virulence of several problematic Gram-positive pathogens. Our lab and others have targeted the WTA assembly pathway in several whole-cell screens. Proteins and intermediates of this pathway are not targeted by traditional antibiotic classes. Yet, it is clear that this pathway is druggable. There are many unexploited targets in this pathway to leverage for antibiotic drug discovery and development.

We show herein that authentic WTA substrates are useful probes of WTA assembly. We characterized a process of WTA biosynthesis that had been elusive for decades with these materials. This information has allowed us to design rational whole-cell screens that specifically target this critical process. We

are now poised to validate small molecule inhibitors that should come out of such efforts.

References

- Chan, Y.G.-Y., Kim, H.K., Schneewind, O., and Missiakas, D. (2014). The capsular polysaccharide of *Staphylococcus aureus* is attached to peptidoglycan by the LytR-CpsA-Psr (LCP) family of enzymes. *J. Biol. Chem.* **289**, 15680–15690.
- Eberhardt, A., Hoyland, C.N., Vollmer, D., Bisle, S., Cleverley, R.M., Johnsborg, O., Håvarstein, L.S., Lewis, R.J., and Vollmer, W. (2012). Attachment of capsular polysaccharide to the cell wall in *Streptococcus pneumoniae*. *Microb. Drug Resist.* **18**, 240–255.
- Emami, K., Guyet, A., Kawai, Y., Devi, J., Wu, L.J., Allenby, N., Daniel, R.A., and Errington, J. (2017). RodA as the missing glycosyltransferase in *Bacillus subtilis* and antibiotic discovery for the peptidoglycan polymerase pathway. *Nat. Microbiol.* **2**, 16253.
- Farha, M.A., Koteva, K., Gale, R.T., Sewell, E.W., Wright, G.D., and Brown, E.D. (2014). Designing analogs of ticlopidine, a wall teichoic acid inhibitor, to avoid formation of its oxidative metabolites. *Bioorg. Med. Chem. Lett.* **24**, 905–910.
- Farha, M.A., Leung, A., Sewell, E.W., D'Elia, M.A., Allison, S.E., Ejim, L., Pereira, P.M., Pinho, M.G., Wright, G.D., and Brown, E.D. (2013). Inhibition of WTA synthesis blocks the cooperative action of PBPs and sensitizes MRSA to β -lactams. *ACS Chem. Biol.* **8**, 226–233.
- Grzegorzewicz, A.E., De Sousa-d'Auria, C., McNeil, M.R., Huc-Claustre, E., Jones, V., Petit, C., Angala, S.K., Zemanová, J., Wang, Q., Belardinelli, J.M., Gao, Q., Ishizaki, Y., Mikusova, K., Brennan, P.J., Ronning, D.R., Chami, M., Houssin, C., and Jackson, J.M. (2016). Assembling of the *Mycobacterium tuberculosis* cell wall core. *J. Biol. Chem.* **291**, 18867–18879.
- Hancock, I.C., Carman, S., Besra, G.S., Brennan, P.J., and Waite, E. (2002). Ligation of arabinogalactan to peptidoglycan in the cell wall of *Mycobacterium smegmatis* requires concomitant synthesis of the two wall polymers. *Microbiology (Reading, Engl.)* **148**, 3059–3067.

Harrison, J. (2016a). Biochemical characterization of pivotal enzymes involved in *Mycobacterium tuberculosis* cell wall biosynthesis. University of Birmingham. Ph.D. thesis.

Harrison, J., Lloyd, G., Joe, M., Lowary, T.L., Reynolds, E., Walters-Morgan, H., Bhatt, A., Lovering, A., Besra, G.S., and Alderwick, L.J. (2016b). Lcp1 Is a phosphotransferase responsible for ligating arabinogalactan to peptidoglycan in *Mycobacterium tuberculosis*. *MBio*. 7, e00972–16.

Hübscher, J., Lüthy, L., Berger-Bächi, B., and Stutzmann Meier, P. (2008). Phylogenetic distribution and membrane topology of the LytR-CpsA-Psr protein family. *BMC Genomics*. 9, 617–16.

Ishizaki, Y., Hayashi, C., Inoue, K., Igarashi, M., Takahashi, Y., Pujari, V., Crick, D.C., Brennan, P.J., and Nomoto, A. (2013). Inhibition of the first step in synthesis of the *Mycobacterial* cell wall core, catalyzed by the GlcNAc-1-phosphate transferase *WecA*, by the novel caprazamycin derivative CPZEN-45. *J. Biol. Chem.* 288, 30309–30319.

Kawai, Y., Marles-Wright, J., Cleverley, R.M., Emmins, R., Ishikawa, S., Kuwano, M., Heinz, N., Bui, N.K., Hoyland, C.N., Ogasawara, N., et al. (2011). A widespread family of bacterial cell wall assembly proteins. *EMBO J.* 30, 4931–4941.

Köster, S., Upadhyay, S., Chandra, P., Papavinasasundaram, K., Yang, G., Hassan, A., Grigsby, S.J., Mittal, E., Park, H.S., Jones, V., Hsu, F-F., Jackson, M., Sasseti, C.M., and Philips, J.A. (2017). *Mycobacterium tuberculosis* protected from NADPH oxidase and LC3-associated phagocytosis by the LCP protein CpsA. *Proc. Natl. Acad. Sci.* 374, 201707792–10.

Larson, T.R., and Yother, J. (2017). *Streptococcus pneumoniae* capsular polysaccharide is linked to peptidoglycan via a direct glycosidic bond to β -D-N-acetylglucosamine. *Proc. Natl. Acad. Sci. U.S.A.* 201620431.

Leclercq, S., Derouaux, A., Olatunji, S., Fraipont, C., Egan, A.J.F., Vollmer, W., Breukink, E., and Terrak, M. (2017). Interplay between penicillin-binding proteins and SEDS proteins promotes bacterial cell wall synthesis. *Sci. Rep.* 7, 43306.

Lee, K., Campbell, J., Swoboda, J.G., Cuny, G.D., and Walker, S. (2010). Development of improved inhibitors of wall teichoic acid biosynthesis with potent activity against *Staphylococcus aureus*. *Bioorg. Med. Chem. Lett.* 20, 1767–1770.

Lehar, S.M., Pillow, T., Xu, M., Staben, L., Kajihara, K.K., Vandlen, R., DePalatis, L., Raab, H., Hazenbos, W.L., Morisaki, J.H., et al. (2015). Novel antibody-antibiotic conjugate eliminates intracellular *S. aureus*. *Nature*. *527*, 323–328.

Li, L., Woodward, R.L., Han, W., Qu, J., Song, J., Ma, C., and Wang, P.G. (2016). Chemoenzymatic synthesis of the bacterial polysaccharide repeating unit undecaprenyl pyrophosphate and its analogs. *Nat. Protoc.* *11*, 1280–1298.

Ling, L.L., Schneider, T., Peoples, A.J., Spoering, A.L., Engels, I., Conlon, B.P., Mueller, A., Schäberle, T.F., Hughes, D.E., Epstein, S., Jones, M., Lazarides, L., Steadman, V.A., Cohen, D.R., Felix, C.R., Fetterman, K.A., Millett, W.P., Nitti, A.G., Zullo, A.M., Chen, C., and Lewis, K. (2015). A new antibiotic kills pathogens without detectable resistance. *Nature*. *517*, 455–459.

Lovering, A.L., Lin, L.Y.-C., Sewell, E.W., Spreter, T., Brown, E.D., and Strynadka, N.C.J. (2010). Structure of the bacterial teichoic acid polymerase TagF provides insights into membrane association and catalysis. *Nat. Struct. Mol. Biol.* *17*, 582–589.

Mann, P.A., Müller, A., Wolff, K.A., Fischmann, T., Wang, H., Reed, P., Hou, Y., Li, W., Müller, C.E., Xiao, J., et al. (2016). Chemical genetic analysis and functional characterization of Staphylococcal wall teichoic acid 2-epimerases reveals unconventional antibiotic drug targets. *PLoS Pathog.* *12*, e1005585.

Meeske, A.J., Riley, E.P., Robins, W.P., Uehara, T., Mekalanos, J.J., Kahne, D., Walker, S., Kruse, A.C., Bernhardt, T.G., and Rudner, D.Z. (2016). SEDS proteins are a widespread family of bacterial cell wall polymerases. *Nature*. *537*, 634–638.

Munch, D., Muller, A., Schneider, T., Kohl, B., Wenzel, M., Bandow, J.E., Maffioli, S., Sosio, M., Donadio, S., Wimmer, R., and Sahl, H-G. (2014). The lantibiotic NAI-107 binds to bactoprenol-bound cell wall precursors and impairs membrane functions. *J. Biol. Chem.* *289*, 12063–12076.

Müller, A., Ulm, H., Reder-Christ, K., Sahl, H.-G., and Schneider, T. (2012). Interaction of Type A lantibiotics with undecaprenol-bound cell envelope precursors. *Microb. Drug Resist.* *18*, 261–270.

Over, B., Heusser, R., McCallum, N., Schulthess, B., Kupferschmied, P., Gaiani, J.M., Sifri, C.D., Berger-Bächi, B., and Meier, P.S. (2011). LytR-CpsA-Psr proteins in *Staphylococcus aureus* display partial functional redundancy and the deletion of all three severely impairs septum placement and cell separation. *FEMS Microbiol. Lett.* *320*, 142–151

Pereira, M.P., Schertzer, J.W., D'Elia, M.A., Koteva, K.P., Hughes, D.W., Wright, G.D., and Brown, E.D. (2008). The wall teichoic acid polymerase TagF efficiently synthesizes poly(glycerol phosphate) on the TagB product Lipid III. *ChemBioChem*. *9*, 1385–1390.

Ramos, J.C.M. (2017). Structure based drug design for the discovery of promising inhibitors of human Bcl-2 and *Streptococcus dysgalactiae* LytR proteins. Universidade NOVA De Lisboa. Ph.D. thesis.

Schaefer, K., Matano, L.M., Qiao, Y., Kahne, D., and Walker, S. (2017). *In vitro* reconstitution demonstrates the cell wall ligase activity of LCP proteins. *Nat. Chem. Biol.* *13*, 396-401.

Schertzer, J.W., and Brown, E.D. (2003). Purified, recombinant TagF protein from *Bacillus subtilis* 168 catalyzes the polymerization of glycerol phosphate onto a membrane acceptor *in vitro*. *J. Biol. Chem.* *278*, 18002–18007.

Schertzer, J.W., and Brown, E.D. (2008). Use of CDP-glycerol as an alternate acceptor for the teichoic acid polymerase reveals that membrane association regulates polymer length. *J. Bacteriol.* *190*, 6940–6947.

Schertzer, J.W., Bhavsar, A.P., and Brown, E.D. (2005). Two conserved histidine residues are critical to the function of the TagF-like family of enzymes. *J. Biol. Chem.* *280*, 36683–36690.

Sewell, E.W.C., Pereira, M.P., and Brown, E.D. (2009). The wall teichoic acid polymerase TagF is non-processive *in vitro* and amenable to study using steady state kinetic analysis. *J. Biol. Chem.* *284*, 21132–21138.

Sigle, S., Steblau, N., Wohlleben, W., and Muth, G. (2016). Polydiglycosylphosphate transferase PdtA (SCO2578) of *Streptomyces coelicolor* A3(2) is crucial for proper sporulation and apical tip extension under stress conditions. *Appl. Environ. Microbiol.* *82*, 5661–5672.

Sobhanifar, S., Worrall, L.J., King, D.T., Wasney, G.A., Baumann, L., Gale, R.T., Nosella, M., Brown, E.D., Withers, S.G., and Strynadka, N.C.J. (2016). Structure and mechanism of *Staphylococcus aureus* TarS, the wall teichoic acid β -glycosyltransferase involved in methicillin resistance. *PLoS Pathog.* *12*, e1006067.

Sobhanifar, S., Worrall, L.J., Gruninger, R.J., Wasney, G.A., Blaukopf, M., Baumann, L., Lameignere, E., Solomonson, M., Brown, E.D., Withers, S.G., and Strynadka, N.C. (2015). Structure and mechanism of *Staphylococcus aureus*

TarM, the wall teichoic acid α -glycosyltransferase. *Proc. Natl. Acad. Sci.* **112**, E576–E585.

Sutterlin, H.A., Malinverni, J.C., Lee, S.H., Balibar, C.J., and Roemer, T. (2017). Antibacterial new target discovery: Sentinel examples, strategies, and surveying success. In: *Topics in Medicinal Chemistry*. Springer, Berlin, Heidelberg. pp. 1–29.

Swoboda, J.G., Meredith, T.C., Campbell, J., Brown, S., Suzuki, T., Bollenbach, T., Malhowski, A.J., Kishony, R., Gilmore, M.S., and Walker, S. (2009). Discovery of a small molecule that blocks wall teichoic acid biosynthesis in *Staphylococcus aureus*. *ACS Chem. Biol.* **4**, 875–883.

van der Es, D., Hogendorf, W.F.J., Overkleeft, H.S., van der Marel, G.A., and Codée, J.D.C. (2017). Teichoic acids: synthesis and applications. *Chem. Soc. Rev.* **46**, 1464–1482.

Wang, H., Gill, C.J., Lee, S.H., Mann, P., Zuck, P., Meredith, T.C., Murgolo, N., She, X., Kales, S., Liang, L., Liu, L., Wu, J., Santa Maria, J., Su, J., Pan, J., Hailey, J., McGuinness, D., Tan, C.M., Flattery, A., Walker, S., Black, T., and Roemer, T. (2013). Discovery of wall teichoic acid inhibitors as potential anti-MRSA β -lactam combination agents. *Chem. Biol.* **20**, 272–284.

World Health Organization (2017a). Prioritization of pathogens to guide discovery, research and development of new antibiotics for drug resistant bacterial infections, including tuberculosis. WHO/EMP/IAU/2017.12

World Health Organization (2017b). Antibacterial agents in clinical development: an analysis of the antibacterial clinical development pipeline, including tuberculosis. WHO/EMP/IAU/2017.11

Xia, G., Maier, L., Sanchez-Carballo, P., Li, M., Otto, M., Holst, O., and Peschel, A. (2010). Glycosylation of wall teichoic acid in *Staphylococcus aureus* by TarM. *J. Biol. Chem.* **285**, 13405–13415.

Zhou, Z., Ding, W., Li, C., and Wu, Z. (2017). Synthesis and immunological study of a wall teichoic acid-based vaccine against *E. faecium* U0317. *J. Carbohydr. Chem.* **36**, 205–219.

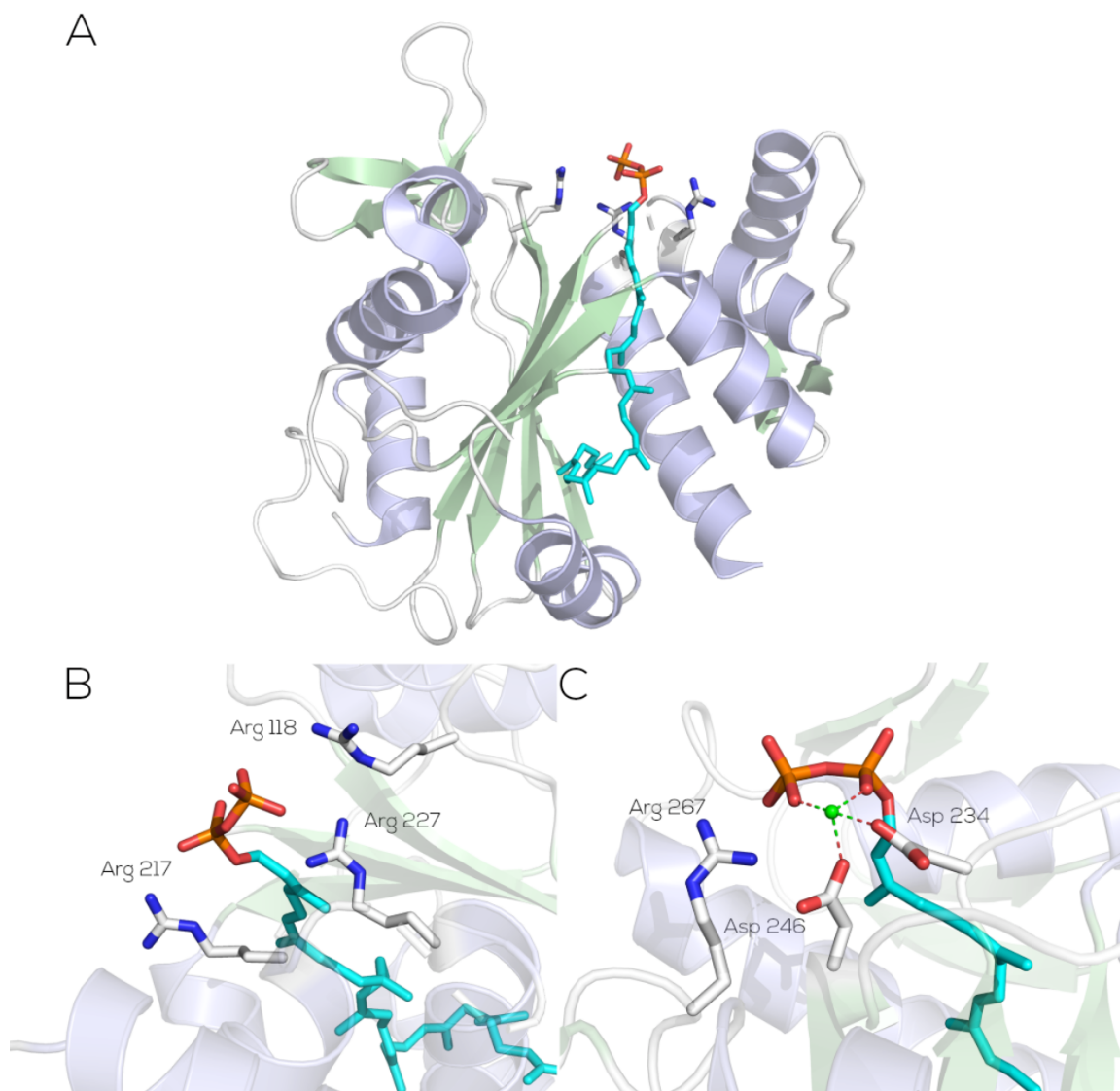


Figure 1. Structural features and conserved residues of LCP proteins. (A) Secondary structure and overall fold representation of *B. subtilis* TagT (PDB 4DE9). **(B)** Conserved arginine residues in putative active site. **(C)** *S. pneumoniae* CPS2A (PDB 2XXP) in complex with Mg^{2+} (green sphere; its coordination with two H_2O molecules are not shown). All structures are in complex with octaprenyl pyrophosphate (cyan sticks). Select conserved residues are shown in stick form and coloured according to heteroatom type.